Chiral Lithium N,P-amide Complexes

Synthesis, applications and structural studies by NMR and DFT

PETRA RÖNNHOLM

UNIVERSITY OF GOTHENBURG

Department of Chemistry

University of Gothenburg

Göteborg, Sweden

2011

DOCTORAL THESIS

Submitted for partial fulfilment of the requirements for the degree of
Doctor of Philosophy in chemistry.

Chiral Lithium N,P-amide Complexes

Synthesis, applications and structural studies by NMR and DFT

PETRA RÖNNHOLM

ABSTRACT

Enantiospecific synthesis reactions are of intense interest, owing to the increasing request for enantiopure compounds in both research and industry. Lithium amides containing a secondary chelating group are a class of powerful ligands for asymmetric addition reactions. Based on earlier experiences with lithium N,O and N,S amides, synthesis and properties of chiral lithium N,P amides and their use in asymmetric addition reactions are investigated in the present thesis.

Several chiral amines were synthesized with previously published methods, which were improved in different ways. A new synthetic route towards chiral aminophosphines via cyclic sulfamidates has been developed. The use of silica in the synthesis of sulfamidate and the chiral aminophosphine shortened the reaction time considerably, compared to previous methods. The reactions are fast, clean and high-yielding. Furthermore, the synthesis could successfully be scaled up with no loss in yield or purity and gives a general and simple route to a wide variety of chiral N,P-ligands from cheap and readily available amino acids.

Solution studies using low temperature ^{6}Li-NMR showed that the chiral lithium N,P-amides form various types of dimers depending on solvent and substituents in the amino acid backbone. The Li-P interactions in these complexes proved much stronger than expected, as indicated by the ^{6}Li-^{31}P coupling constant. A stability study on the aminophosphines with ^{31}P-NMR proved they are relatively air stable.

The newly synthesized lithium N,P amides were used as ligands in the asymmetric 1,2-addition of *n*-BuLi to benzaldehyde. The chiral N,P-ligands were found to induce asymmetry to similar or better extent, compared to previously reported chiral N,O- and N,S-ligands. Enantiomeric ratios up to 98:1 were obtained at −116 °C.

The experiments were complemented by quantum-chemical calculations employing Density-Functional Theory and Molecular Mechanics (MM), in order to rationalize the experimental findings. For the MM calculations, a tailored force field was developed to allow a proper description of the Li-N interaction. Both the aggregation and solvation of the ligand and the reaction mechanism were investigated. The predicted solvation and aggregation states as well as the enantioselectivites were in good accordance with experiment, provided that dispersion interaction was taken into account in a proper way. It was found that Li-π and π-α-H interactions and solvation within the complexes are the major contributions to the energy differences between the more stable *(R)*-transition state compared to its corresponding *(S)*-transition state.

Keywords: ^{6}Li NMR, Asymmetric synthesis, N,P-ligands, DFT, Molecular mechanics.

LIST OF PUBLICATIONS

Publication I:
Petra Rönnholm, Mikael Södergren, Göran Hilmersson, Improved and Efficient Synthesis of Chiral N,P-Ligands via Cyclic Sulfamidates for Asymmetric Addition of Butyllithium to Benzaldehyde, Organic Letter, 2007, 9 (19), pp 3781–3783.

Publication II:
Petra Rönnholm, Göran Hilmersson, NMR studies of chiral lithium amides with phosphine chelating groups reveal strong Li-P-interactions in ethereal solvents. 2011, Arkivoc, WB-5911EP. 200-210.

Publication III:
Petra Rönnholm, Sten O. Nilsson Lill, Jürgen Gräfenstein, Per-Ola Norrby, Mariell Pettersson, Göran Hilmersson, Aggregation and Solvation of Chiral N,P-amide Ligands in Coordinating Solvents - A Computational and NMR Study, 2011. Submitted to European Journal of Organic Chemistry.

Publication IV:
Petra Rönnholm, Jürgen Gräfenstein, Per-Ola Norrby, Göran Hilmersson, Sten O. Nilsson Lill. A Computational Study of the Enantioselective Addition of *n*-BuLi to Benzaldehyde in the Presence of a Chiral Lithium N,P-Amide, 2011. Submitted to Organic & Biomolecular Chemistry.

Publication V:
Petra Rönnholm, Sten O. Nilsson Lill, Tailored force field for lithium amides, 2011. Manuscript.

Publication not included in this thesis:
Göran Hilmersson, Petra Rönnholm, "1,2´-methylenedipyrrolidin, 1-(2-Pyrrolidinylmethyl) pyrrolidine", Encyclopedia of Reagents for Organic Synthesis, 2008.

VIII

CONTRIBUTION REPORT

Publication I:
Development of ligand synthesis, synthesized the ligands, performed parts of the asymmetric addition reactions, made contributions to the interpretation of the results and the writing of the paper.

Publication II:
Synthesis of the ligands, performed the NMR studies.

Publication III:
Development of ligand synthesis, synthesized the ligands, performed most of the NMR studies of the complexes, performed the theoretical calculations and contributed to the writing of the paper.

Publication IV:
Formulated the research problem, performed the experimental and theoretical studies and contributed to the interpretation and writing of the paper.

Publication V:
Performed the DFT, contributed to the interpretation of the results.

x

LIST OF ABBREVIATIONS

Ac   acetyl

Ar   aryl

B3LYP   Becke 3-Parameter, Lee, Yang, Parr

Boc   *tert*-butyloxycarbonyl

Bn   benzyl

Bu   butyl

DABCO   1,4-diazabicyclo[2.2.2]octane

DCC   *N,N'*-Dicyclohexylcarbodiimide

DCE   1,2-dichloroethane

DCM   dichloromethane

DCVC   dry column vacuum chromatography

de   diastereomeric excess

DFT   Density Functional Theory

DMM   di(propylene glycol) dimethyl ether

DMAP   4-dimethylaminopyridine

DMF   *N,N*-dimethylformamide

DMSO   dimethyl sulfoxide

ee   enantiomeric excess

e.r   enantiomeric ratio

Et   ethyl

eq.   equivalents

FF   Force Field

GC   gas chromatography

HOBT   1-hydroxybenzotriazole

i-Pr   isopropyl

i-Bu   isobutyl

IRC   Intrinsic Reaction Coordinate

IUPAC   International Union of Pure and Applied Chemistry

Me   methyl

MM   Molecular Mechanics

MNDO   Modified Neglect of Differential Overlap

MS   mass spectrometry

MTBE	methyl-*tert*-butylether
MW	microwave
n-BuLi	*n*-butyllithium
NMR	nuclear magnetic resonance
Nu	nucleophile
PBF	Poisson Boltzmann Finite
PES	Potential Energy Surface
Ph	phenyl
QM	Quantum Mechanics
QRC	Quick Reaction Coordinate
R, S, Re, Si	descriptors of stereochemistry
RINMR	rapid injection NMR
RT	room temperature
SCF	Self-Consistent Field
SCRF	Self-Consistent Reaction Field
S_N2	bimolecular nucleophilic substitution
Solv	Solvent
TFA	trifluoroacetic acid
THF	tetrahydrofuran
TLC	thin layer chromatography
ZPE	Zero Point Energy

TABLE OF CONTENTS

1. INTRODUCTION

1.1. Organic compounds

The term "organic" in organic chemistry goes back to 1779, when the Swedish chemist Torbern Bergman introduced the concepts of "organic" and "inorganic":[1, 2]

"At med någon ordning kunna överse de nyaste Chemiens framsteg, få bör märkas, är de kroppar, som på Jordklotet förefalla, äro i allmänhet af tväggehanda beskaffenhet. Större delen består och tillkommer af partiklar, som häftas tillsammans utvärtes, utan at ega bestämda rör til närings-safters fördelning. Sådane äro jord-arter, stenar, salter, allehanda mineraler, ja vatten, luft och eld, som derföre kunna kallas oorganiske. Deremot finnes en oräknelig mängd och förändring af andra, hvilka til sin byggnad äro få inrättade, at mångfaldige gröfre och finare canaler föra de til växt och underhåll nödiga vätskor. Hit höra örter och djur, hvilka med et gemensamt namn, kunna kallas organiske kroppar."

The meaning was that certain compounds could only be synthesized from compounds stemming from their classical elements - Earth, Wind, Water and Fire - by organisms possessing a vital force (*vis vitalis*). This was called vitalism or The Vital Force Theory and was questioned in 1824 when Friedrich Wöhler synthesized oxalic acid, which was known to exist in living organisms. In 1828 he accidentally synthesized urea from the inorganic compound ammonium cyanate, this is now referred to as Wöhlers synthesis. Urea was known to occur in urine of living organisms, and thus Wöhler´s synthesis showed that organic compounds actually can be synthesized from inorganic compounds. Friedrich Wöhler was himself very surprised by his results:[3]

"Der Umstand, daß bei der Vereinigung dieser Stoffe dieselben ihre Natur zu verändern schienen und dadurch ein neuer Körper enstände, lenkte von Neuem meine Aufmerksamkeit auf diesen Gegenstand, und diese Untersuchung hat das unerwartete Resultat gegeben, daß bei der Vereinigung von Cyansäure mit Ammoniak Harnstoff entsteht, eine auch in sofern merkwürdige Thatsache, als sie ein Beispiel von der künstlichen Erzeugung eines organischen, und zwar sogenannten animalischen, Stoffes aus unorganischen Stoffen darbietet."

Historians see these findings as the turning point for the vitalism, even though Friedrich Wöhler was very cautious about claiming he had destroyed The Vital Force Theory.

Today an "organic compound" has many definitions, where one is simply that if the compound contains carbon it is an organic compound. Others say the compound needs to have one or more C-H bonds, while others include the C-C bonds. Organic chemistry can be subdivided into groups with heteroatoms such as nitrogen, phosphorus, silicon, sulfur and oxygen, but also into organometallic compounds.

1.2.   Organometallic compounds

Organometallic compounds are molecules containing a carbon-metal linkage, and more specifically it contains an alkyl or aryl radical bonded to a metal. Examples of organometallic compounds are diethylmagnesium (Et_2Mg), ferrocene ($Fe(C_5H_5)_2$) and lithiumorganic compounds such as butyllithium (BuLi). An organolithium reagent is a compound that contains mainly an ionic carbon-lithium bond (90% ionic, 10% covalent).[4-6] These compounds can be prepared by the reaction of lithium metal and a halocarbon or by metal-haloalkane exchange between a solution of, for example, BuLi and an organic halide compound. There are a number of hydrocarbon solutions of various organolithium bases but one of the most frequently used reagents is *n*-BuLi.

The ionic bond between the carbon of the alkyl chain and the lithium ion, resulting in a strong dipole moment, makes organolithium compounds aggregate easily, i.e. form clusters, or complexes. A single carbanionic alkyl chain is not sufficient for stabilization of the electron-deficient lithium cation. The π-system of aromatic groups can form good interaction with lithium atoms, which has a stabilizing effect. Therefore, freezing-point measurements, which show the size of the aggregates, are carried out in aliphatic solvents since the organolithium reagents are then more aggregated compared to in polar solvents.[7] For unfunctionalised organolithiums the aggregation states depend mostly on steric hindrance. For example, primary organolithiums form hexamers in hydrocarbons, but form tetramers when the organolithium is branched β to the lithium atom. Secondary and tertiary organolithiums form tetramers in hydrocarbons and very bulky alkyllithiums, such as benzyllithium, form dimers.[7]

Other compounds with coordinating possibilities, such as ethers, amines or metal alkoxides, can form different aggregates with organolithium compounds. When these potential ligands coordinate to lithium, the higher order aggregates are deaggregated to smaller aggregates. Solvents can also coordinate to lithium and increase the reactivity of the organolithiums. Some important

coordinating solvents or additives used for this purpose are for example: HMPA, (-)-sparteine, DME, THF, t-BuOMe, and Et$_2$O that bind to the lithium ion, acting as ligands.

1.3. Ligands

A ligand is a molecule that binds to a metal atom via one or several bonds to form a coordination or metal complex. The binding to the metal atom can take place in numerous ways depending on the number of atoms involved in the binding to the metal, that is, the denticity. Denticity is derived from dentis, which is the latin word for tooth. If only one atom binds to the metal atom the denticity of the ligand is said to be monodentate, or unidentate (Figure 1). When two atoms of the ligand bind to the metal atom the ligand is said to be bidentate. Ligands with three bonding atoms are called tridentante, with four bonding atoms tetradentate. When more than two atoms are bonded the ligand is polydentate or multidentate. Ambidentate ligands, on the other hand, can bond to the metal in more than one way. If the ligand coordinates via two or more atoms it is also called a chelate, a term that comes from the greek word chelè for claw.
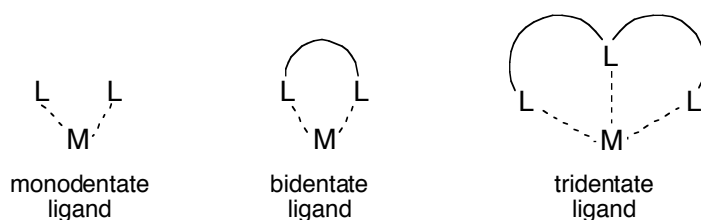

Figure 1. Examples of denticity of ligands.

Among polydentate ligands there are hybrid ligands, which contain at least two different types of coordinating atoms, in contrast to homofunctional ligands.[8] These atoms often have very different character, where one can be a soft and the other a hard donor atom in the sense of HSAB (Hard and Soft Lewis Acids and Bases) theory.[9-11] According to HSAB , oxygen, for example, is a hard atom, i.e. small and weakly polarizable, whereas sulfur is soft, i.e. large and strongly polarizable.[12] It has previously been shown that the combination of a hard and soft donor can give a very selective ligand in the enantioselective addition of *n*-BuLi to benzaldehyde (Scheme 1).[13]
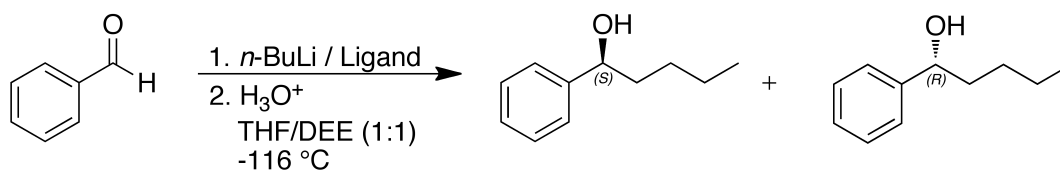
Scheme 1. The enantioselective addition of *n*-BuLi to benzaldehyde.

By increasing the softness/hardness ratio of the donor atoms the ee can be improved.[13] In our group, N,O-ligands were studied first and gave good enantiomeric excess (ee). To further investigate the possibility to improve the ee, the oxygen was replaced by sulphur to study N,S-ligands. It was, however, uncertain if this approach would work well in lithium chemistry, since soft donors usually do not bind well to lithium, which is a very hard atom. It was thus surprising to us that the ee of N,S-ligands was substantially increased compared to N,O-ligands.[13, 14] Examples on ligands previously studied in our group are shown in Figure 2.[15]

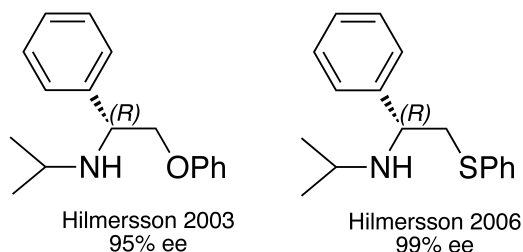
Figure 2. N,O- and N,S-ligands studied in our group.[16, 17]

Chiral N,P-ligands have many applications in asymmetric catalysis, where different metal-complexes can be formed. Some examples are Ir-catalyzed asymmetric hydrogenation, Pd-catalyzed allylic alkylation and Cu-catalyzed conjugate addition of diethylzinc to ketones.[15, 18, 19] However, N,P-ligands in asymmetric reactions with organolithiums are scarce.

## 1.4.   Previously synthesized ligands used in asymmetric butylation reaction

1.4.1.   Synthesis of N,N-ligands

N,N-ligands have long been investigated and were the first ligands studied in our group. One of Koga´s chiral N,N-ligands can be synthesized by starting with commercially available *(R)*-phenylglycine and using a number of steps to the desired diamine.[20] Another synthesis of this diamine has also been published, where *(R)*-styrene oxide is converted to the diamine in fewer steps (Scheme 2).[21, 22]
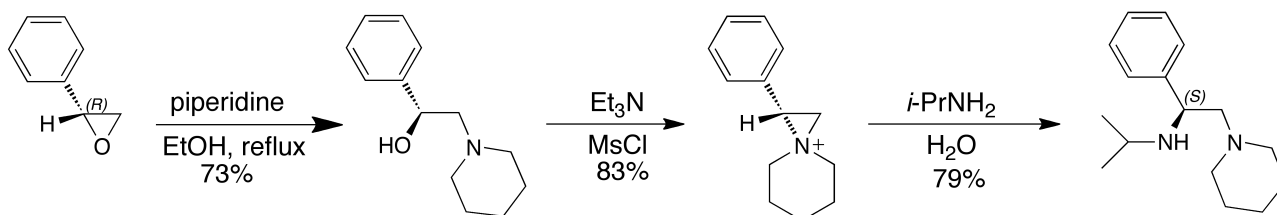

Scheme 2. Ring opening of *(R)*-styrene oxide and the aziridinium ion.

Another common diamine is *N*-methyl-1-phenyl-2-(1-pyrrolidinyl)ethanamine, which has been synthesized in a three step route, from commercially available amino acid, by *N*-protection, amide formation and reduction (Scheme 3).[23]
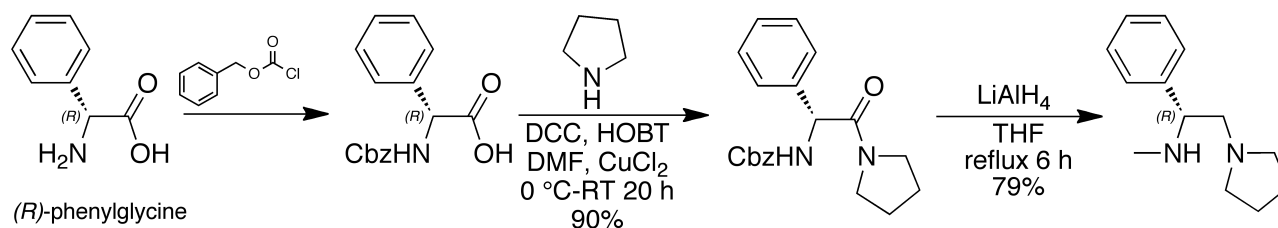
Scheme 3. Synthesis of *N*-methyl-1-phenyl-2-(1-pyrrolidinyl)ethanamine from *(R)*-phenylglycine by Singh et al.

There is also a one pot synthesis that yields higher ee than the previous one and starts either by *(R)*-styrene oxide or *(S)*-phenylglycinol and proceed via mesylation and formation of an aziridinium ion (Scheme 4).[24-26]
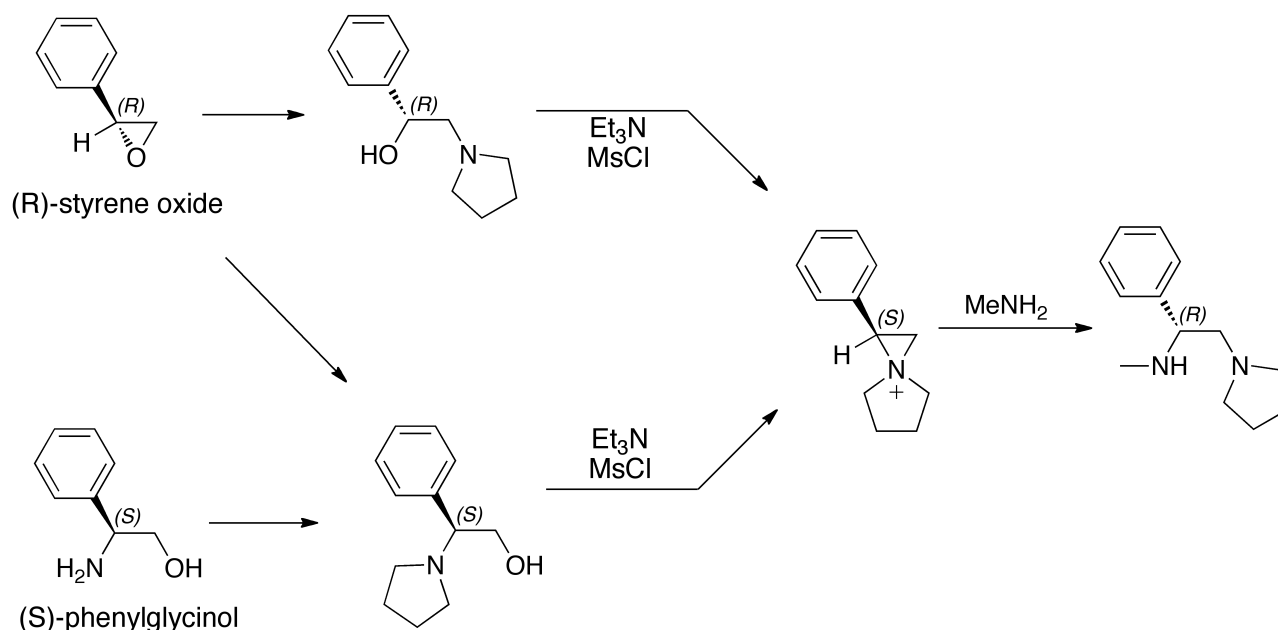
Scheme 4. Two routes for the synthesis of a diamine via mesylation and aziridinium ion.

1.4.2. Synthesis of N,O-ligands

Various N,O-ligands have been studied in our group and they are easily prepared from readily available amino acids. The amino acids were first reduced with LiAlH$_4$, followed by reductive amination of the amine to give the *N*-alkylated amino alcohol (Scheme 5). The respective amino ethers were obtained by adding NaH to the secondary amino alcohol in dry THF and adding the respective alkyl halide.[14]
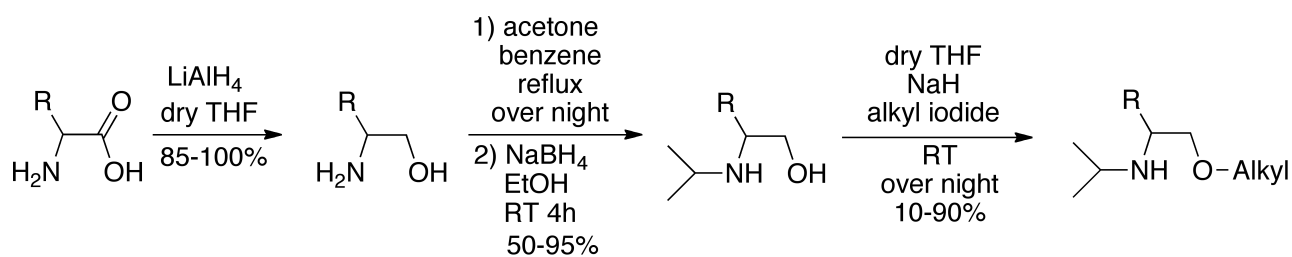
Scheme 5. Synthesis of previously studied amino ethers.
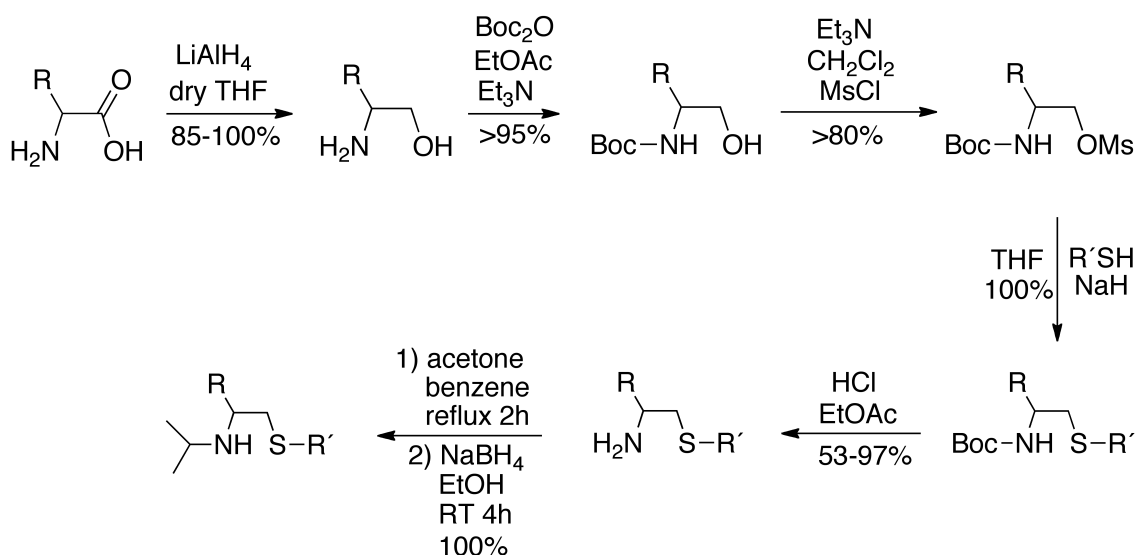
1.4.3.   Synthesis of N,S-ligands

In many cases N,S-ligands give rise to higher enantioselectivity compared to N,O-ligands[16] and this has been rationalized to the higher polarizability of sulphur, the higher thiophilicity of some metals towards sulphur and the fact that metal thiolates have less tendency to diminish the Lewis acidity of a metal compared to metal alcoholates.[27-31]

Anderson et al. synthesized N,S-ligands either via aziridine or Mitsunobu/reduction procedures, where the latter procedure is more reliable (Scheme 6).[27]
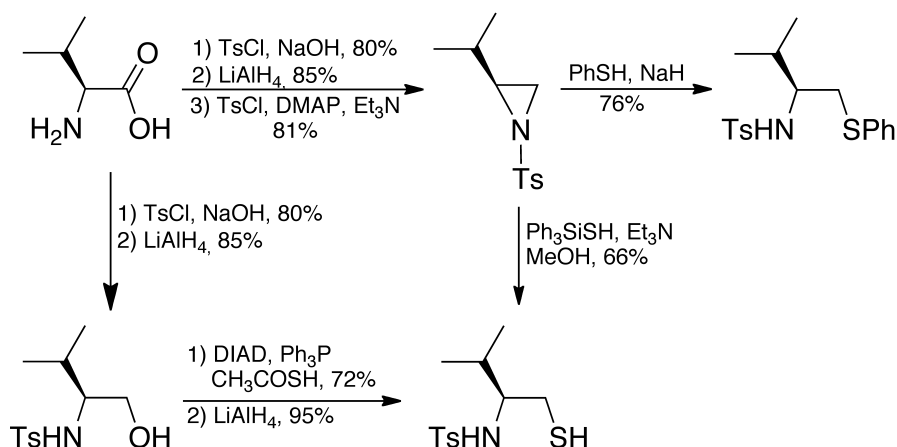
**Scheme 6.** Synthesis of N,S ligands.

In our group the N,S-ligands were prepared by reduction of a readily available amino acid, Boc-protection of the amine and mesylation the alcohol (Scheme 7). This was followed by the addition of the thiol as nucleophile.[13] The Boc group was then deprotected by hydrochloric acid and the free amino sulfide was subjected to reductive amination with acetone and $NaBH_4$.

Scheme 7. Previous procedure to synthesize N,S-ligands.

1.4.4.   Synthesis of N,P-ligands

The previously most common method for synthesizing N,P-ligands has been by a similar procedure as for the N,S-ligands, and was used by Saitoh et al. (Scheme 8).[32]
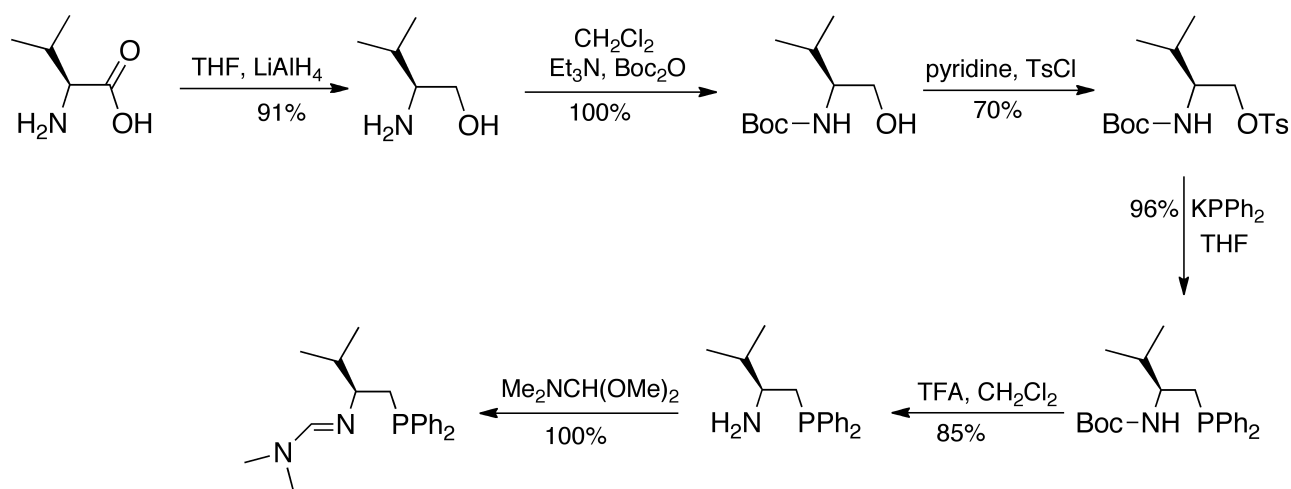
Scheme 8. Synthesis of the chiral amidine.

Quirmbach et al. tried to synthesize the N,P-ligand of valine from the Boc- and tosylated amino alcohol with LiPPh₂ as the nucleophile, but they found that various by-products were formed (Scheme 9).[33] Instead, a better reaction sequence was used, by deprotecting the amine with HBr/ HOAc and protecting the amine as the ammonium salt. LiPPh₂ in THF was added and in a S_N2-reaction the N,P-ligand was obtained in 43% yield
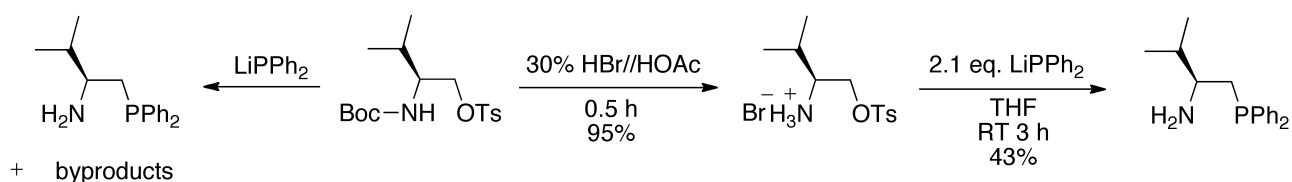
Scheme 9. Synthesis of N,P-ligand via ammonium salt and tosylated alcohol.

The difficulty in synthesizing the N,P-ligand was also experienced by Anderson et al.[34] They deprotected the Boc- and tosylated amino alcohol with $KPPh_2$ and received only aziridine as isolated product, even with various counterions, solvents and temperature (Scheme 10).[34] However, by using the anion of phosphine borane, which is less basic than the anion of the free phosphine, the borane complex was obtained in good yield (71%). Liberation of the free aminophosphine was achieved by deprotection with DABCO in toluene, followed by deprotecting the Boc-group with TFA (93% yield).
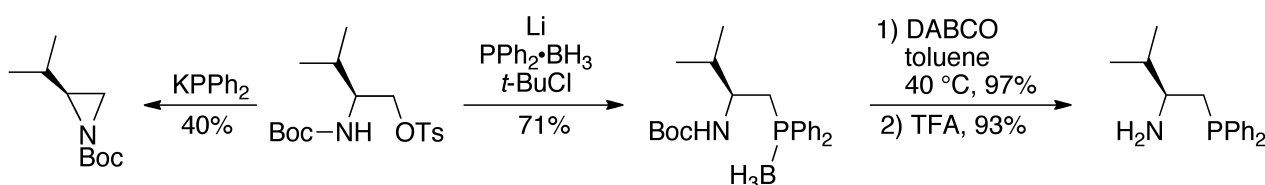
Scheme 10. Synthesis of N,P-ligand via borane complex.

Ring opening of aziridines have also been a way to synthesize N,P-ligands. When $KPPh_2$ was added to aziridine of ephedrine the isolated products were $HPPh_2$ and aziridine, i.e. the aziridine had not reacted at all. However, by adding Et_2OBF_3 the nitrogen was activated and the ring opening of aziridine was possible, giving the desired N,P-ligand (Scheme 11).
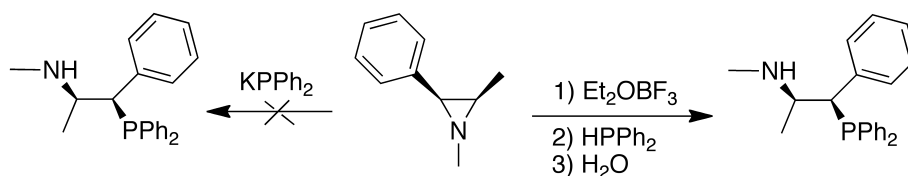
Scheme 11. Ring opening of aziridine by activation of the nitrogen.

The N,P-ligand of L-proline was synthesized by Kanai et al. by refluxing the tosylate with PPh_2Cl and sodium in dioxane/THF, followed by deprotection of the Boc-group using TFA to give the aminophosphine ligand in 78% yield (Scheme 12).[35]
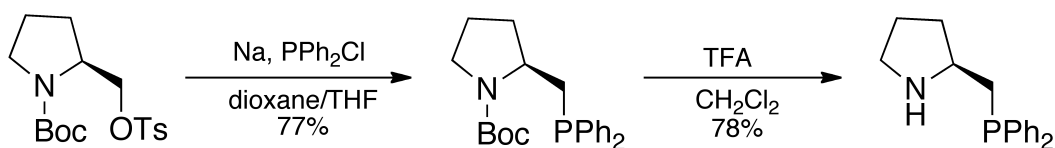
Scheme 12. Synthesis of chiral phosphine of L-proline.

N,P-ligands have received much attention due to their unsymmetrical nature and the bonding versatility they give.[36] In addition, they enable tuning of the electronic and steric properties of the donor atoms, such as hemilability, and this represents an efficient way of controlling the selectivity of catalytic processes.

1.5.   Alkylation reactions

In organic chemistry carbon-carbon bond formation is one of the most important reactions. Due to the increased demand for chiral substances, such as pharmaceuticals, it is often required to perform these reactions in a stereoselective fashion, and various ways of achieving this have been developed through the years. By adding organometallics to aldehydes at low temperature in the presence of a chiral ligand as chiral auxiliary and catalyst a chiral alcohol can be afforded in various ee´s (Scheme 13).
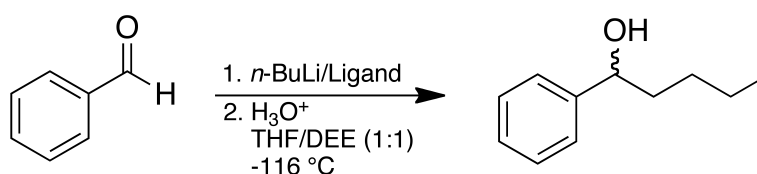
Scheme 13. Asymmetric addition of *n*-BuLi to benzaldehyde in the presence of a chiral ligand.

Previously used ligands in the addition reaction are both mono-, di- and tridentate and those ligands have historically been based on hard chelates such as sp^3 nitrogen and/or oxygen donor groups. Some examples of ligands are given in Figure 3.[37-42]
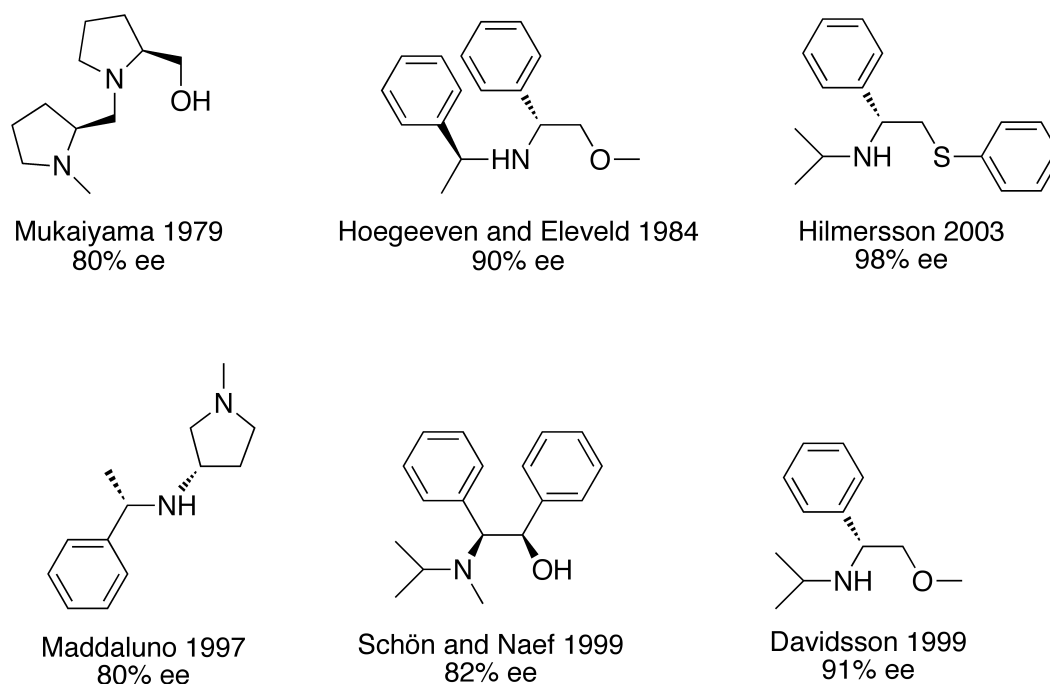
Figure 3. Examples of chiral ligands with hard and soft chelates, used in enantioselective reactions.[37-40, 42, 43]

One of the early studies of the asymmetric alkylation of benzaldehyde was performed by Mukayiama et al.[37] Based on their earlier work and the good results in the asymmetric reduction of various aryl ketones they decided to study the asymmetric addition of organometallic reagents to benzaldehyde. It was found that the tridentate ligand was a very good ligand in terms of enantioselectivity and one the enantiomers of the alcohol was obtained in 95% ee (Scheme 14).
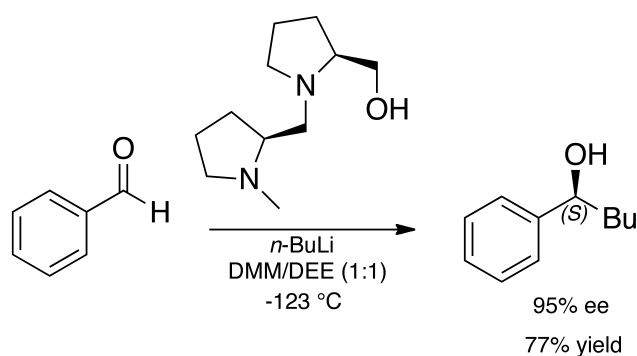
Scheme 14. Addition of *n*-BuLi and tridentate ligand to benzaldehyde by Mukaiyama et al.

Cram et al used a diamine as the chiral ligand in the asymmetric addition to benzaldehyde.[44] One alcohol was obtained in 95% ee (Scheme 15).
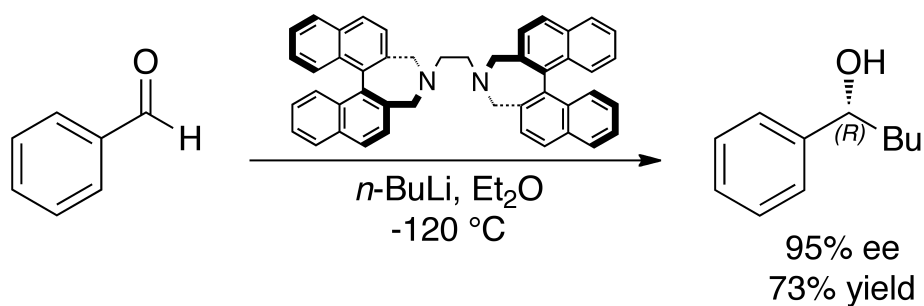
Scheme 15. Addition of n-BuLi to benzaldehyde in the presence of a diamine by Cram et al.

Hogeveen and Eleveld synthesized various N,O-ligands for their study of the asymmetric addition to benzaldehyde (Scheme 16).[40]
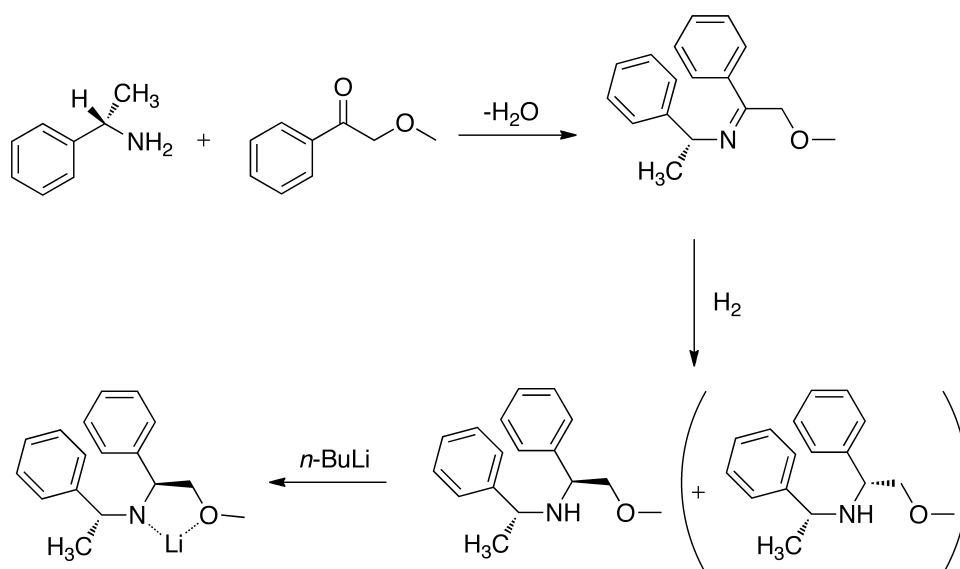
Scheme 16. Synthesis of an N,O-ligand by Hogeveen and Eleveld.

Different chiral lithium amides were investigated where the highest ee (90%) was obtained from (S)-(−)-α-methylbenzylamine, 2-methoxyacetophenone and n-BuLi in DMM/Et$_2$O (1:1) at -120 °C (Scheme 17).
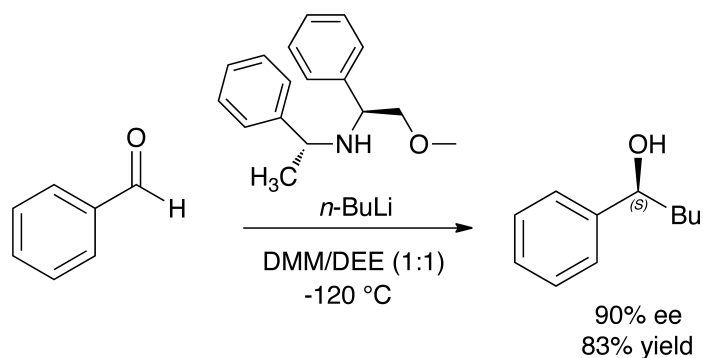
Scheme 17. Addition of *n*-BuLi to benzaldehyde in the presence of an amino ether by Hogeveen and Eleveld.

Other chiral amino ethers recently studied have given 89% ee of the *(R)*-enantiomer of the alcohol in Et$_2$O/THF (Scheme 18).[14]
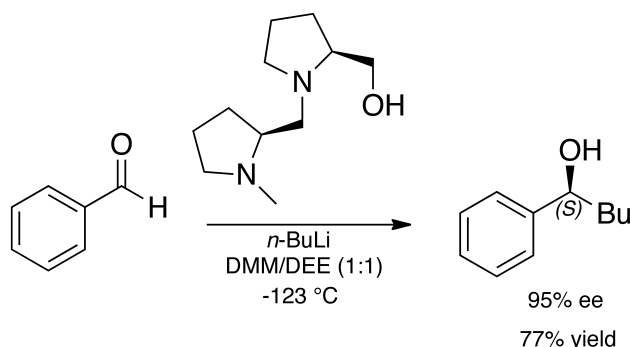
Scheme 18. Addition of *n*-BuLi and an amino ether to benzaldehyde by Hilmersson et al.

Also, in previous work on N,O-ligands it was found that a less bulky alkyl group on the oxygen atom in the chelate result in a higher ee (Scheme 19).[14] To further investigate if the enantiomeric excess could be improved chiral amido sulfide ligands were also tested in the asymmetric addition to benzaldehyde[13] In comparison to the previous N,O-ligands the enantioselectivity was improved.[14] The ee´s improved in Et$_2$O/THF and ee´s up to 98.5% and 88% were obtained (Scheme 19).
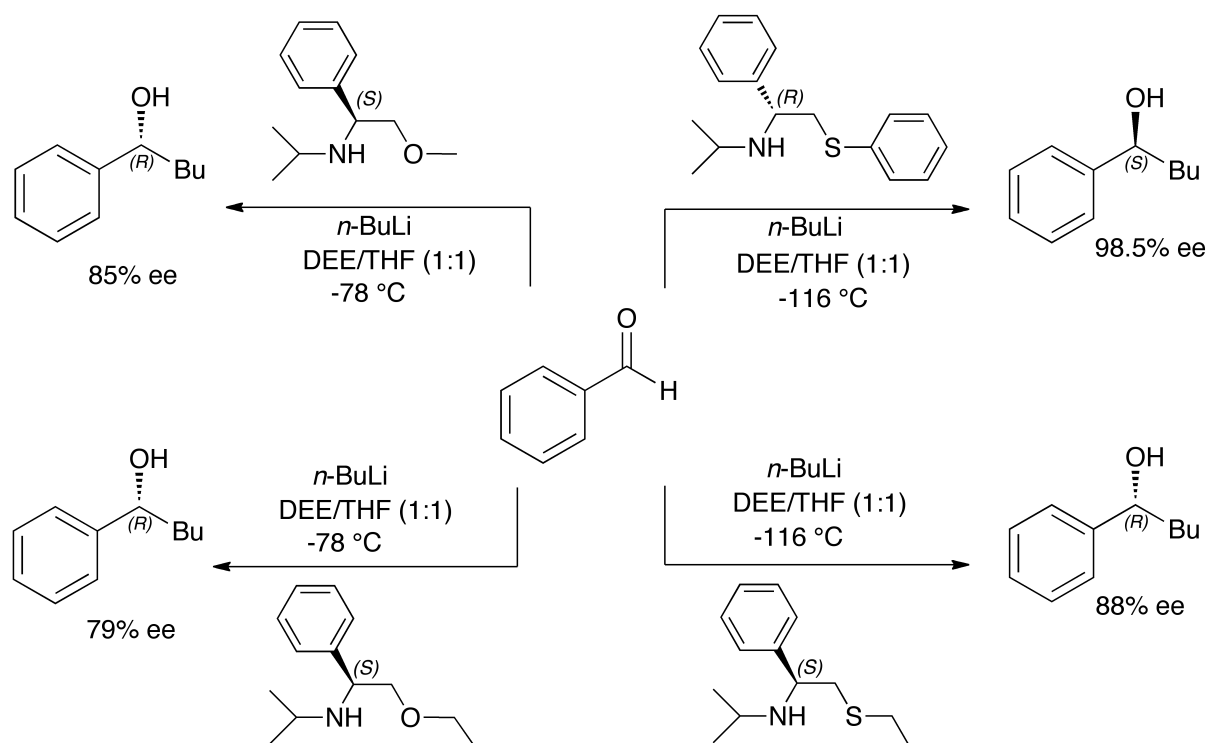
Scheme 19. Chiral amido sulfide ligands in the asymmetric additon of benzaldehyde.

With tridentate Li-amides the enantioselectivity is low and the highest ee is 48% with benzaldehyde. There is also a larger solvent dependence for tridentate than for bidentate Li-amides and in non-coordinating solvents low ee was obtained.[14] When using MeLi as the alkylating reagent in the alkylation reaction a racemic mixture was obtained with tridentate, possibly due to that the non-ligand mediated methylation reaction is faster. With bidentate ligands a 45% ee was obtained.

1.6.   NMR - structures and experiments

NMR - Nuclear Magnetic Resonance - is used to characterize and investigate properties and structures of organic, bioorganic and inorganic molecules, in both solution and solid state. A first milestone in the history of NMR was the work of Uhlenbeck and Goudsmit.[45] Rabi received the Nobel Prize 1944 "for his resonance method for recording the magnetic properties of atomic nuclei."[46] In 1952 that same prize was shared between Purcell and Bloch "for their development of new methods for nuclear magnetic precision measurements and discoveries in connection therewith".[46] After these findings NMR has gained a lot of interest and been continuously used throughout the years. In 1971, Jean Jeener presented a suggestion to add a second probing frequence. In this way, 2D NMR became possible and more information on the structures would be obtained.This idea was, however, not published until 1976 by Richard Ernst, who published the first 2D-NMR.[47] Richard R. Ernst received the Nobel Prize in chemistry 1991 for his contributions to the development of the sensitivity and the resolution of NMR. In 2002 Kurt Wüthrich received the Nobel Prize in chemistry for his application of NMR in determining the three-dimensional structure of biological macromolecules in solution.

NMR is a quantitative, non-destructive, analysis technique to study the chemical and physical properties of pure compounds and mixtures. The analysis is performed on the nucleus of the atom and not the electrons. Some nuclei have an overall spin (I) resulting from unpaired spins of the nuclear particles. The rules for determining the overall spin of a nucleus are:

1.   If the number of neutrons and the number of protons are both even:
   - the nucleus has no spin.
2.   If the number of neutrons plus the number of protons is odd:
   - the nucleus has a half-integer spin (i.e. 1/2, 3/2, 5/2)
3.   If the number of neutrons and the number of protons are both odd:
   - the nucleus has an integer spin (i.e. 1, 2, 3)

The overall spin is important due to the fact that the higher the spin the more often it is difficult to observe, owing to its too fast relaxation. The number of possible quantum states of the nucleus can be determined with: number of orientations $= 2I + 1$

A magnetic field applied at the nucleus gives an energy splitting between the different spin-orientation states of the nucleus. This splitting can be measured very accurately by radio frequency applied simultaneously. If the energy of the radio frequency quanta equals the energy difference between neighbouring spin states a sharp absorption resonance is observed. The resonance condition can be expressed as

$$h\nu = \mu B \qquad\qquad \text{Eq. 1}$$

where ν is the radio frequency, μ the magnetic moment of the nucleus, and B the applied magnetic field. Now the crucial point with NMR is that the magnetic field B at the nucleus is not equal to the externally applied magnetic field B_0. The electrons surrounding the nucleus shield the nucleus and slightly increase or decrease the applied field, such that $B = (1 + \sigma) B_0$, which can be observed as a slight change in the resonance frequency. The sign and size of the so-called chemical shielding σ arises from several processes: All electrons, in particular s electrons, make a positive contribution to σ by diamagnetic shielding. The shift caused by the shielding is termed diamagnetic shift or the upfield shift and result in a low chemical shift. p or d electrons in the vicinity of the investigated nucleus give rise to a negative paramagnetic contribution to σ. The p- and d-electrons produce a larger magnetic field at the nucleus, which is deshielding the nucleus and is said to have a paramagnetic or lowfield shift, resulting in a high chemical shift. Thus, the total σ value at a nucleus depends on its chemical environment and is characteristic for a certain atom in a certain compound.

In practice, one measures not the shieldings σ (which are related to a bare nucleus) but the so-called chemical shifts δ, i.e. the shieldings relative to the shift σ_0 of a reference compound: $\delta = \sigma_0 - \sigma$. Note the sign convention, which implies that paramagnetic effects make shift values more positive. Usually, a compound with weak paramagnetic shielding (and thus high σ value) is used as reference, such that δvalues are typically positive. However, a few unusual compounds may have even higher shieldings than the reference, and hence, negative shifts. Possible causes are bonds to metals or specific orientations in very anisotropic molecules. The intensity of the signals is proportional to the number of nuclear sites at that specific resonance frequency, allowing quantification of equivalent nuclei. Both σ and δ are given in parts per million (ppm).

Often, the observed NMR absorption lines prove to be multiplets consisting of equidistant lines with characteristic intensity ratios (1:1 for dublets, 1:2:1 for triplets, 1:3:3:1 for quartets, etc.) This splitting is caused by (indirect) nuclear spin-spin coupling: If there is an additional NMR-active nucleus (the so-called perturbing nucleus) close to the investigated one, its magnetic moments generates an extra magnetic field at the site of the investigated nucleus. The sign and size of this field depends on the spin orientation of the perturbing nucleus, and the different possible spin orientations give rise to the different components of the multiplet. The transmission of the magnetic field between the nuclei is performed by the electron system. Thus, spin-spin coupling is a (very sensitive) antenna for the electronic structure, which provides complementary information. The splitting between the multiplet components is independent of the applied external field and is called spin-spin coupling constant J for the pair of nuclei. In distinction from δ, J is isotope-dependent.

There are various nuclei to be studied in NMR and the most studied nuclei in organic and bioorganic molecules are ^{13}C and ^{1}H, due to their relatively high natural abundance. ^{1}H-NMR detects only the ^{1}H-isotope of the hydrogen, which has a a natural abundance of 99.984%. In ^{13}C-NMR the ^{13}C-isotope is only detected and not the ^{12}C-isotope due to its zero spin. Some other nuclei that can be studied in NMR are ^{31}P and ^{7}Li (see Table 1).

Table 1 Different nuclei, their spins and natural abundance.

nuclei	spin	natural abundance (%)	gyromagnetic ratio $\gamma/2\pi$ (MHz/T)
1 h	1/2	99.985	42.576
^{2}H (D)	1	0.015	6.536
^{12}C	0	98.89	0
^{13}C	1/2	1.109	10.705
^{31}P	1/2	100	17.235
^{6}Li	1	7.5	6.265
^{7}Li	3/2	92.5	16.546
^{15}N	1/2	0.37	-4.316
^{17}O	5/2	0.0373	-5.772

The shift caused by this shielding is termed diamagnetic shift or the upfield shift and result in a low chemical shift. The p-electrons, on the other hand, produce a larger magnetic field at the nucleus,

which is deshielding the nucleus and is said to have a paramagnetic or lowfield shift, resulting in a high chemical shift.

In the late 1960′s and early 1970′s some work on ^{7}Li-NMR was published[48-50] which opened up new methods in the field of lithium NMR. ^{7}Li, which is the most abundant isotope, gives broader signals in NMR compared to ^{6}Li due to its higher quadrupole moment. By synthesizing ^{6}Li-enriched reagents,[51-54] and with ^{6}Li-NMR available, it became feasible to study simple organolithium reagents and their aggregates in solution.

In ^{6}Li NMR the signals give a special pattern for phosphorus containing compounds, due to lithium coupling to phosphorus. One lithium coupling to one phosphorus, give rise to a doublet and one lithium coupling to two phosphorus give rise to a triplet.

The lithium cation often adopts a tetracoordinated ligation, which has been identified from solid state structures of organolithium compounds.[55] In addition, it is well established that *n*-BuLi occurs as a tetramer in Et$_2$O and as a tetramer in equilibrium with a dimer in THF. In non-coordinating solvents higher aggregates easily form, as was shown in Paper II as well as by other authors.[56, 57] Hence, in hydrocarbon solvents such as cyclohexane, *n*-BuLi exists predominantly as a hexamer.[58] A dimeric form was identified using ^{13}C- and ^{6}Li-NMR [54] and this dimeric complex increases in abundance with the addition of TMEDA and decreases with temperature. The high reactivity of *n*-BuLi in strongly coordinating solvents, such as THF, compared to less coordinating, such as Et$_2$O, is due to the higher concentration of a less aggregated complex.[59, 60] The internal motions in THF molecules are much more restricted compared to Et$_2$O due to its constraints that the five-membered ring of oxygen and carbon forms, with mainly ring-puckering remaining.[61] The difference in the ability of Li to coordinate THF compared to Et$_2$O is partly caused by the greater loss in vibrational entropy, mainly internal rotational entropy, for Et$_2$O compared to THF. Besides, Et$_2$O loses enthalpy when coordinating to Li since it has to adopt the gauche-gauche rather than the most stable (trans-trans) conformation.

When chiral amino ethers are mixed with *n*-Bu^{6}Li in THF and Et$_2$O chiral lithium amides are formed, which can aggregate to various degrees, depending on solvent and temperature (Figure 4).
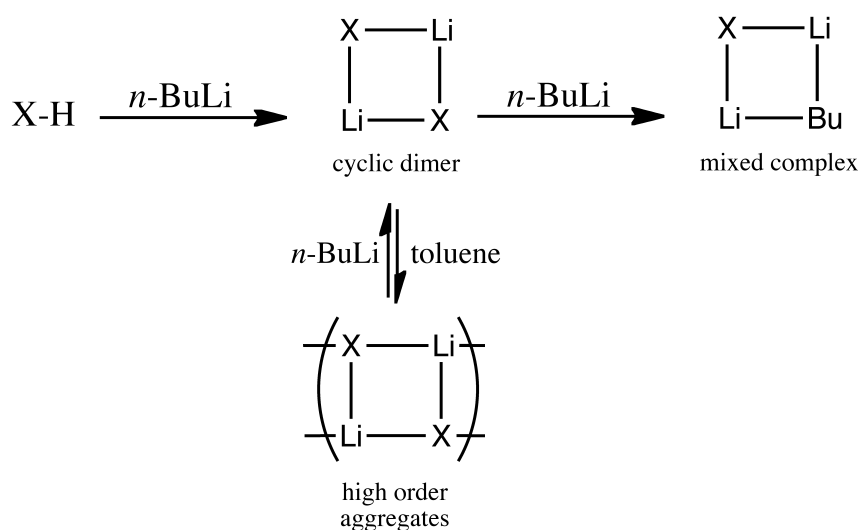
16

Figure 4. Aggregates formed in ^{6}Li-NMR (-90 °C) with *n*-BuLi in Et$_2$O and THF . $\times$ = C, N, O.

Addition of one equivalent (eq.) of *n*-BuLi to a chiral amino ether in Et$_2$O forms one single species, a mixed complex. Adding more than one eq. of *n*-BuLi results in various dimers, depending on solvent and substituents of the amino ether. It was found that when THF was added to the Et$_2$O solution of the Et$_2$O-solvated mixed complex (**Et$_2$O•Li-amide/*n*-BuLi**), ^{6}Li-NMR showed that the equilibrium between the solvated mixed complex and monomeric complex (**THF$_n$•Li-amide**) was solvent dependent (Scheme 20).[62]
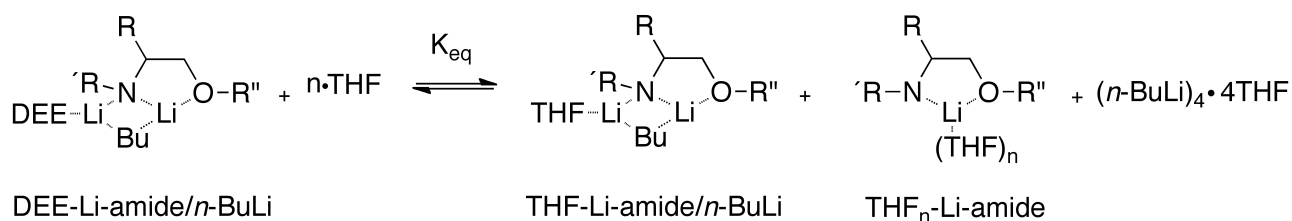
Scheme 20. The solvent dependence of the equilibrium between solvated monomer and mixed dimer.

In the addition of less than one equivalent of *n*-BuLi to a chiral amino sulfide in Et$_2$O at -78 °C a dimer with nonequivalent lithiums is formed (Scheme 21). Further addition of *n*-BuLi breaks up the dimer and resulted in a mixed complex .[16]

17
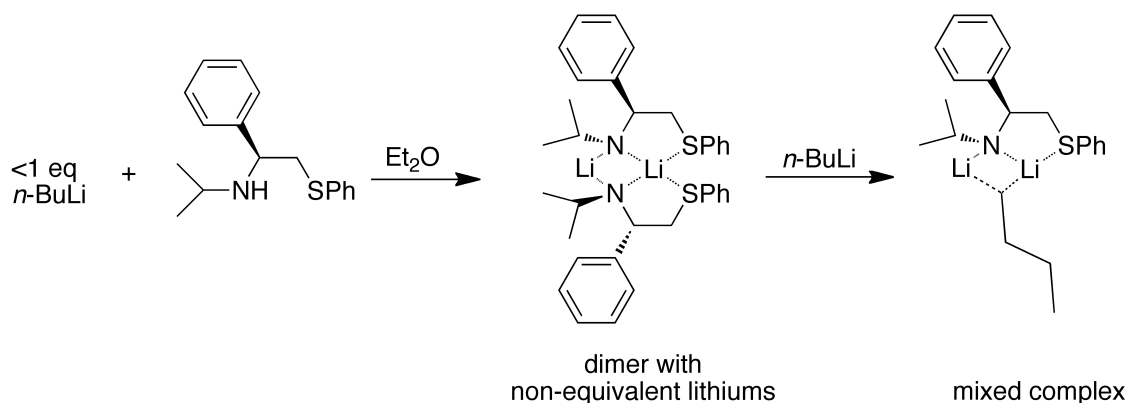
Scheme 21. The aggregates formed with chiral lithium amino sulfides depending on solvent and amount of *n*-BuLi added.

NMR is superior to any other solution-state technique in structure elucidation of organolithium compounds. The aggregates mentioned above can be analyzed with ^{6}Li-NMR, and often needs to be run at low temperature, to avoid deprotonation of the protons α to heteroatoms in the amino acid backbone.[62] Low temperatures may give rise to a number of problems in NMR measurements:

1. Precipitation of the solute
2. Freezing of solvent
3. Unattainable temperatures
4. B$_0$ field homogeneity problems
5. Solvent property changes; change of shift and line broadening due to increasing solvent viscosity
6. Increased propensity for equipment failure

Another useful method for structure elucidation of compounds, that avoids the mentioned problems, is theoretical calculations.

1.7.   Theoretical methods

Experimental methods, in particular NMR, play a crucial role for structure elucidation in the present work. A valuable complement to these measurements are quantum-mechanical calculations. Such calculations allow to determine properties that are not available for experiments and they give clues to rationalize experimental findings. For example, differences in bond strength can be related to structural features. In the following, we describe the theoretical methods used in this thesis.

1.7.1. Modelling theories

In its quantum mechanical description, the properties and the state of a system (atom, molecule, complex) are described by its Hamilton operator H and its many-particle wave function Ψ, respectively. The two quantities are related by the Schrödinger equation, which in its time-independent form reads:

$$H \, \Psi = E \, \Psi \qquad \text{Eq 2}$$

where E is the ground-state energy of the chemical system. Here, Ψ comprises the state of both the electrons and the nuclei. In the Born-Oppenheimer approximation,[63] which is commonly used in quantum chemistry, the Schrödinger equation is divided up in two parts: the electronic structure for spatially fixed nuclei and the motion of the nuclei. This can be performed because electrons are much lighter than nuclei, and therefore the nucleus is almost stationary.

The Schrödinger equation cannot be solved exactly except for very simple systems. Efficient and reliable computational schemes are therefore necessary to do quantum chemistry for real systems. Today, the majority of all quantum-chemical calculations are based on density-functional theory (DFT). DFT rests on the Hohenberg-Kohn theorem,[64] which states that all properties of a chemical system are fully determined by its ground-state electron density. Thus, it is not necessary to calculate the rather complex many-particle wave function.

Based on the Hohenberg-Kohn theorem, Kohn and Sham[65] developed the Kohn-Sham (KS) formalism, which is the basis of practically all current DFT calculations. In the KS formalism, the real interacting electrons of the systems are replaced by a set of non-interacting electrons that move in an effective potential. This so-called KS potential accounts for (i) the electron-nucleus attraction, (ii) the electrostatic (Hartree) electron-electron repulsion, (iii) exchange (X) interaction between electrons and (iv) electron correlation (C) effects. Whereas (i) through (iii) can be calculated exactly, (iv) contains the electronic many-body effects and needs to be approximated in practical calculations. In most KS calculational schemes, (iii) is treated approximately as well for several technical reasons. The choice of XC approximation distinguishes the different KS schemes that are in use and governs their accuracy. In the local-density approximation (LDA),[65, 66] XC is treated as if the electron gas were homogeneous at each point of the molecules. LDA schemes are, however, hardly used in molecular science due to their insufficient accuracy. The breakthrough of DFT in molecular modelling was initiated by the so-called Generalized Gradient Approximation (GGA)

schemes,[67-70] which instead use an inhomogeneous electron gas with linearly varying density as model for XC. More recently, hybrid GGA functionals[71] were devised, which combine the exact and the approximate (i.e. GGA-like) description of exchange effects. These hybrid XC schemes are now used most widely in quantum chemistry; the Becke-3-parameter/Lee-Yang-Parr[72] functional accounting for more than half of all DFT calculations in quantum chemistry.[73] The development of more accurate XC functionals both on and beyond the GGA and hybrid-GGA levels is an active field of current quantum chemistry.[74-77]

While KS-DFT is a fairly efficient computational scheme it is still too expensive for really large systems (several 10,000 atoms) as well as for extensive investigations (e.g. conformational searches) at moderate-size systems. Molecular mechanics (MM) is an alternative approach to be used in such cases. The idea of MM was developed in the early years of quantum mechanics,[78] it has been used regularly since about the seventies.[79, 80] In MM, molecules are described by a ball-and-spring model with balls for the atoms and springs for the bonds; additional springs are added for several types of non-covalent interactions (e.g. electrostatic, hydrogen-bond, or dispersion interaction). The movement of the system is then described by classical (Newton) mechanics. In MM, the quantum character of the molecules is no longer explicit; rather, it is hidden in the parameters of the model, such as rest lengths and harmonic and possibly anharmonic force constants of the springs. The values of those parameters, which define the MM force field, are determined from a set of reference molecule based either on experimental data, quantum chemical calculations, or a combination of both.[81] The accuracy of MM calculations may be competitive to that of a DFT calculation at much lower costs, provided that the system under investigation is sufficiently similar to the molecules in the reference set. Thus, most force fields are suitable for purely organic compounds but are severely limited in their application to metal complexes. Moreover, a given force field cannot be applied to a system that contains atom or bond types not present in the training set.

1.7.2.   Potential Energy Surface, geometry optimizations, thermochemistry

In the Born-Oppenheimer approximation, the energy of the system is a function of the set of nuclear coordinates. This function, the so-called potential-energy surface (PES), contains valuable information on the chemical behaviour of the system, such as possible reaction paths, relative stability of different structures, etc (Figure 5). Thus, quantum-chemical studies typically amount to exploring the PES of a system.
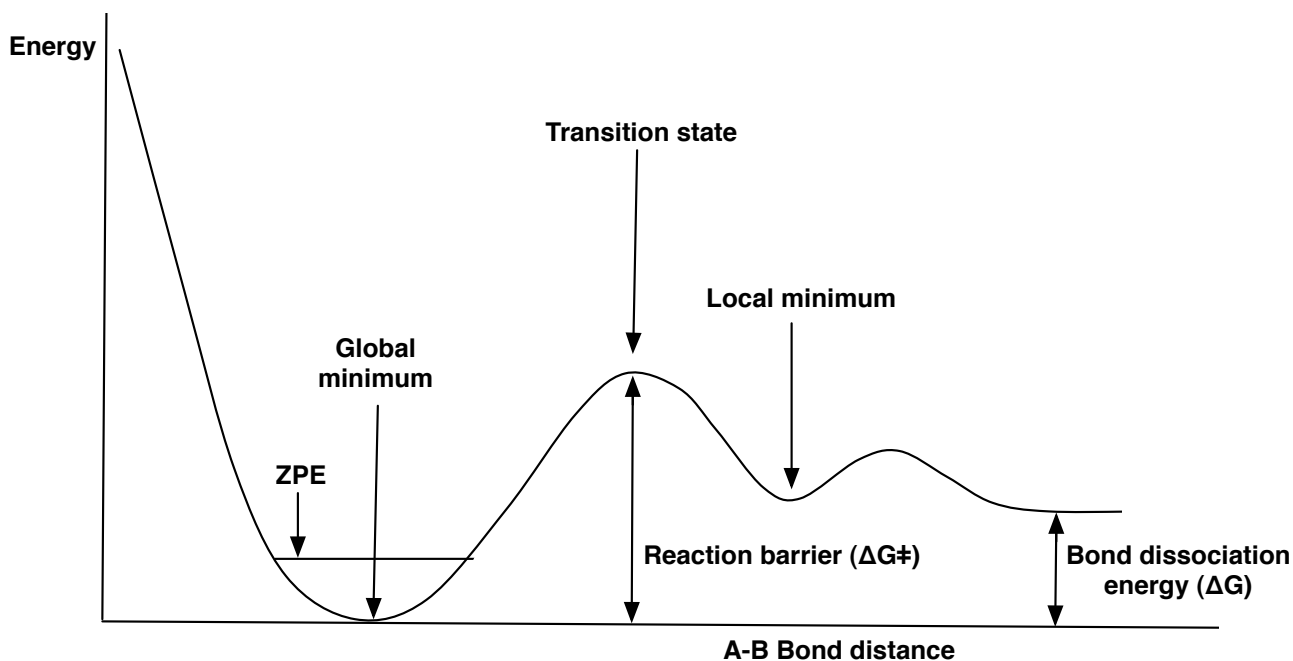
Energy

Transition state

Local minimum

Global
minimum

ZPE

Reaction barrier (ΔG‡)

Bond dissociation
energy (ΔG)

A-B Bond distance

Figure 5. Schematic picture of the Potential Energy Surface (PES).

The complete PES is by far too complex to be scanned systematically. Instead, one focuses on distinguished points, lines, or regions on the PES that are relevant for the behaviour of the system. Of particular interests are stationary points of the PES, i.e. points where the gradient of the energy vanishes. The chemical relevance of a stationary point depends on its stability, which can be determined from the signature of the eigenvalue spectrum of the so-called Hessian, i.e. the matrix of the second derivatives of the energy at the stationary point:

- If all eigenvalues are positive, the point represents a local minimum of the energy and thus a locally stable geometry of the system. This may be the equilibrium structure for a molecule in general, one of the stable conformers for a flexible molecule, or the reactants, intermediates, or products for a reacting systems of molecules.

- If just one of the eigenvalues is negative, the point represents a transition state (TS), that is, a saddle point on the path between two stable points on the PES, such as between two stable conformers or between reactants and products.

- If there are two or more negative eigenvalues, the point is a higher-order saddle point with no immediate chemical relevance.

Frequency calculations can be used to characterize stable points on the PES. The total energy of the system is actually higher than the electronic energy represented by the PES: Due to the Heisenberg

uncertainty principle, the nuclei of the system are never fully at rest. The zero-point vibrations of the nuclei give rise to a zero-point energy (ZPE) contribution, which is added to the electronic energy. From the relative energies of the minima of products and reactants the thermochemistry of the reactions can be calculated. Reaction rates are obtained from the profile and height of the mountain pass separating the valleys of the products and reactants. At finite temperatures, the thermodynamics of the system is governed not by energy alone but by a balance between energy minimization and entropy maximization. As a consequence, the key quantity for thermochemistry is not the energy E but the Gibbs free energy G. The enthalpy and entropy corrections contained in G can in principle be calculated quantum-chemically. However, in some cases (e.g. when solvation plays a role, see Section 1.7.4), empirical entropy terms may be more reliable than the calculated ones.

Properties like polarizability, dipole moments, NMR shielding etc depend on the response of the energy to applied electric and magnetic fields and can thus be related to an extended PES, where the mentioned fields are additional parameters.

The starting point when studying a chemical reaction in computational chemistry is consequently to locate and characterize the reactants, products and transition states on the PES. This is done by geometry-optimization algorithms, where an initial guess for the geometry is improved stepwise until the geometry of the stationary point is located with a specified accuracy. At every optimization step, the energy, the energy gradient and possibly the Hessian are calculated and used as a guide to find the next improved guess for the geometry. Generally, the geometry of a stable state is easier to find than that of a TS. This has two reasons: (i) Making a good guess for bond lengths, angles, etc. is easier with a stable state than a TS. (ii) The energy at points around the TS may be either higher or lower than at the TS, thus, it is more difficult to set up a search strategy. Typically, TS searches need to be performed with Newton methods; sometimes, dedicated methods are used for the optimization of a TS.[82-84]

Analyzing complicated reaction processes can be quite intricate in some cases. Even if a saddle point is found that has one imaginary frequency and is, thus, a TS one cannot always be sure that this TS is connected to the desired product(s) and reactant(s). In these cases one has to trace the reaction path from the TS to the reactant(s) and product(s). The reaction path in the PES is the steepest descent path from the TS down to both product and reactant sides. By following the path along the imaginary frequency in both directions, i.e. down the reaction coordinate, the minimum

energy pathway is found, and one sees which reactants and products are connected to the TS. This Intrinsic Reaction Coordinate (IRC)[85, 86] approach can be performed automatically and is quite robust. However, for stability, the reaction path has to be scanned with a small step width, which causes high computational effort. A cheaper alternative is the Quick Reaction Pathway (QRC) approach, which comprises two steps:[87] At first two structures are generated that correspond to a short step forwards and backwards along the imaginary-frequency mode, which is followed by an energy minimization of each of these two structures.

The relative energy of each stationary point determines its population by Maxwell-Boltzmann statistics according to:

$$\frac{N^i}{N^{tot}} = \frac{e^{-\left(\frac{E^i}{RT}\right)}}{Z} \qquad \text{Eq. 3}$$

where T is the temperature and R the ideal gas constant. This implies that not all stable structures on the PES really are observed: Only structures within a certain energy range above the energy of the global minimum show a noticeable population. At 298 K, population decreases with a factor of 10 for an energy difference of 1.4 kcal/mol.

The rate constant k of a reaction is mainly determined by its activation energy $\Delta G^{\ddagger}$. The enantiomeric ratio (e.r) of a stereospecific reaction will depend only in the difference in the calculated Gibbs free energies of the two possible TS and can be described with a reaction coordinate free energy diagram (Figure 6) and equation 2. Allow any prochiral reactant, R_R and P_S R, that give enantiomeric products, P_R and P_S, in a reaction under conditions of kinetic control.
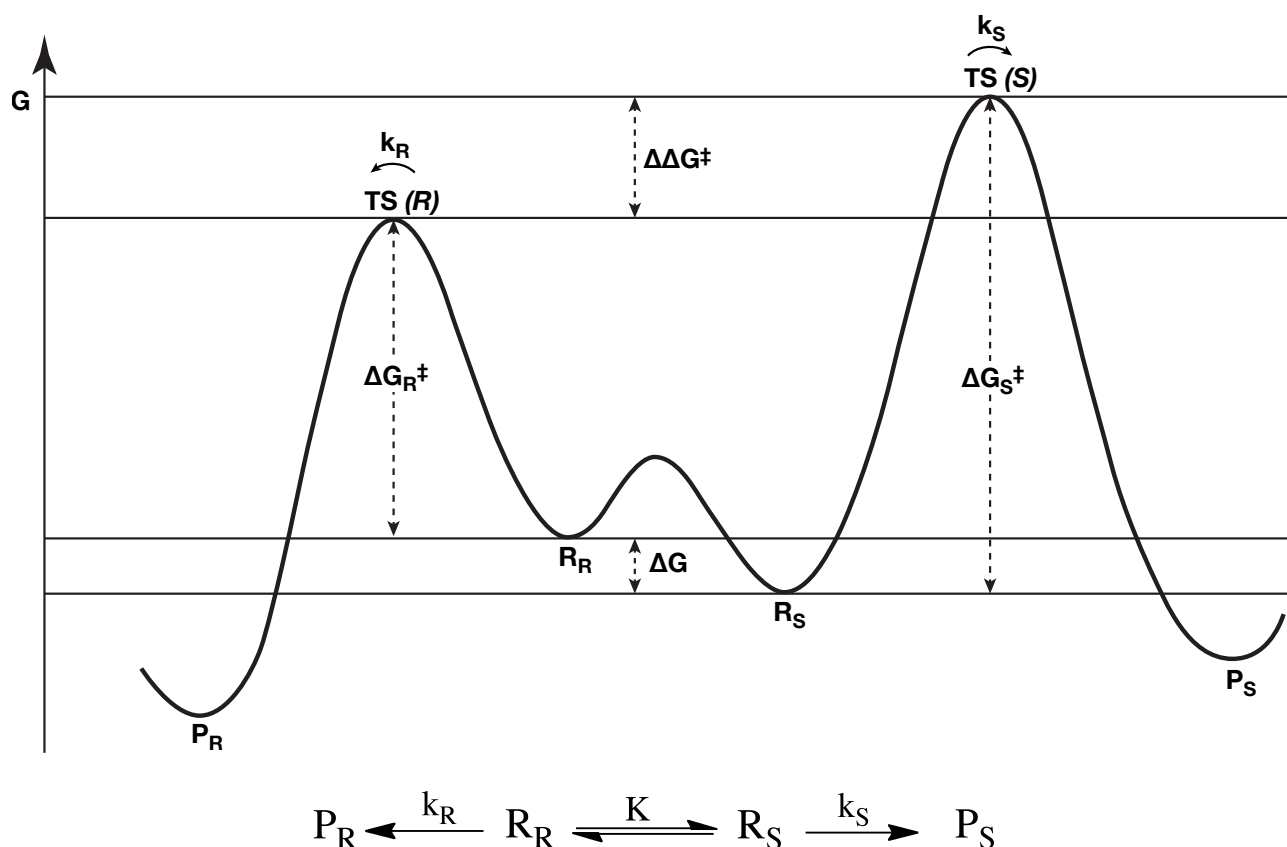
Figure 6. The reaction coordinate free energy diagram for an irreversible reaction.

The product ratio (R/S) is determined by the relative rates of reaction, and is given by Eq 4.

$$er = \frac{R}{S} = e^{-\frac{\Delta\Delta G^{\ddagger}}{RT}} \qquad \text{Eq. 4}$$

$$\Delta\Delta G^{\ddagger} = \Delta G_R^{\ddagger} - \Delta G_S^{\ddagger}$$

where $\Delta\Delta G^{\ddagger}$ is the standard change of reaction in Gibbs free energy and determines the product ratio. In this reaction, product P_S will be the minor product because $\Delta G_S^{\ddagger}$ is lower in energy.

1.7.3. Gas-phase vs solvation

Quantum-chemical calculations for an isolated molecule reflect the situation in gas phase (vacuum) and do not account for the influence of solvent molecules on energy and geometries etc[88]. An accurate description of solvated molecules needs to correct this shortcoming, which can be done in two essential ways:

1. Implicit solvation, or continuum solvation, where the solvent is not described as individual solvent molecules but as a continuous medium.[88]

2. Explicit solvation, where a number of solvent molecules are incorporated in the quantum chemical description.

Implicit solvation models are most suitable for non-specific solvation processes, where the solvent molecules move randomly around the solute molecule. In specific solvation processes, in contrast, one or a few solvent molecules bind to the solute at a certain position and in a well-defined orientation, for example, by coordinative bonds. Specific solvation processes are described most reasonably by explicit solvation. Typically, both specific and non-specific solvation processes occur around a solute; consequently, explicit and implicit solvation models are often combined: a complex consisting of the solute and one or more coordinated solvent molecules is surrounded by a continuum solvent model. A number of models have been developed for the description of implicit solvation. In the present work, the SM8 model by Truhlar et al. is used.[89-91]

1.7.4. Dispersion

Dispersion forces, also known as London forces, are pure correlation effects giving long-range attractive forces between separated molecules.[92, 93] They arise from interaction between electrons belonging to the densities of two otherwise not directly interacting atoms, molecules, or fragments. It has been well known for decades that commonly used DFT such as B3LYP functionals do not describe long-range dispersion interactions correctly,[94-96] which was originally discovered on rare gas dimers and later also on $(N_2)_2$ dimers and in base-pair stacking.[97] The structure of weakly bonded systems often depends on a delicate balance between intra- and intermolecular interactions, such as long-range dispersion/vdW forces and hydrogen bond. Dispersion effects are essential not only for a proper description of noncovalent interactions but also to reach a high level of chemical accuracy in the theoretical description reaction thermodynamics.[98]

There are currently different approaches to deal with the problem of dispersion, which includes:

- Explicitly non-local van der Waals functionals (vdW-DFs)[99-101]

- Standard-type XC functionals that have been reparameterized against suitable training sets to incorporate dispersion interaction[74, 98, 102]

- Dispersion-correcting atom-centered non-local one-electron potentials[103-105]

- Explicit (MM-like) energy terms covering the dispersion energy.[98, 106, 107]

Grimme has developed a sequence of methods according to the last of the four approaches, the so-called DFT-D methods. DFT-D2, an update of the earlier DFT-D1 method.[108] is today the most widely used DFT-D method. This method has recently been refined regarding higher accuracy, broader range of applicability, less empiricism. The most recent version of the method is called DFT-D3[108-110] and can be used as a general tool for the computation of the dispersion energy and for optimization of molecules and solids of any kind.

2. RESULTS AND DISCUSSION

2.1. Synthesis

The aim in this part of the project was to synthesize alkylated N,P-ligands from amino acids via reduction to an alcohol and substitution to the N,P-ligand (Scheme 22).
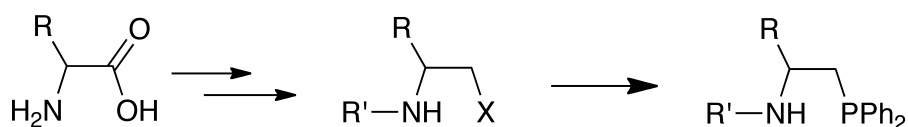
Scheme 22. The general procedure for synthesizing N,P-ligands. R= *i*-Pr, Ph, Bn. × = OH, OSO and OSO$_2$.

2.1.1. Phosphination

The phosphination reaction was found to be more difficult to perform than anticipated, and therefore several known methods were explored. Firstly, the nucleophilic addition of KPPh$_2$ or HPPh$_2$ to the Boc protected and OMs-activated *β*-aminoalcohols that has been reported by Anderson et al[34] proved problematic due to *N*-deprotonation and rapid formation of aziridine and oxazolidinone by the competing S$_N$2 intramolecular ring closure.[111] Phosphination using iodine as the leaving group as well as deprotonation of a borane complex that have previously been reported proved to give mostly by-products. Since all these methods did not give satisfactory yields the nitrogen was protonated. The protonation itself was easily performed but the following phosphination turned out to be very unpredictable. In some cases it was possible to obtain the desired aminophosphine but only in low yields and in small scale. During scale-up the yields dropped considerably yielding aziridine and complex product mixtures that could not be purified to satisfaction. Different protecting groups for the acylated nitrogen were explored (Fmoc, Boc, isopropyl) to avoid N-deprotonation but neither of them were successful.

Although several methods for the construction of chiral β-aminophosphines have been reported in the literature none could be employed with success to provide the target chiral N,P ligands in acceptable yields and purity. Therefore, the route via cyclic sulfamidate was used, which involves a simultaneous N-protection and O-activation, thus avoiding the formation of aziridine, oxazolidinone as well as reducing the need for protection/deprotection (Figure 7).
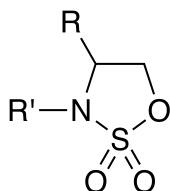

Figure 7. The structure of sulfamidate used in this thesis.

The phosphination reactions using cyclic sulfamidate were found to be very efficient and after some optimization of previously developed methods very good yields were obtained, with high purity and very low amounts of oxidized product. In addition, the resulting aminophosphines turned out to be less air sensitive than expected.

2.1.2.   Synthesis of N, P-ligands via Boc-protected amine

The reduction of the amino acids resulted in their respective amino alcohols in excellent yields (Scheme 23).[112] The following protection of the free amino alcohol was performed with Boc-anhydride and Et$_3$N in EtOAc. Mesylation of the Boc-protected amino alcohol was performed with methanesulfonyl chloride, Et$_3$N in CH$_2$Cl$_2$, and good yields were obtained.
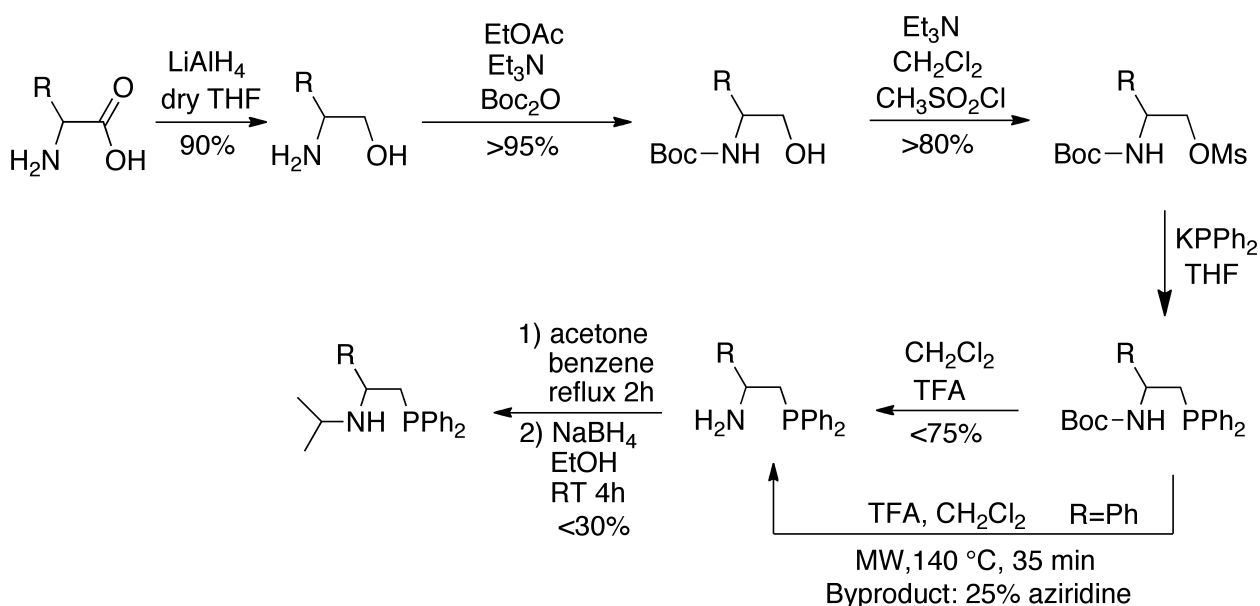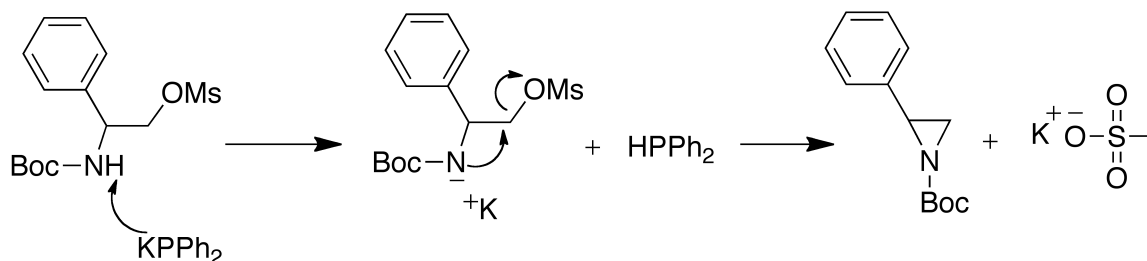

Scheme 23. Synthesis of N,P-ligands via Boc-protected amine. R=i-Pr, Ph, Bn.

The addition of KPPh$_2$ to the Boc-protected amine and mesylated alcohol in THF at -78 °C resulted in the free aminophosphine in low yield, since many impurites were formed. In this reaction, cyclization can occur and aziridine and/or oxazolidinone can be formed as the major products (Scheme 24).[113, 114]
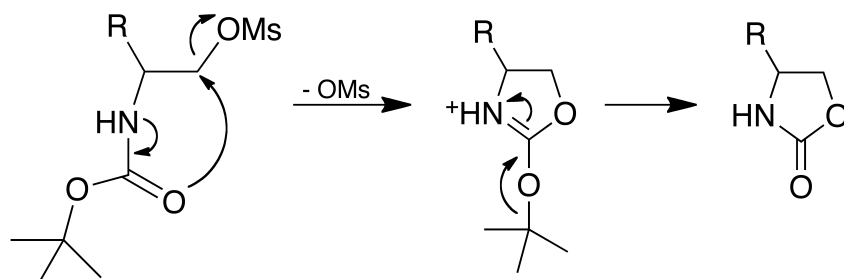

Scheme 24. Oxazolidinone formation from ring closure of Boc-protected and mesylated aminoacid.

The cyclization can occur by intramolecular displacement of the mesyl group with the carbamate carbonyl for the oxazolidinone and the amine for the aziridine (Scheme 24 , Scheme 25).[113-115] Other phosphination methods were screened, but always resulted in low yield (Scheme 26).


Scheme 25. Intramolecular aziridination.
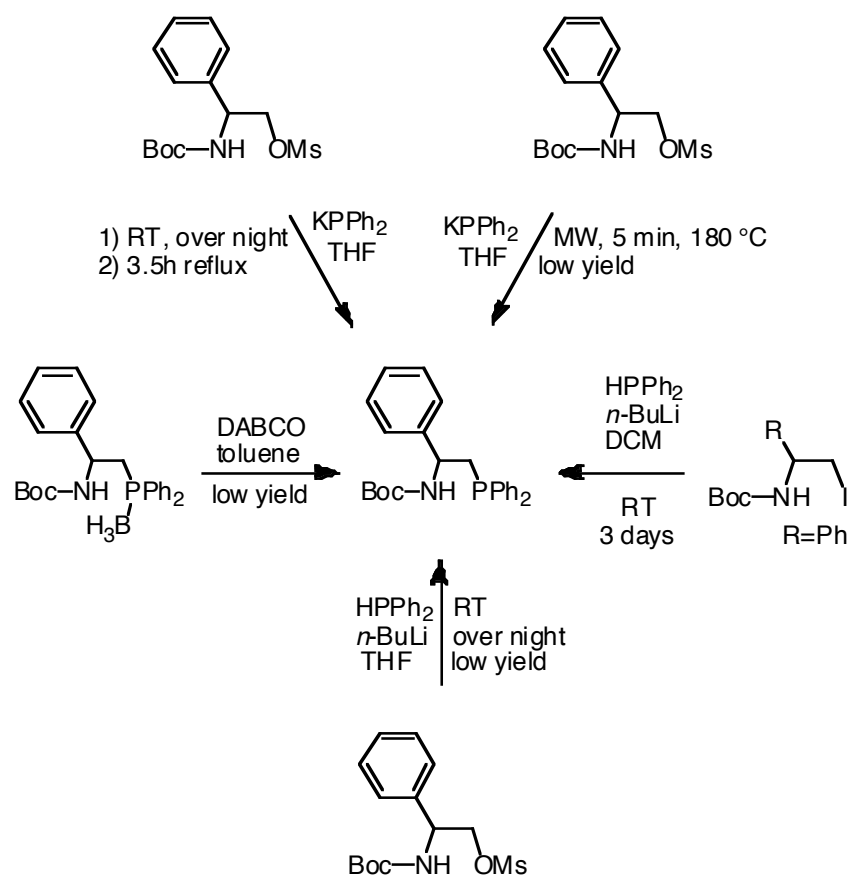
Scheme 26. Different methods previously used for the synthesis of N,P-ligand.

Upon deprotection of the Boc-group with TFA in CH$_2$Cl$_2$ at RT the free aminophosphine was obtained in moderate to good yields, although with impurities. The deprotection of the Boc group was also performed using microwave irradiation (140 °C, 35 min) and resulted in the desired product and some impurities, where ca 25% was aziridine (Scheme 26). To obtain the final N,P-ligand, reductive amination was performed by refluxing the free aminophosphine with NaBH$_4$ in acetone and benzene using. A high yield was obtained with with *(R)*-phenylglycine (90%) as the amino acid and lower with L-valine (37%). In general, a substantial formation of oxide products was observed. Previous published results show similar yields.[116]

In the search for conditions avoiding the undesired cyclization, the *N*-alkylated amino alcohol was formylated with ethyl formate by microwave irradiation, to prevent cyclization. *N*-(2-hydroxy-1-phenylethyl)formamide was obtained as the main product in low yield (Scheme 27).
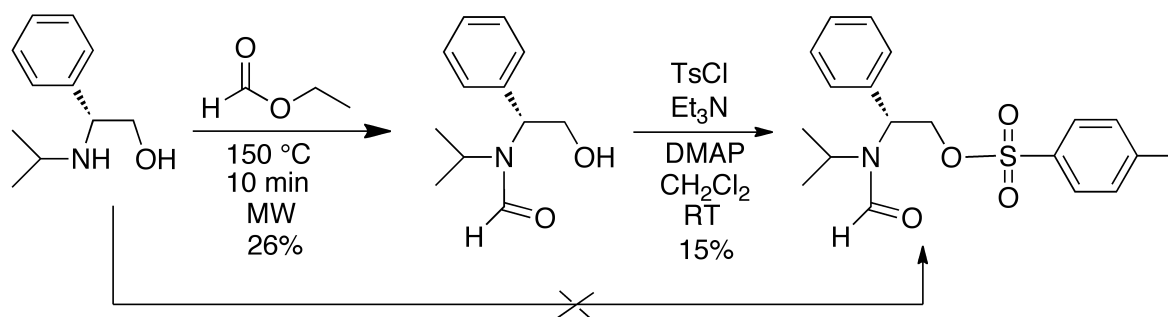
**Scheme 27.** Acylation and tosylation of the secondary amino alcohol.

Tosylation of the acylated amino alcohol was only successful with purified TsCl using a Soxlet and low yield was obtained after flash chromatography. Tosylation of the *N*-alkylated amino alcohol was not successful. However, with mesylation of Boc-protected amino alcohol a higher yield was obtained. Phosphination with PPh$_2$BH$_3$ resulted in the desired borane complex in 60% yield (Scheme 28). The following deprotection of the borane with DABCO in refluxing toluene did only give traces of the desired product.
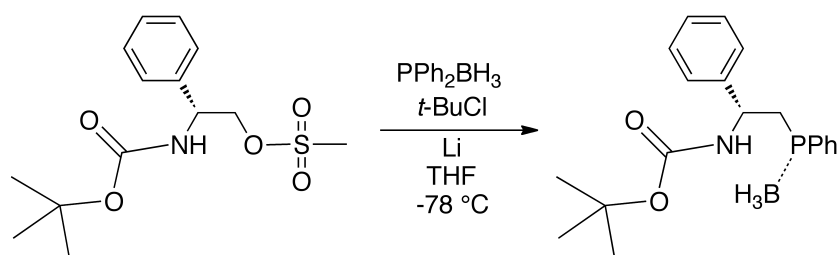
Scheme 28. The borane complex from the mesylate.

2.1.3.   Synthesis of N, P-ligands via bromide-salt

In the search of finding a reliable method that did not produce the by-products received earlier during the phosphination, it was attempted to deprotect the Boc-group with a solution of HBr in HOAc (45% w/w), resulting in a bromide salt (Scheme 29).[33]
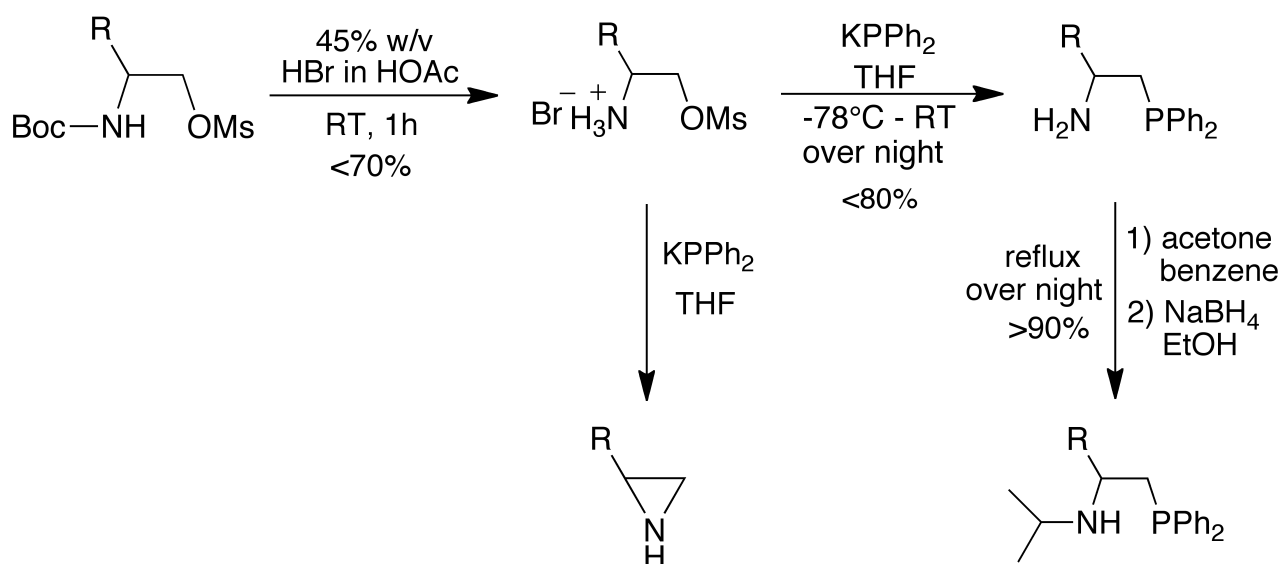
Scheme 29. Synthesis of N,P-ligands via ammonium salt. R= *i*-Pr, Ph, Bn

The bromide salt was obtained in moderate to good yields (50-70%), depending on the amino acid. A lower yield was obtained with L-valine as the amino acid, compared to *(R)*-phenylglycine. However, this method was not reproducible enough and aziridine was often formed (Scheme 30).
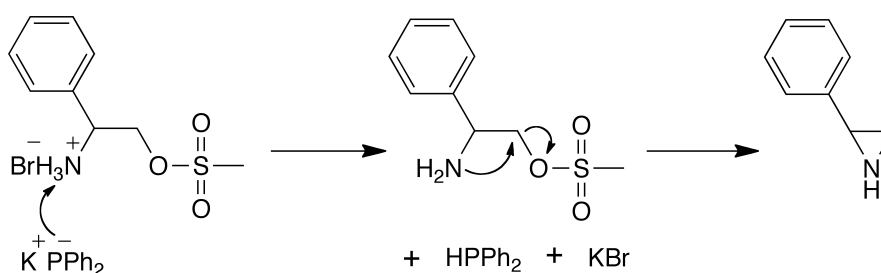

Scheme 30. Formation of aziridine.

The free aminophosphine was obtained by addition of KPPh$_2$ in THF at -78 °C. The reaction also resulted in a considerable amount of oxidized aminophosphine, and this method was therefore abandoned .

2.1.4. Synthesis of N,N- and N,P-ligands via sulfamidate (Paper I)

The use of various protecting groups to the primary amino alcohol was problematic and the synthesis of the desired N,P-ligands proved to be very challenging. By using the cyclic sulfamidate the amine was both protected and the alcohol made a good leaving group. This decreased the number of steps in the synthesis to the final N,P-ligand and avoided the by-products from the earlier methods (Scheme 31). In addition, this made it feasable for the alkylation to be performed in the beginning and the crucial phosphination in the last step.
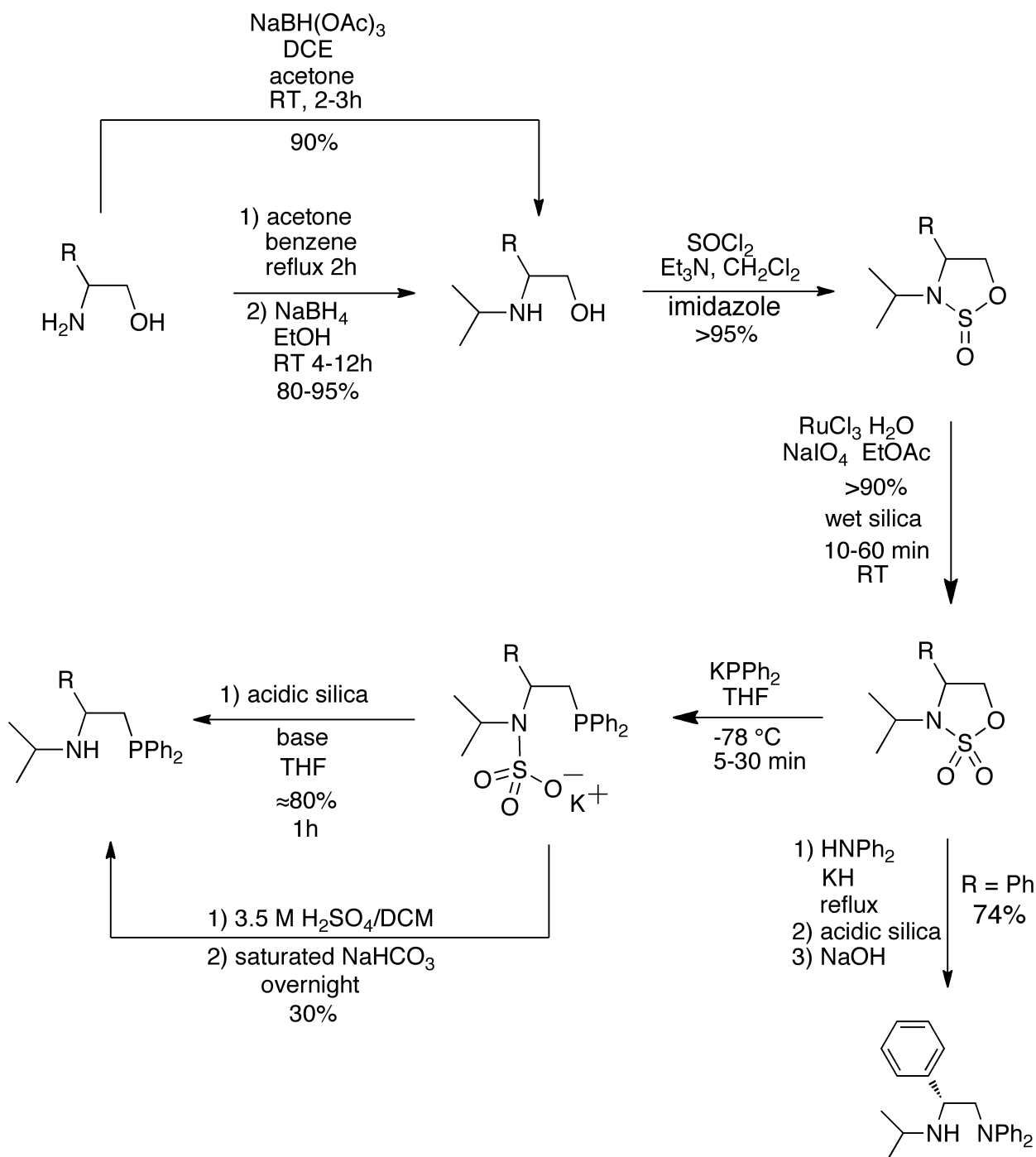
Scheme 31. New synthetic route to N,N- and N,P-ligands via sulfamidate.

Reductive amination of the free amino alcohol resulted in almost quantitative yield. Acetone and NaBH(OAc)₃ in DCE at RT was found to yield the alkylated amine in high yields and in considerably shorter time.[117] The alkylated aminoalcohol was then transformed into a mixture of diastereomeric five membered sulfamidites, using thionyl chloride, imidazole and Et₃N in dry CH₂Cl₂. Depending on the amino acid and the amount of amino alcohol the cyclization to sulfamidite was completed after 30 min-4 h in moderate to excellent yields. One way of improving

the yield would be by reversing the addition, i.e. adding the amine to the thionyl chloride.[113] In addition, the sulfamidite is very sensitive to hydrolysis. Hence, when purifying the sulfamidite with Kugelrohr distillation it was hydrolyzed to the amino alcohol.

The biphasic system in the standard version for oxidizing the sulfamidite to sulfamidate proved to be very unreliable. Instead, efficient transformation of sulfamidite to sulfamidate was achieved via sodium periodate oxidation, catalyzed by $RuCl_3$ in the presence of silica gel, water and EtOAc.[118] The success of this reaction required a special procedure. A solution of RuO_4 was first generated in situ by the addition of $RuCl_3$ in water followed by the addition of $NaIO_4$. This RuO_4 solution was added dropwise to silica gel, followed by stirring until a homogenous and free flowing powder. was obtained. This silica is referred to as "wet silica", since it contains water. EtOAc was added to the silica-RuO_4 before the sulfamidite, dissolved in EtOAc, was added dropwise. Slow addition of the sulfamidite to the slurry of wet silica is important to prevent exotherm reaction, which probably gives β-elimination. It was found that the use of EtOAc as solvent was crucial in this reaction and resulted in best isolated yield. The use of other solvent systems (CH_3CN/H_2O, $CH_2Cl_2/EtOAc/H_2O$ or $CCl_4/CH_3CN/H_2O$) only resulted in significantly lower isolated yields of the sulfamidate (45-78%).[119] Even in the case when CH_2Cl_2 was used to dissolve the sulfamidite upon addition to the EtOAc/wet silica slurry, a lower yield was again obtained.

The reaction was followed by a workup by simply filtrating the solids through a short pad of silica. Due to the use of wet silica a drastic augmentation in yield was observed and the reaction time decreased to 10-60 min, making the oxidation reproducible and very attractive. The short reaction time is most likely a result of the inhomogeneous reaction mixture with its high surface to volume ratio (SA:V) which is important to avoid the formation of by-products due to over oxidation and cyclization. Using wet silica instead of $RuCl_3/H_2O/NaIO_4$ in EtOAc improved the reaction time and purity considerably. Oxidation in the microwave using wet silica, $NaOI_4$ and OsEnCat as the catalyst in EtOAc for 10 minutes resulted in a very clean desired product, according to TLC. In addition, it appears crucial that the oxidation in the microwave is performed with high temperature and short reaction time rather than long reaction time and low temperature, in order to receive the desired product. Oxidizing sulfamidite with OsEnCat at RT did not work at shorter reaction times. However, when the reaction was run over night the oxidation worked. The yield was decreased when CH_2Cl_2 was used to dissolve the starting material.

The oxidation seems to be very general since various 5- and 6-membered rings have been successfully oxidized using this method. Huibers et al oxidized various sulfites to sulfates in a 3-step sulfation called the sulfitylation-oxidation protocol.[120] The yields of the sulfites were low, probably due to the concomitant formation of the β-D- symmetrical sulfite diesters formed from the in situ alkyl chlorosulfite. However, the following oxidation with $RuCl_3/H_2O/NaIO_4$ in $CH_2Cl_2/MeOH$ proceeded fast and in excellent yields. This protocol was also used by Al-Horani and Desai when using various secondary alcohols, diols, sugars and aromatic alcohols as the starting material, which also proceeded clean and in high yields.[121]

Direct cyclization of the acyclic, alkylated amino alcohols with sulfuryl chloride to sulfamidate was not very successful and did not form the desired sulfamidate, but many impurities.[122] The flexible, acyclic amino acids easily formed aziridine with sulfuryl chloride in a two-step route and is even a better route to aziridines than the well-established Okawa two-step procedure (Scheme 32).[123]
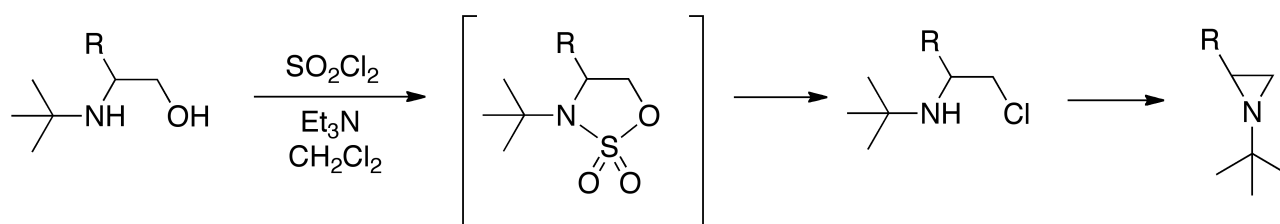

Scheme 32. Aziridine formation in the Okawa two-step procedure.

The phosphination proceeds through an efficient and fast one-pot reaction with $KPPh_2$ in THF and was in general very rapid and completed in about 5 minutes. There are different representative systems for the following hydrolysis of the formed sulfamic acid, i.e. the $N-SO_3H$ group. One alternative is to evaporate the reaction mixture of the sulfamic acid and then perform the hydrolysis in a biphasic system of CH_2Cl_2/HCl (0.1 M, 1:1) over night, followed by deprotonation of the protonated amine with saturated $NaHCO_3$ to give the desired product. Here, the biphasic system of H_2SO_4/CH_2Cl_2, without evaporating the sulfamic acid, was used at first. However, this reaction produced a lot of oxidized product and previous work had shown that to achieve the desired chemoselectivity, as low an amount of water as possible is crucial. Therefore, the goal was to find a more efficient way for the hydrolysis.[124]

Inspired by the good result with the silica mediated oxidation the use of silica in the hydrolysis was also explored. H_2SO_4 (2 M) was therefore adsorbed on silica gel (SiO_2), still giving a biphasic

system but with a much higher SA:V ratio during the hydrolysis. This increased the rate of the hydrolysis of the sulfamic acid, which normally is slow in acidic media. Therefore, stirring the sulfamic acid in 20% aqueous H_2SO_4 (pH 1) adsorbed on SiO_2 for 1 h, followed by basic workup with saturated $NaHCO_3$ or 2 M NaOH (pH 10), filtration and column chromatography, where no oxygen free conditions are necessary, obtained the desired aminophosphine in excellent yield and purity. The use of silica proved to be very successful and not only did the silica shorten the reaction time by two days compared to the original method, but impurities are probably also bonded to the silica and thereby making the desired product less impure. Using this method the aminophosphine was produced from the sulfamidate in about 2 h and proved to be very reproducible and reliable concerning the yield. It could successfully be scaled up to >5 g with no loss in yield or purity and gives a general and simple route to chiral N,P-ligands from cheap and readily available amino acids. In addition, the stability of the aminophosphines were tested by leaving a sample in the hood in open air and after six weeks no oxidation of the phosphorus was observed in ^{31}P-NMR. However, the aminophosphines decomposed in DMSO which is consistent with previously published findings.[125]

Methylated N,P-ligands were also synthesized in order to test them in the butylation reaction. Methylating the free amino alcohol of phenylalanine as well as *(R)*-phenylglycine were carried out with formaldehyde in $NaBH(OAc)_3$ and obtained the *N*-alkylated amino alcohol in good yields. (Scheme 33). In addition, to investigate the versatility of sulfamidate, N,N-ligands were also synthesized, using the same method as for the *N*-iPr-ligands.
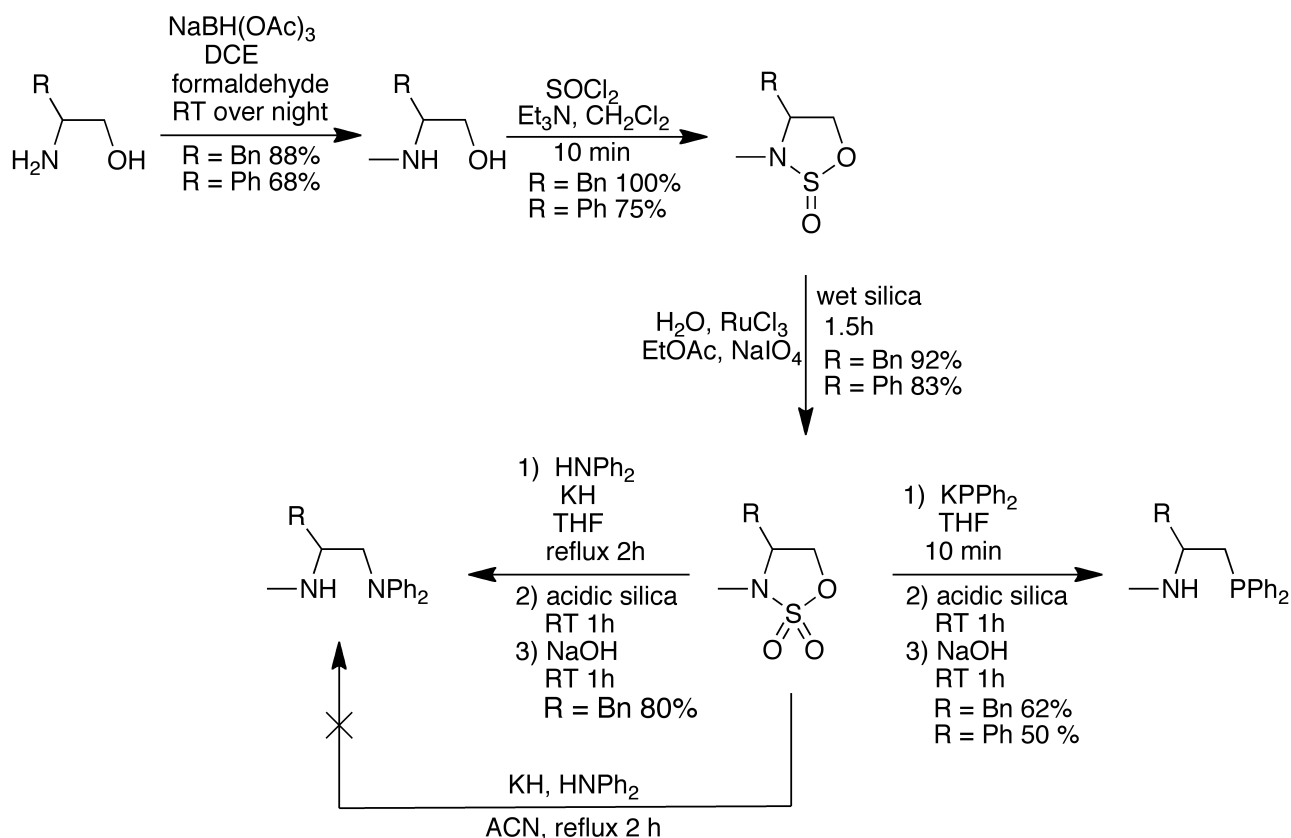
**Scheme 33.** Synthesis of methylated N,N- and N,P-ligand via sulfamidate of phenylalanine. R= *i*-Pr, Ph, Bn.

The amination of sulfamidate to the diamine proceeds in a one-pot reaction with $HNPh_2$ and KH in THF under reflux. In the case of *(R)*-phenylglycine the synthesis of methylated N,P-ligand was performed with the same procedure as for the N,P-ligands, with *i*-Pr on nitrogen (Scheme 33). In addition, when KH was used as base under reflux the yield improved and showed that the sulfamic acid is able to solvolyze in situ during the reflux without adding any mineral acid or acidic silica and is probably due to the proton-rich reaction mixture.[126] Refluxing with KH followed by addition of acidic silica to hydrolyze the sulfamic acid increased the yield considerably (74%) (Scheme 34).
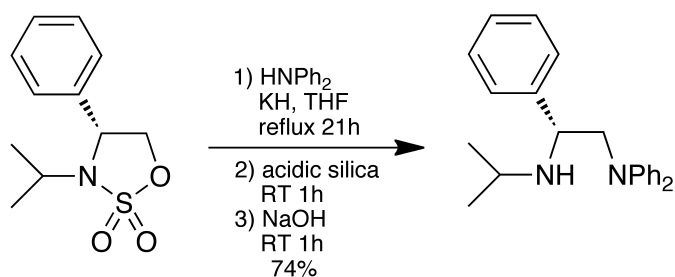
Scheme 34. Ring opening of sulfamidate to the N,N-ligand.

To investigate the applicability of sulfamidate further aminophosphines were synthesized. Reduction of L-proline was performed with $LiAlH_4$ in THF to give quantitative yield of the
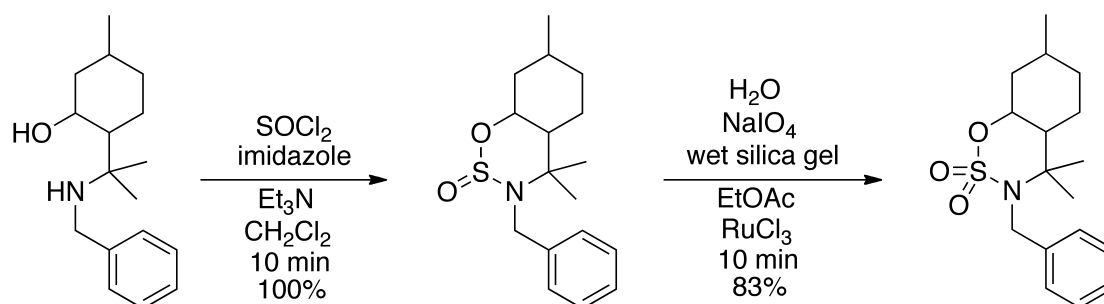
aminoalcohol (Scheme 35)[112]. The sulfamidite was then succesfully synthesized in thionyl chloride, imidazole, Et$_3$N and dry CH$_2$Cl$_2$ to give a mixture of isomers in 1:2 to 1:2.8 ratio in good yield (68-97%). In benzene, these ratios of the isomers are 3:1.[125] It was difficult avoiding triethylamine salt in the resulting product. Oxidation of the sulfamidite to sulfamidate was performed by adding RuCl$_3$ in water followed by the addition of NaIO$_4$ to give a yellow solution of RuO$_4$. The RuO$_4$ solution was then added dropwise to dry silica gel during stirring, until a homogenous and free flowing powder had formed. EtOAc was added to this silica-RuO$_4$ powder and sulfamidate dissolved in EtOAc was added dropwise at 0 °C. The yields were moderate to good (39-71%), which can be due to the fact that during the concentration of the sulfamidate it was found to have a very low boiling point and evaporates during concentration in vacuo at 40°C.[127, 128]
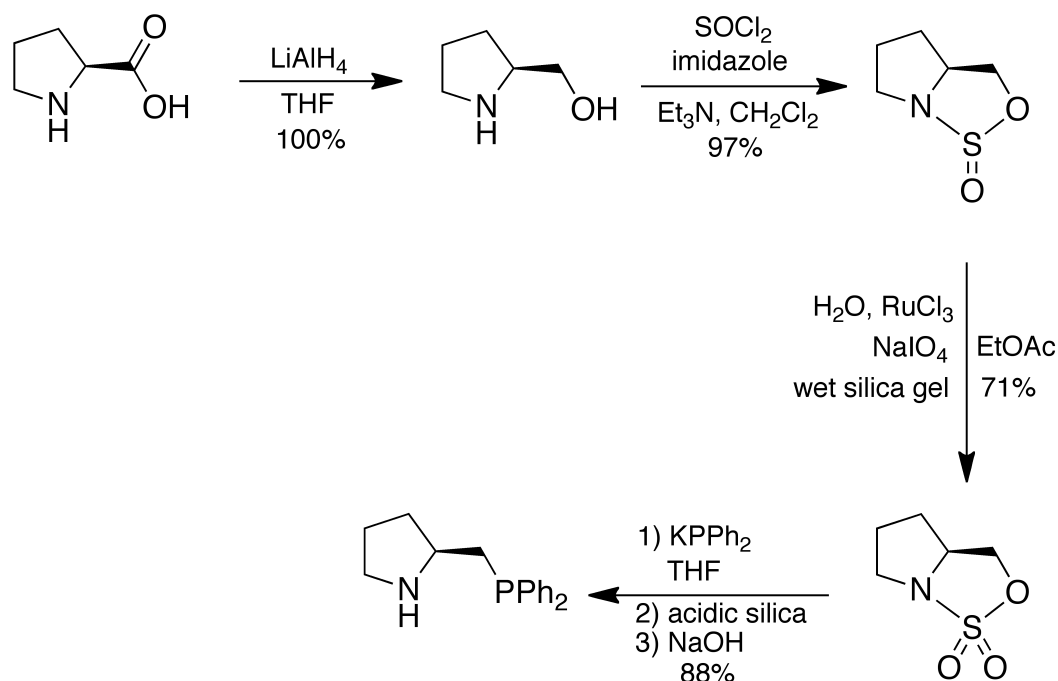
Scheme 35. Synthesis of the N,P-ligand of L-proline.

Direct cyclization of L-prolinol using sulfuryl chloride, Et$_3$N in dry CH$_2$Cl$_2$ at 0 °C was successful in 72% yield.[129] This is probably due to its cyclic form, making it more rigid than the acyclic amino acids in this thesis.[122] However, this reaction contained more impurities than the cyclization via sulfamidite. The following S$_N$2 reaction with KPPh$_2$ in THF, followed by hydrolysis and reduction was not as simple as with the other amino acids and seemed in general to be somewhat more sensitive. Some oxidized product was formed and the yields were not reproducable. However, this method via sulfamidite and sulfamidate offers an easy and better way to the free aminophosphine of L-proline than previous methods.[116]

To further investigate the versatility of sulfamidate and its applicability on different chiral amino alcohols we tested an amino alcohol more sterically hindered compared to the previous (Scheme 36).

Scheme 36. Synthesis of a sulfamidate from a sterically hindered amino alcohol.

The amino alcohol was converted to sulfamidite with thionyl chloride, imidazole and Et$_3$N in CH$_2$Cl$_2$ at 0 °C. The reaction was completed after only 10 min and afforded the sulfamidite in a very clean reaction in quantitative yield. The following oxidation with RuCl$_3$/NaIO$_4$/H$_2$O adsorbed on wet silica was also very clean and again completed after 10 min to give in very good yield (83%). The synthesis of the sulfamidate from the amino alcohol could probably also have been achieved by direct synthesis to sulfamidate with sulfuryl chloride, due to the rigid structure of this amino alcohol.

2.2. Structural studies (Paper II, III)

2.2.1. Experimental NMR studies

The aim of the solution studies using low temperature ^{6}Li-NMR, typically at -80 °C, was to evaluate the dynamics and aggregates that the aminophospines **1a-e** can form with *n*-BuLi, depending on solvent and substituents in the amino acid backbone (Figure 8).
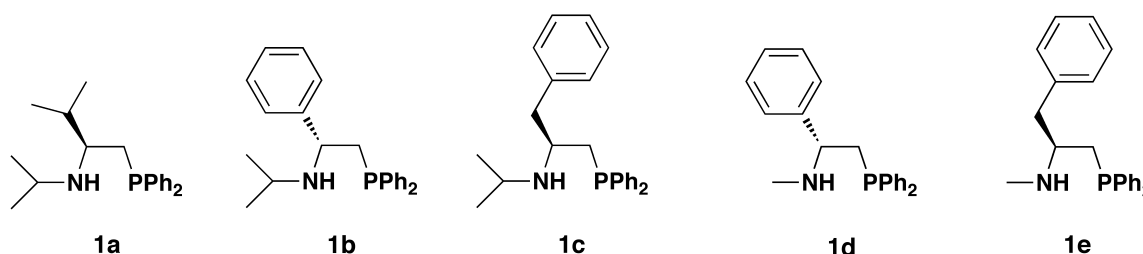

Figure 8. The chiral aminophosphines used in the experimental NMR studies

NMR-studies on N,O- and N,S-ligands have previously been performed in our group. A pronounced difference in the order of aggregates, when going from coordinating to non-coordinating solvents,

was observed. In non-coordinating solvents, such as toluene, with an excess n-BuLi, mixed trimers, cyclic trimers and ladder complexes are formed.[130-132] Among these aggregates the cylic trimer is the most stable complex in toluene.[132] In coordinating solvents, such as ethers, the chiral lithium amides may also exist as dimers with non-equivalent or equivalent lithiums.[132] When adding Et$_2$O to the toluene solution of the mixed trimer, a dimer with non-equivalent lithium, a mixed complex and free *n*-BuLi are formed.[133] In coordinating solvents, such as Et$_2$O or THF, other aggregates are formed. In a mixture of a aminophosphine with one equivalent of *n*-BuLi, a dimer with non-equivalent lithiums is formed.[13] In a 1:1 ratio of the chiral lithium amide and *n*-BuLi in coordinating solvents a 1:1 mixed complex is formed.[16, 61] Even though the complexes of the N,O- and N,S-ligands are similar there are differences in the Li-O and Li-S interactions, where the latter bond is weaker, which is one of the features that affects the reactivity. Continuing this work it was obvious to proceed with NMR experiments with the synthesized chiral aminophosphines.

For one of the aminophosphines ^{31}P-NMR, COSY, HSQC and HMBC were performed.[57] For the N,P-ligands ^{1}H-, ^{13}C- and ^{6}Li-NMR were performed at low temperature. The ^{6}Li-NMR studies were performed at -80 °C in NMR tubes, equipped with an airtight Teflon valve system, which allows sequential addition via gas-tight syringes under nitrogen atmosphere. Dried, deuterated solvents and *n*-Bu^{6}Li were used in the NMR studies described in this thesis.

Although the Li-P bond is expected to be even weaker interaction, compared to Li-O and Li-S bonds, it was found that N,P-ligands aggregate in a similar way, in both coordinating and non-coordinating solvents (Figure 9).
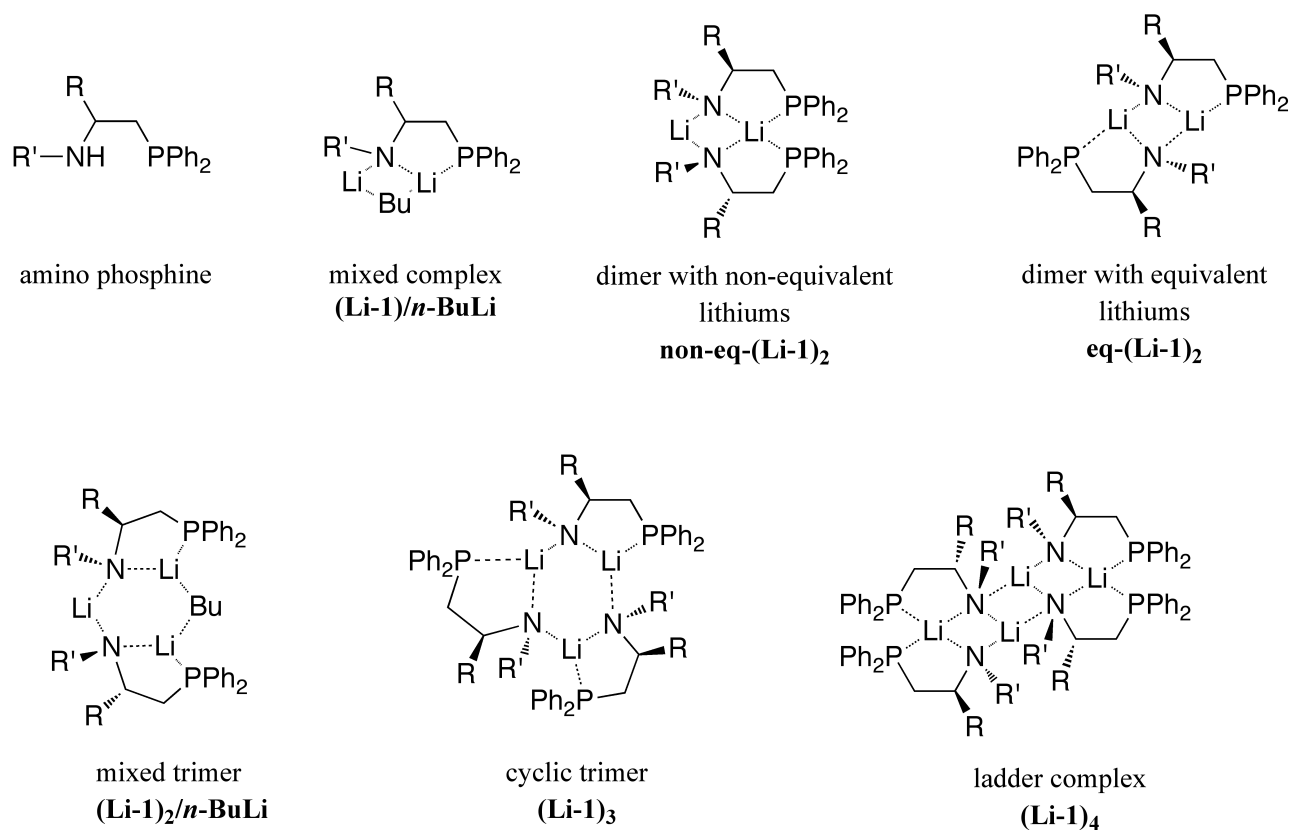
Figure 9. The aminophosphines and complexes that can form in the addition of *n*-BuLi to various amino phosphines. R' = Me, *i*-Pr and R = Bn, Ph, *i*-Pr. Solvent is excluded for clarity.

2.2.1.1. Non-coordinating solvents

In toluene, a non-coordinating solvent, high order N,P aggregates, such as cyclic and mixed trimers **(Li-1)₃** and ladder-complexes **(Li-1)₄**, are formed (Figure 10).[134-136] Hence, in the addition of 1.5 eqivalent of *n*-BuLi to the aminophosphine **1a** (0.3 M) in toluene a mixed trimer is formed. In ^{6}Li-NMR this is observed as a doublet at δ 2.25 ppm, ($^1J(^6Li,^{31}P)$=16 Hz) and singlet at δ 1.80 ppm in a 2:1 ratio, indicating that only one species is formed (Figure 10). In ^{13}C and ^{1}H NMR only one set of signals is observed.
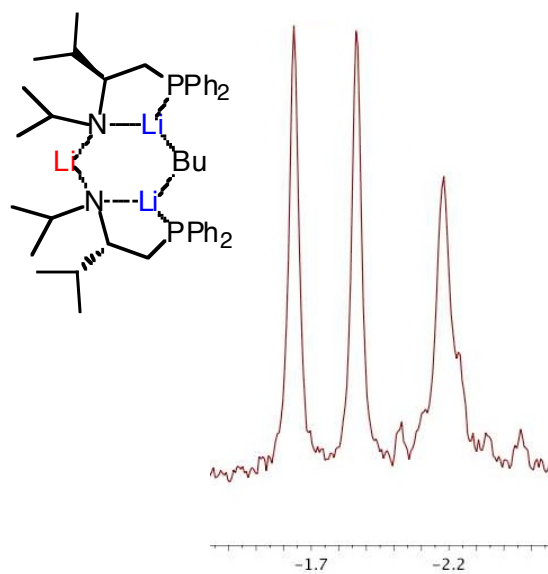
Figure 10. ^{6}Li NMR of the mixed trimer in toluene at -80 °C.

Adding more of **1a** to the toluene solution results in two more species (Figure 11). The triplet at δ -2.16 ($^1J(^6Li,^{31}P)$=15.5 Hz) and singlet at δ -3.39 are assigned to a ladder complex and the doublet at δ -2.21 ($^1J(^6Li,^{31}P)$=18.4 Hz) to a cyclic trimer. The singlet of the mixed trimer is overlapping the triplet of the ladder complex, hence the high intensity of the central peak of the triplet.
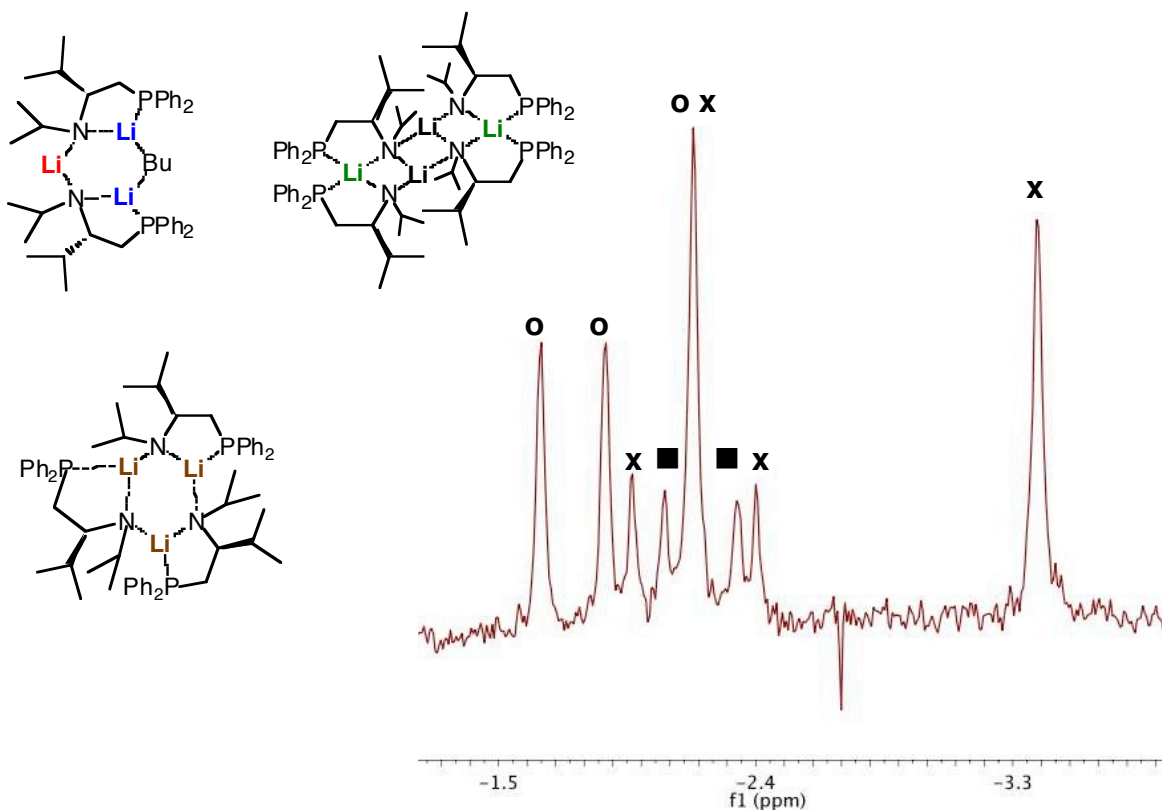

Figure 11. ^{6}Li-NMR with a mixture of the mixed trimer (**o**), the cyclic trimer (**■**) and the ladder complex (**x**).

Further addition of **1a** results in disappearance of the remaining mixed trimer and only the ladder and cyclic trimer are observed in the ^{6}Li-NMR spectra (Figure 12). Now the intensities of the triplett at δ 2.13 also show the expected 1:2:1 ratio.
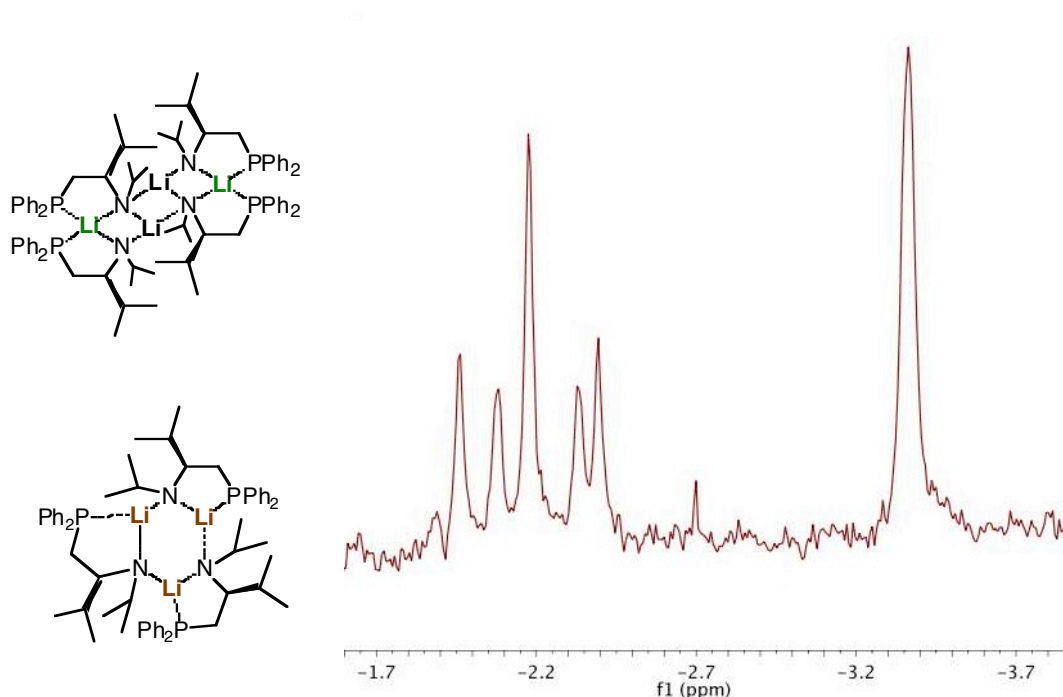

Figure 12. The remaining trimer and ladder complex after adding additional **1a**.

When Et$_2$O is added to the solution of **1a** in toluene a Et$_2$O-solvated **non-eq-(Li-1a)$_2$** is obtained, according to ^{6}Li-NMR (Figure 13).
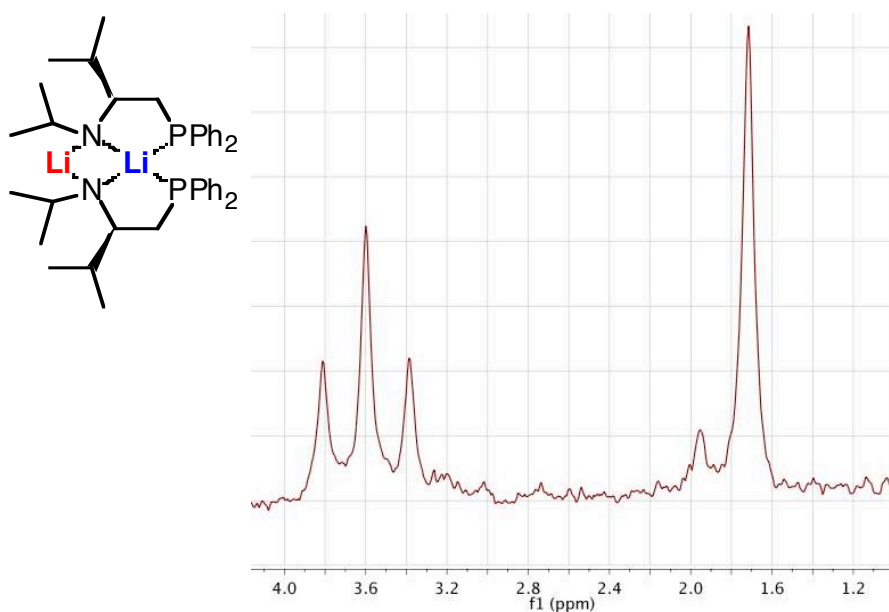

Figure 13. The triplet and singlet in ^{6}Li-NMR indicating a dimer with non-equivalent lithiums.

2.2.1.2. Coordinating solvents

In Et_2O and THF, addition of one eq. n-BuLi to aminophosphine ligands produces dimers of two types; a dimer with equivalent lithiums, **eq-(Li-1)$_2$**, or a dimer with non-equivalent lithiums, **non-eq-(Li-1)$_2$**.[16] In a mixture of one eq. of n-BuLi and **1a** in Et_2O the dimer of **non-eq-(Li-1a)$_2$** is formed, which is revealed in the ^{6}Li-NMR by a triplet at δ 3.8 ppm ($^1J(^6Li,^{31}P)$=13.2 Hz) and a singlet at δ 2.2, in a 1:1 intensity ratio (Figure 14).
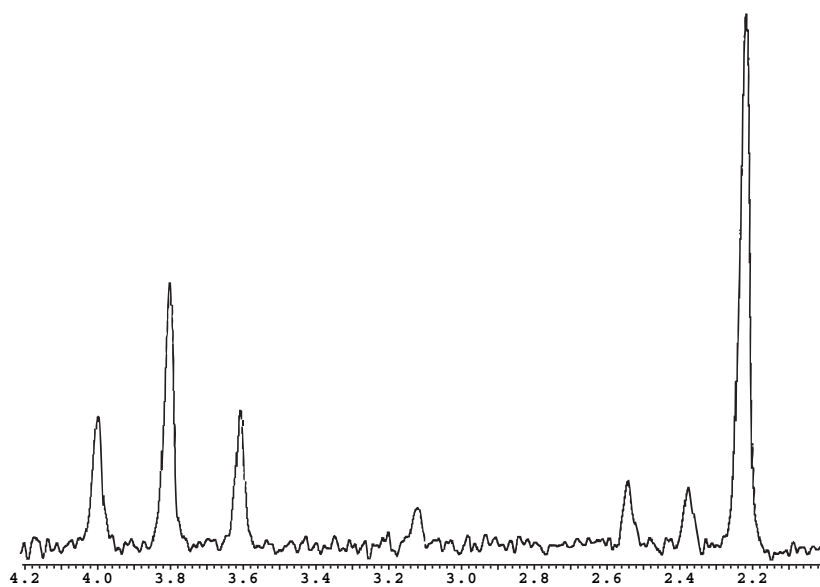

Figure 14. ^{6}Li-NMR of **non-eq-(Li-1a)$_2$** in Et_2O.

Upon addition of n-BuLi the dimer disappears and the mixed complex, **n-BuLi/Li-1a**, is formed. The ^{6}Li-NMR shows a singlet at δ 3.4 ppm and a doublet at δ 3.05 ppm ($^1J(^6Li,^{31}P)$=11.0 Hz) in a 1:1 ratio (Figure 15). Excess of n-BuLi gives rise to a signal at δ 1.9 ppm, corresponding to free n-BuLi, that is **(n-BuLi)$_4$**.
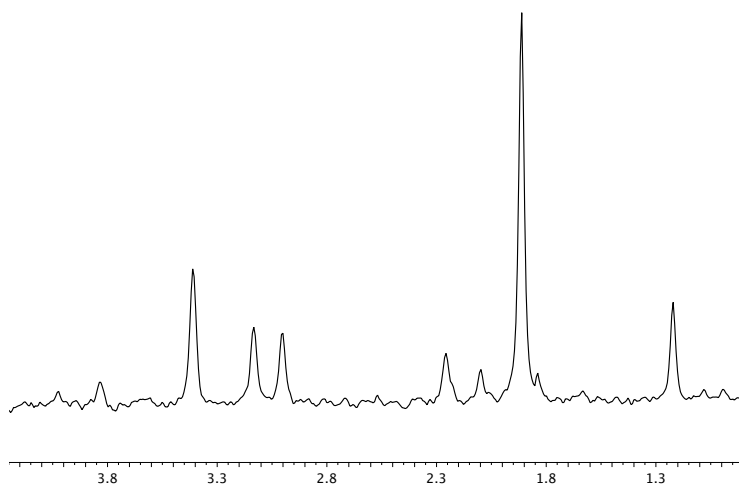

Figure 15. A mixed complex formed when adding n-BuLi to **1a**.

The solvent dependence was tested by titration of THF into an approximately equimolar mixture of **non-eq-(Li-1a)₂** and **n-BuLi/Li-1a** in Et₂O (Scheme 37). In ^{6}Li-NMR this mixture is observed as a triplet at δ 3.84 ((^1J(^{6}Li,^{31}P)=37.5 Hz), a singlet at δ 3.42 , another singlet at δ 2.25, and a doublet at δ 3.08 (^1J(^{6}Li,^{31}P)= 6.6 Hz) (Figure 16). THF was titrated into this mixture. At ca 10% THF the **n-BuLi/Li-1a** is THF-solvated and its singlet (δ 3.1 ppm) is shifted upfield and the doublet (δ 3.24 ppm, (^1J(^{6}Li,^{31}P)=5.9 Hz) is shifted slightly downfield. Both signals for **non-eq-(Li-1a)₂** remains constant. At ca 20% THF the singlet of **n-BuLi/Li-1a** again shifts 0.3 ppm upfield to δ 2.80 ppm , while the doublet (δ 3.24 ppm, (^1J(^{6}Li,^{31}P)=5.9 Hz) still remains constant (Figure 16). Hence, only **n-BuLi/Li-1a** is strongly affected by the addition of THF whereas the effect on **non-eq-(Li-1a)₂** is only marginal.
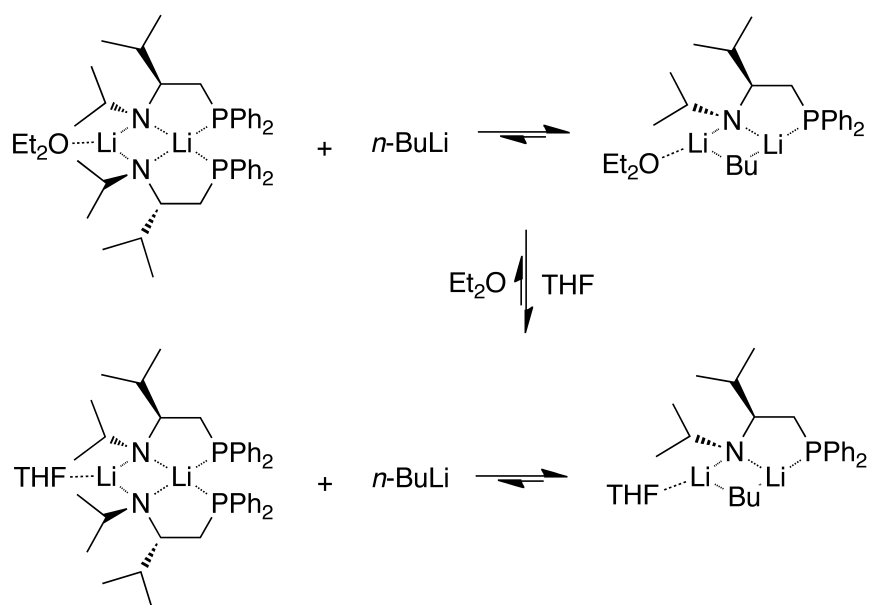
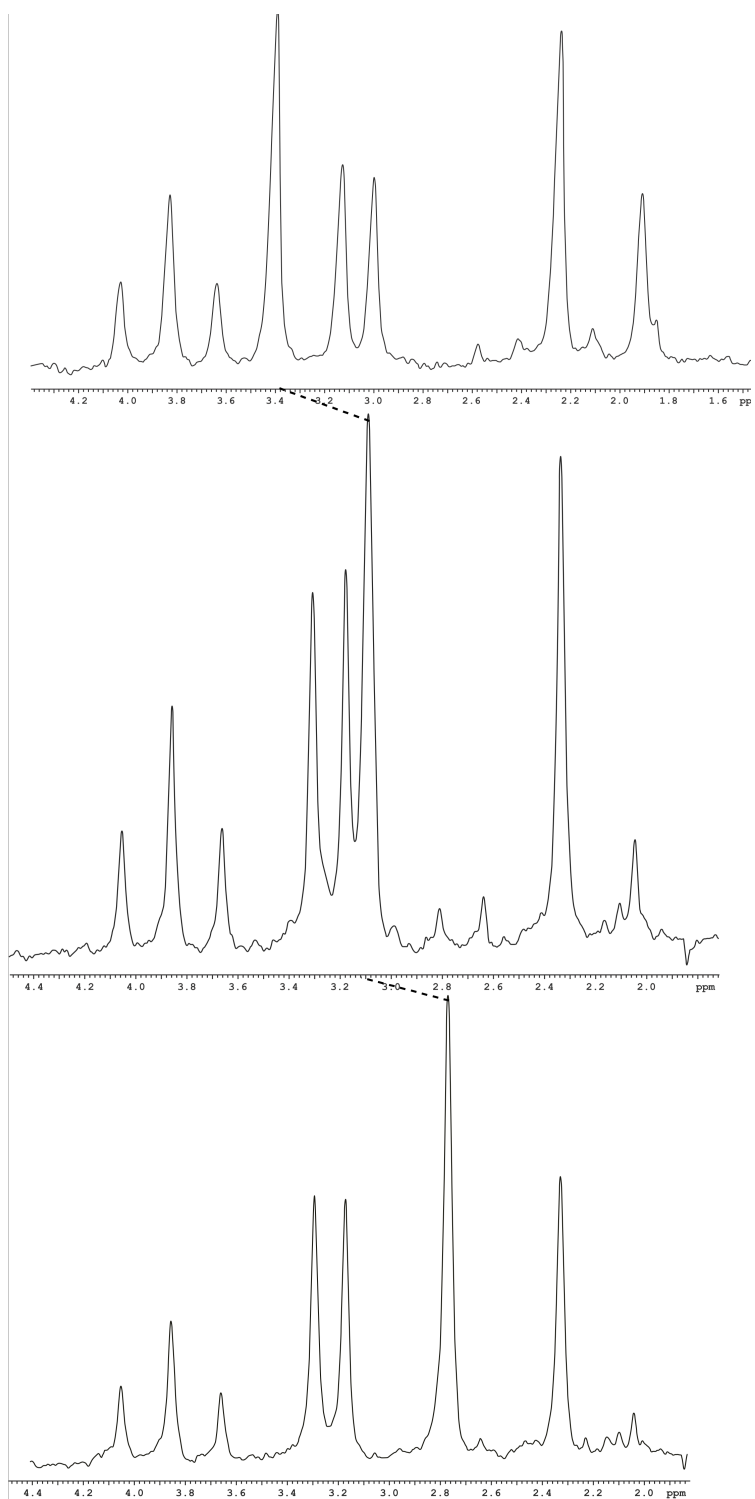**Scheme 37.** Et₂O- and THF solvated dimers.

Figure 16. [6]Li-NMR of the titration of THF to **_n_-BuLi/Li-1a** and **non-eq-(Li-1a)₂**.

In a solution of _n_-BuLi and **1b** in 600 μl Et₂O and 35 μl THF at -80 °C **non-eq-(Li-1b)₂** is formed. This is indicated in [6]Li-NMR by a triplet at δ 3.6 and a singlet at δ 1.7 ppm.
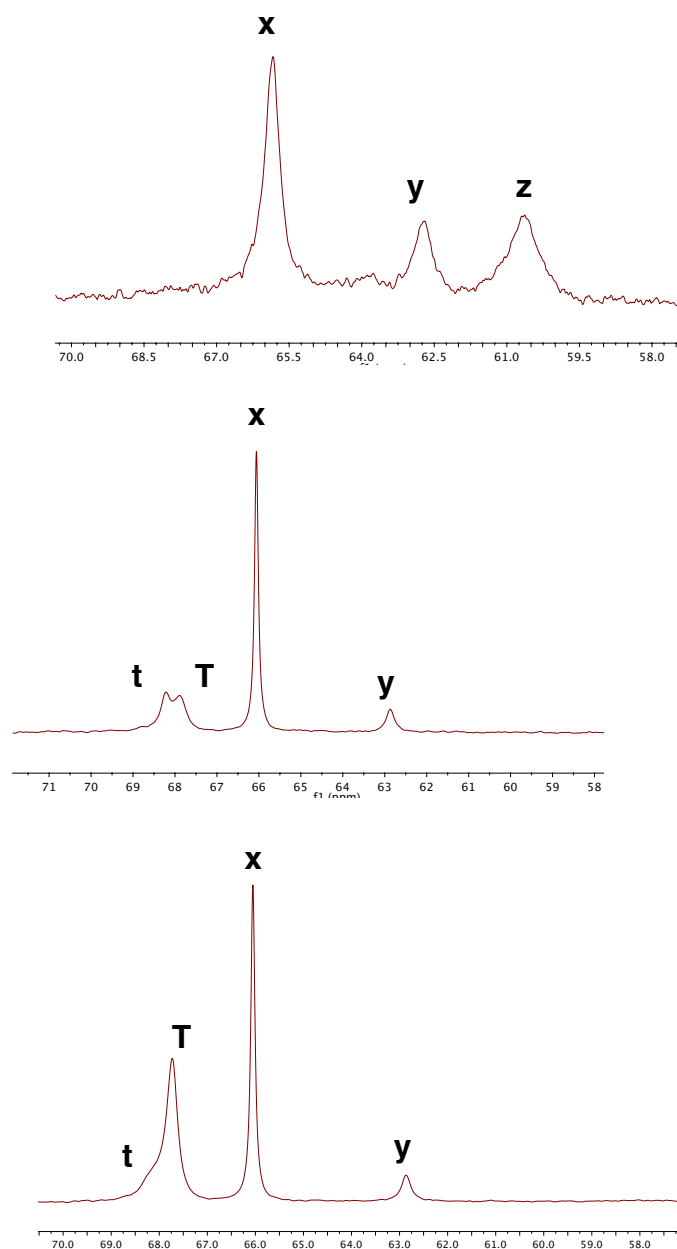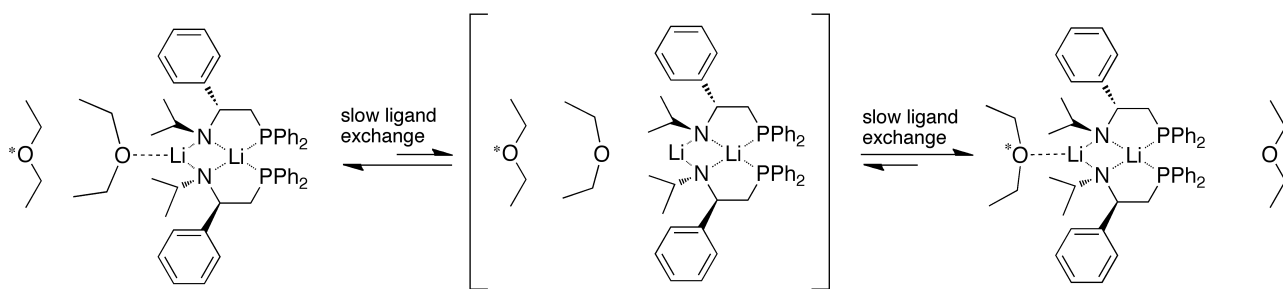
Figure 17. ^{13}C-NMR showing free Et$_2$O (**x**) , THF (**T**) and Et$_2$O- (**z**) and THF-solvated (**t**) **non-eq-(Li-1b)$_2$**, indicating slow ligand exchange. **y**=α-C in the amino acid backbone of **non-eq-(Li-1b)$_2$.**

^{13}C-NMR of **non-eq-(Li-1b)$_2$** shows signals for both coordinated and free Et$_2$O indicative of slow ligand exchange on the NMR time scale at -80 °C (Figure 17). Upon addition of 2 eq. of THF to

**non-eq-(Li-1b)$_2$** in Et$_2$O there is still a slow ligand exchange according to ^{13}C-NMR. However, in ^{6}Li-NMR there is no visible difference on the triplet and singlet of **non-eq-(Li-1b)$_2$** when adding THF. Upon addition of THF to **non-eq-(Li-1a)$_2$** in Et$_2$O the signals in ^{6}Li-NMR are unaffected. However, in excess THF the complex is clearly mainly THF-solvated, as shown by ^{13}C NMR.

In Et$_2$O and *n*-BuLi **1a-b** exist mainly as **non-eq-(Li-1)$_2$•Et$_2$O** but since THF is coordinating stronger to lithium than Et$_2$O, titrating THF results first in the formation of the **non-eq-(Li-1)$_2$•THF** (Scheme 38).[61] Upon higher concentration of THF the mixed complex **(Li-1/*n*-BuLi)**, is formed, hence, the equilibrium is shifted towards **Li-1/*n*-BuLi** in THF with R' = *i*-Pr.
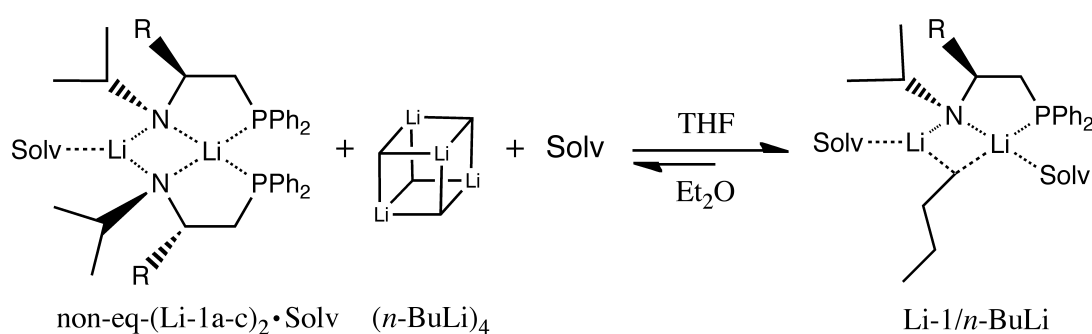
Scheme 4. The equilibrium in THF and Et$_2$O in ^{6}Li-NMR. R = Ph, Bn, *i*-Pr and Solv= THF or Et$_2$O.

For the methylated amino acids, **1d-e**, in Et$_2$O the equilibrium is shifted to **eq-(Li-1)$_2$•Et$_2$O** and upon addition of THF the complexes deaggregates to **(Li-1/*n*-BuLi)** (Scheme 39).
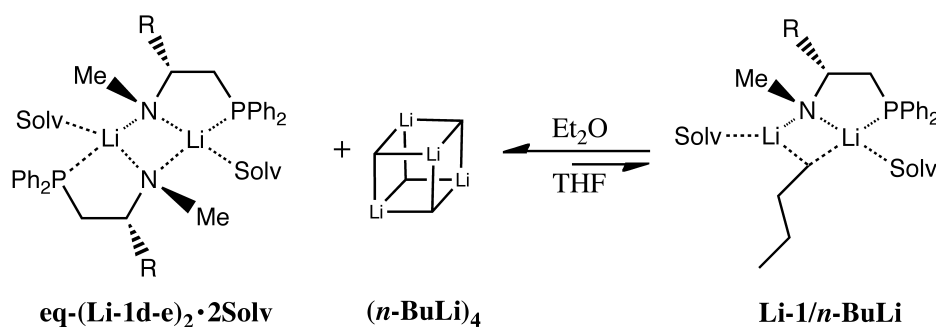
Scheme 39. The equilibrium in THF and Et$_2$O in ^{6}Li-NMR. R = Ph, Bn, and Solv= THF or Et$_2$O.

2.2.2. Computational studies

The aim of this computational study was to rationalize the findings described in the experimental part, that is, to understand what features (sterical hindrance, coordinative bonds, dispersion

interaction) that determine the different aggregation states observed for **Li-1a-e**. In this study, we focus on the homo dimers, without excess *n*-BuLi added (Figure 18).
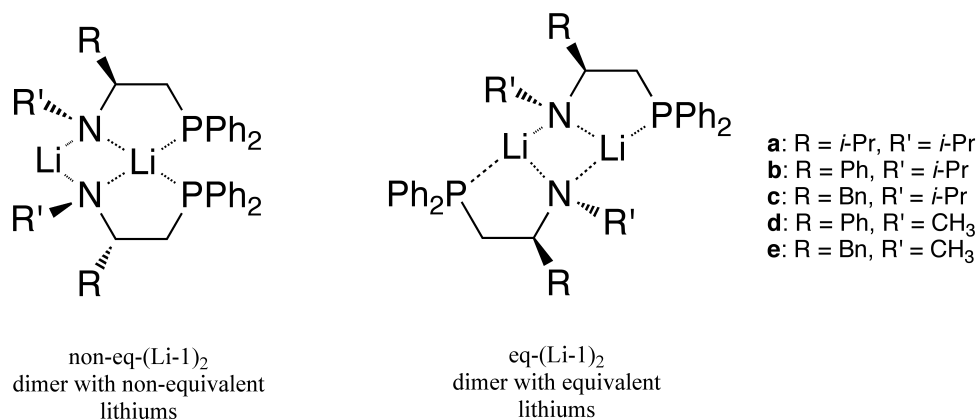

a: R = *i*-Pr, R' = *i*-Pr
b: R = Ph, R' = *i*-Pr
c: R = Bn, R' = *i*-Pr
d: R = Ph, R' = CH₃
e: R = Bn, R' = CH₃

non-eq-(Li-1)₂
dimer with non-equivalent
lithiums

eq-(Li-1)₂
dimer with equivalent
lithiums

Figure 18. The homo dimers included in this computational studie. Solvent is excluded for clarity.

We determined the low-energy conformations for each of the ligand dimers for different explicit solvation states. Given the complex structure of the PES for the dimers, the conformation search requires a systematic strategy. This strategy is shown schematically in Scheme 40. The individual steps are described in greater detail in Paper III.[57] Firstly, optimization was performed for the monomers and dimers of **Li-1d** and all other conformations were reconstructed from these optimized structures. The following steps needed to be taken:

1.   All momomers were optimized on the DFT level.

2.   The **non-eq(Li-1d)₂** was optimized with DFT. This calculation provided two results for the following steps:
     - A template for the modelling of the other dimers to be used for (equivalent as well as non-equivalent ones)
     - A tailored force field for the description of the non-classical N–Li bonds in the dimers (see Section 2.3).

3.   With the template from step 2, all conformers of all dimers were constructed and the geometries were optimized on the MM level with the tailored force field from step 2.

4.   For each structure, the lowest conformer and all conformers at most 8 kJ mol⁻¹ in energy above were reoptimized with DFT. The lowest-energy conformer was selected. The geometries found in this step are used for the calculation of chemical shieldings, which are compared with the experimental shifts (see further below in this section).

5.   For the lowest-energy conformers from step 4, one calculates:

- The energy in solution[106, 137-141] with the SM8 model and an extended basis set (6-31+G** instead of 6-31G**).
- Dispersion corrections on the DFT-D3 level, and a scaled free energy correction.

6. From the corrected energies from step 5, the equilibria between different structures and solvation states are calculated.

The space around lithium does not allow more than four ligands. An attempt to add further solvents beyond tetrahedral coordination lead to the breaking of either one or both Li-P bonds.
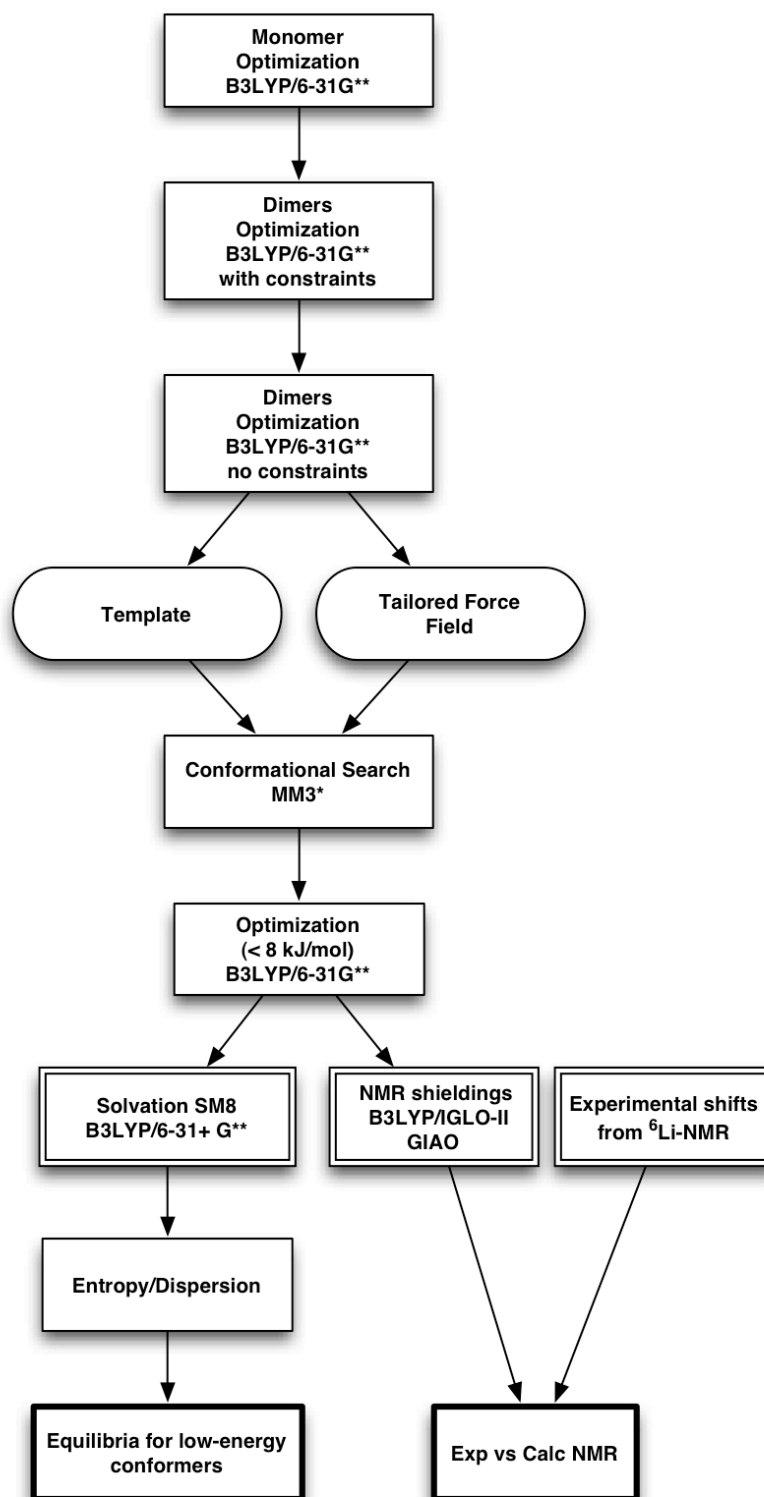
Scheme 40. Prodecure for the calculations of energies and NMR chemical shieldings.

The calculations predict that for amino acids **1a-c** the complexes of **non-eq-(Li-1)2•2DME** are overall the most stable conformations (Table 2). For amino acids **1d-e** the **eq-(Li-1)2•2DME** complexes are the most stable conformations. Among the unsolvated conformations the **eq-(Li-1a-e)2** are strongly favoured over the **non-eq-(Li-1)2**, which also was found for the N,S-ligands.[16]

50

Table 2. Relative free energies at 183 K, kJ mol-1, with scaling[a]

Dimer	Ligand				
	1a	1b	1c	1d	1e
eq-(Li-1)$_2$	8	33	41	34	53
eq-(Li-1)$_2$·sol	2	1	2	9	13
eq-(Li-1)$_2$·2sol	14	6	8	0	0
non-eq-(Li-1)$_2$·sol	0	0	0	20	23
non-eq-(Li-1)$_2$·2sol	41	43	36	27	8

[a] 20% dispersion, $T\Delta S = 6$ kJ mol^{-1}

The low-energy conformations of **eq-(Li-1)$_2$** are folding themselves to structures that resemble cage compounds and prefer to be disolvated (Figure 19). The low-energy conformations of **non-eq-(Li-1)$_2$** have a more butterfly-like structure and are preferentially monosolvated (Figure 20).

eq-(Li-1d)$_2$•2DME   **eq-(Li-1e)$_2$•2DME**
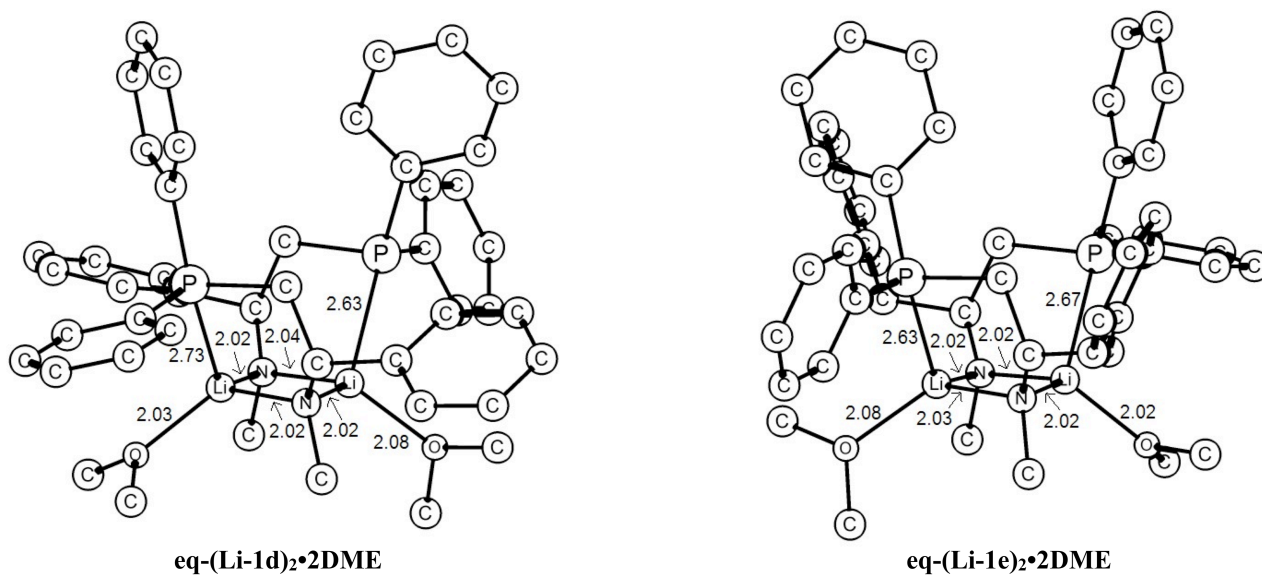
Figure 19. The calculated most stable dimeric complexes with equivalent lithium for each ligand. The hydrogens are omitted for clarity.

non-eq-(Li-1a)₂•DME

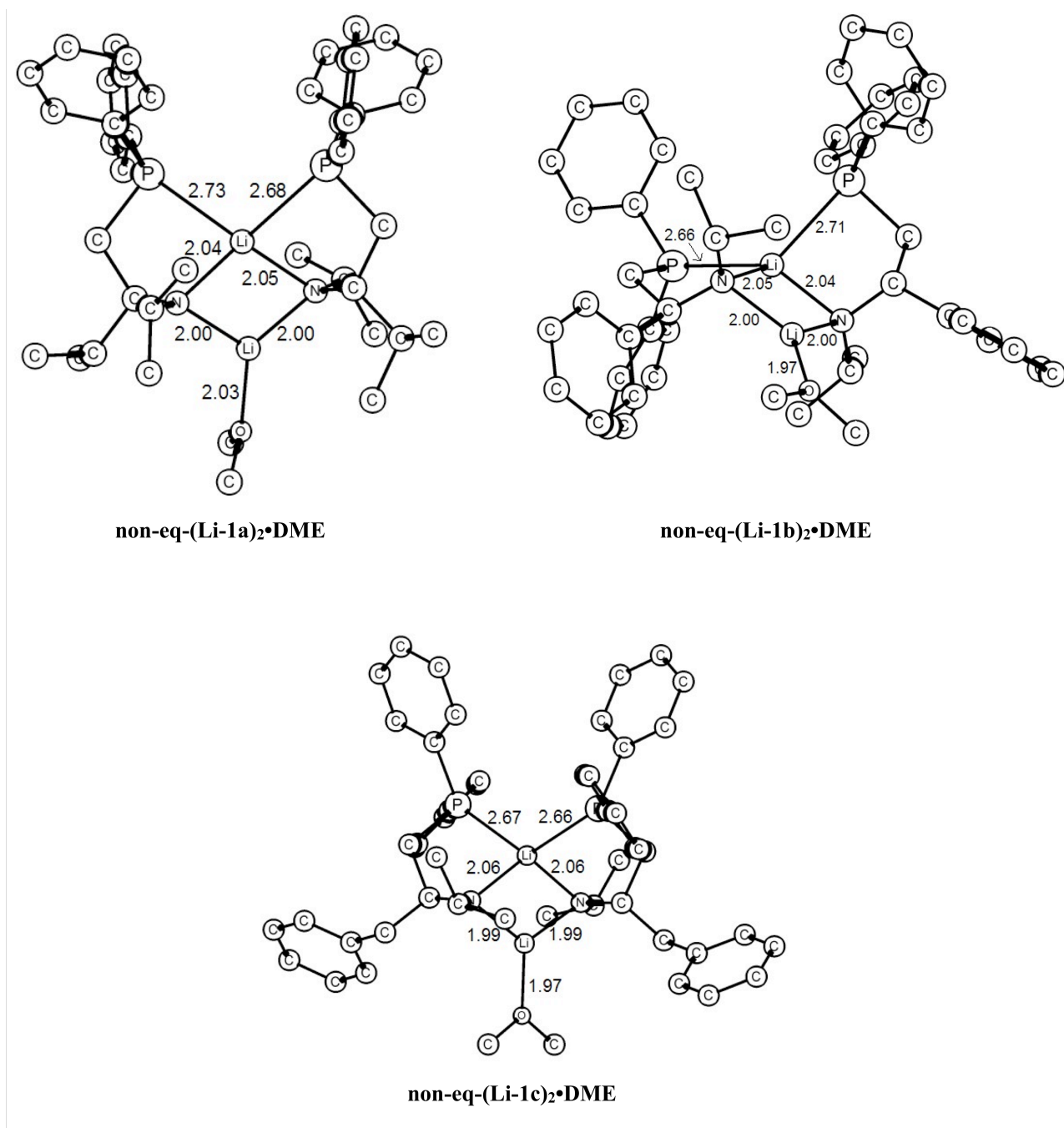non-eq-(Li-1b)₂•DME

non-eq-(Li-1c)₂•DME

Figure 20. The calculated most stable dimeric complexes with non-equivalent lithium for each ligand.Hydrogens are omitted for clarity.

Selecting the best member of each class, we then attempted to reproduce the experimentally preferred dimer type (**eq** or **non-eq**) for each of the five ligands by adding scaled free energy and dispersion contributions.

The evaluation of the measured ^{6}Li-NMR spectra indicated an equilibrium between dimers of both **eq-(Li-1a)₂** and **non-eq-(Li-1a)₂**. We found that the results of the calculation depend sensitively on the choice of the dispersion and entropy corrections. The best agreement with experiment was

obtained if dispersion corrections were scaled to 20% and the entropy correction was chosen to 6.3 kJ/mol instead of the calculated value of 26 kJ/mol.(Refs) This finding is rationalized in Paper III. [136, 142]

The experimental NMR studies had shown that the Li-P bonds are stronger than previously anticipated. We calculated selected chemical shieldings and spin-spin coupling constants to compare them with experiments and to gain insight in the nature of the Li–P bonds. Comparing experimental and calculated shifts allowed verification of the aggregates in solution (Figure 21).
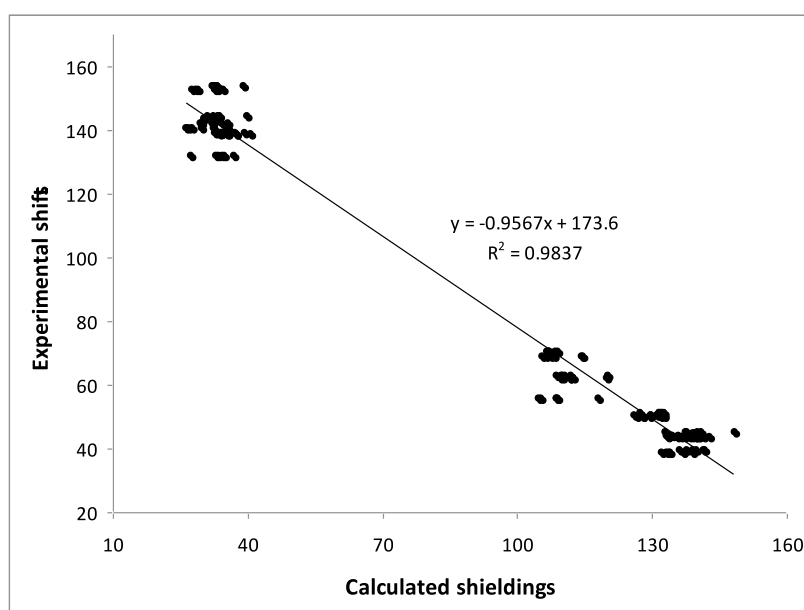

Figure 21. Experimental ^{13}C NMR chemical shifts (in ppm) of the observed dimeric complexes vs calculated shieldings.

A direct comparison of calculated shielding with experimental shift values would require determination of the shielding of the reference compound. However, we are interested in changes of a given shift upon solvation, conformational changes etc. For these changes, the value of the reference shielding cancels, and we can compare the calculated changes in the shieldings with the measured changes in the shifts directly. In uncertain cases experimental shifts were not assigned explicitly and we then assigned experimental and calculated values according to their order. The calculations showed a clear relationship between the calculated shieldings and experimental shifts, and the resulting relationship between calculated shieldings and measured shifts can be used to facilitate the assignment of NMR properties for new complexes (Figure 22).[57]
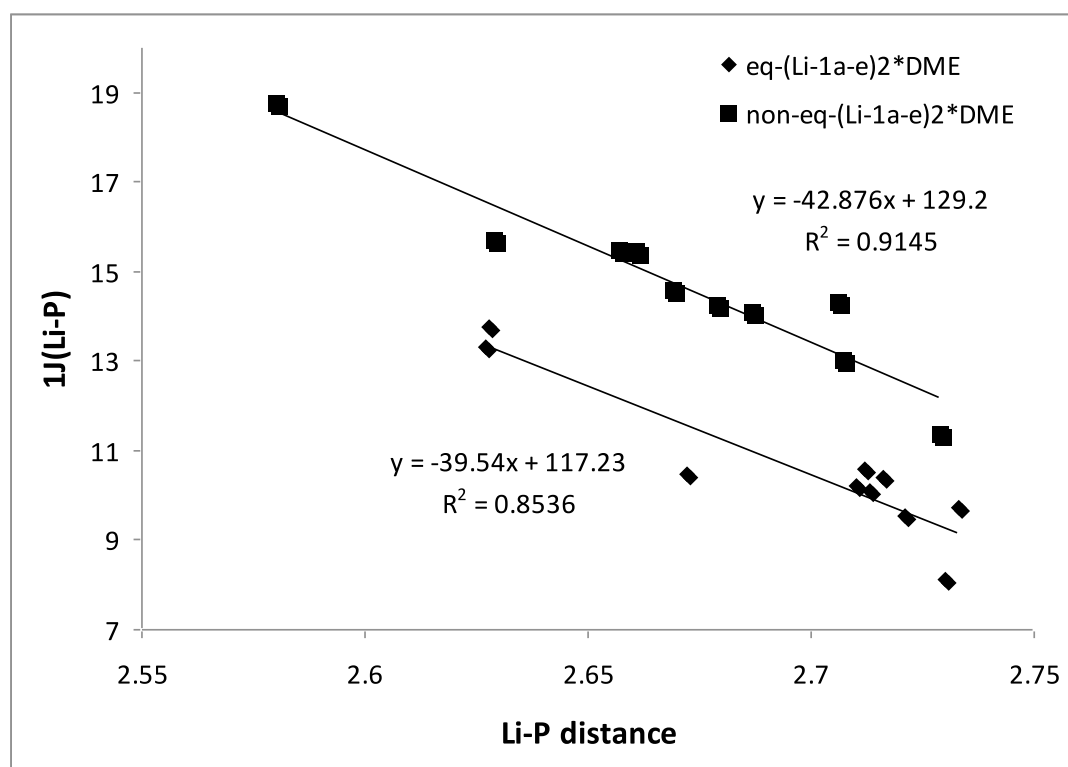
Figure 22. Calculated $^1J_{LiP}$ (Hz) vs calculated ^6Li-^{31}P distance (Å).

The calculations showed linear correlations between calculated $^1J_{LiP}$ values and Li-P distances r_{LiP} (see Figure 8 in Paper III), where $^1J_{LiP}$ decreases with increasing r_{LiP}. It is noteworthy, that there are distinctly different relationships between $^1J_{LiP}$ and r_{LiP} for **non-eq-(Li-1b-c)$_2$•DME** and **eq-(Li-1a-e)$_2$•DME**, where the slope is about the same but the interception points differ markedly. Thus, $^1J_{LiP}$ is indeed an indicator for r_{LiP} (and thus for the Li-P bond strength); however, this relationship is sensitive to the aggregation state of the ligands.

2.3. Tailored force field for lithium organic complexes (Paper V)

The chiral lithium amides are very flexible and therefore have a complex PES. A large manifold of conformations was therefore expected from the geometry optimization. Thus, in order to limit the computational effort, we wanted to use MM for pre-screening of the conformers and then reoptimizing only the most promising candidates with DFT. A limitation in the standard force field (FF) is that it does not cover lithum amide complexes. Hence, we tailored a new FF by augmenting MM3*. Structural parameters were determined on the basis of B3LYP geometries of the lithium amide complexes.[143-147]

Owing to the MM prescreening, DFT calculations were necessary for only a set of chiral lithium amide complexes. The DFT bond lengths in the dimers are well reproduced with MM3* (Figure 23).
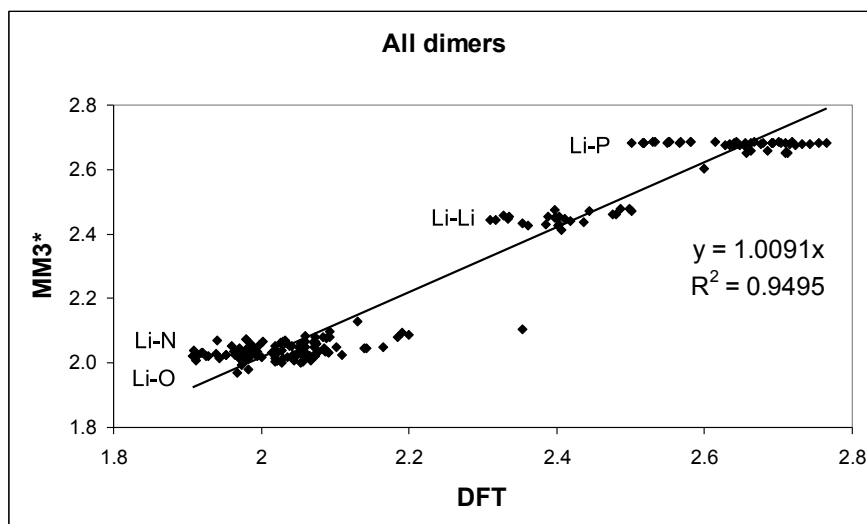

Figure 23. Comparison between MM3* and DFT optimized bond lengths for all investigated dimers.

The calculations show similar structures for MM3* compared to those from DFT and, thus, by using this new force field it is possible to limit the computational effort (Figure 24). The force field developed herein is useful for optimizing structures of lithium amides with a high accuracy. It is shown that different sorts of dimers (**A** as well as **B**) and with different degrees of solvation is covered by the new MM3* parameters. The force field is easily modified to include also lithium N,N-, N,O-, and N,S-ligands, important ligands in for example asymmetric addition reactions.
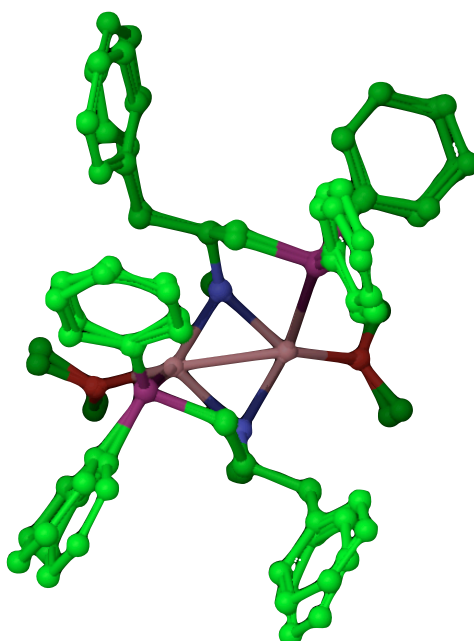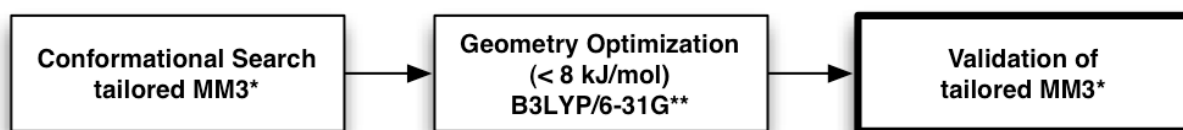

Figure 24. Overlay of **eq-(Li-1c)₂** from the optimization using the new tailored force field and DFT.

The procedure for calculating the low-energy conformations with the new force field are showed in Scheme 41.

Scheme 41. Procedure for calculating the various dimers with the tailored MM3* force field.

2.4.   Enantioselective addition of *n*-BuLi to benzaldehyde (Paper IV)

2.4.1.   Experimental studies on the enantioselective addition

In the butylation reaction of benzaldehyde the stability of the tetramers of *n*-BuLi, **(*n*-BuLi)₄**, increases the activation barrier for the nucleophilic addition, making the (background) reaction path slow (left side reaction, Scheme 42). However, with a ligand present the tetramers deaggregate and form a mixed complex, **B**, which increases the reaction rate of the formation of the alcohol.
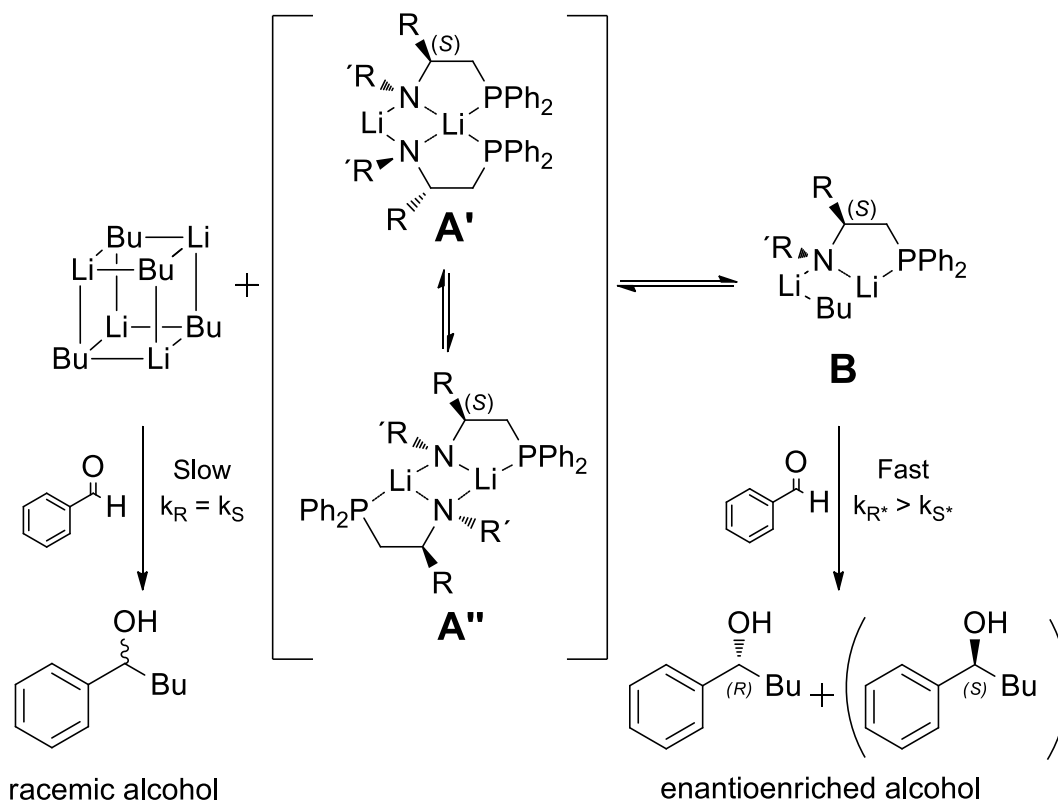
Scheme 42. Asymmetric addition of *n*-BuLi to benzaldehyde with various ligands. With no ligand added a racemic mixture is formed. R = *i*-Pr, Ph, Bn. R' = *i*-Pr, CH₃.

The mixed complex reacts with benzaldehyde in an 1,2-addition reaction and upon quenching 1-phenyl-1-pentanol is formed (Scheme 43). With no ligand present a racemic mixture of the alcohol is formed (Scheme 42).
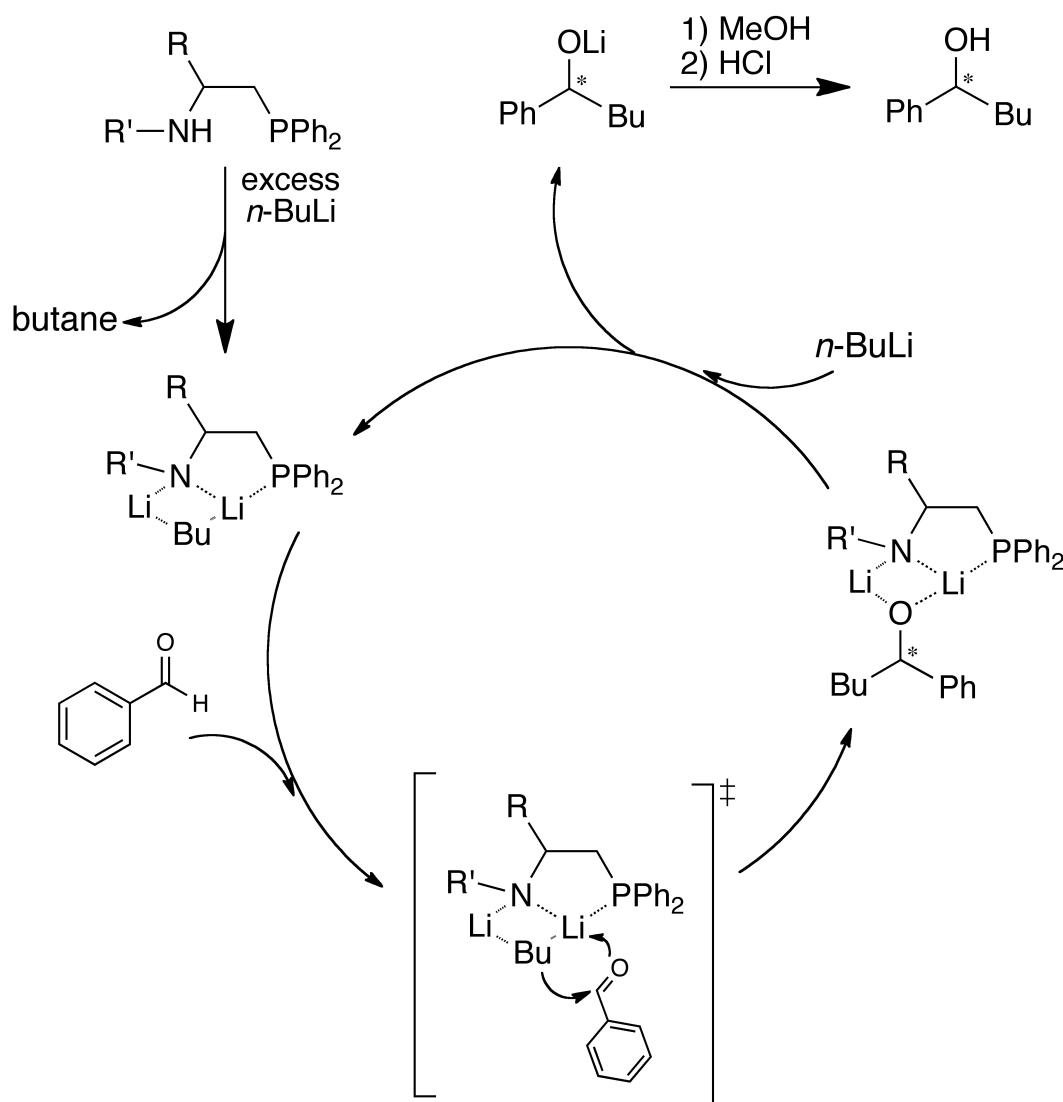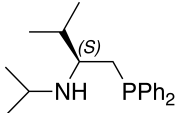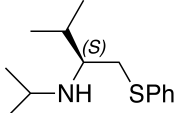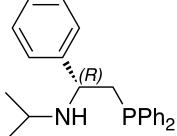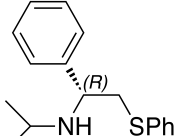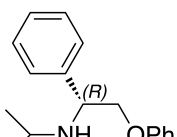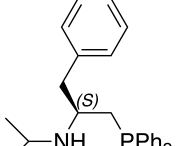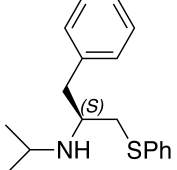
Scheme 43. The suggested mechanism of the addition of *n*-BuLi to benzaldehyde with a N,P-ligand. R = *i*-Pr, Ph, Bn. R' = *i*-Pr, CH$_3$ Solvents are excluded for clarity.

All asymmetric butylation reactions were clean and high-yielding and the e.r´s were higher than the corresponding N,O-ligands and similar to N,S-ligands, reported from our group (Table 3).[148] **Li-1a** yields lower e.r than its corresponding **Li-2a** (Entry 1, 2). **Li-1c**, however, yields a higher e.r than **Li-2c** (Entry 6, 7). **Li-1b** yields the highest e.r among the N,P-ligands in this study, where N,S-ligand **Li-2b** yields a slightly better e.r (Entry 3, 4). The corresponding N,O-ligand **Li-3b** yields a lower e.r (Entry 5). In previous studies N,O-ligands have been designed to form strong 5-membered chelates to lithium between the amide nitrogen and a hard Lewis base, like an ether group. However, the results with N,P-ligands show that an increase in softness of the atom of the chelate

results in comparable and also higher e.r. Thus, a weaker 5-membered chelate is giving a higher asymmetric induction compared to the stronger chelates in N,O-ligands. Similarly as the chiral N,O- and N,S-ligands the chiral N,P-ligands catalyzed the formation of the alcohol with the opposite configuration.[13, 14]

Table 3 Asymmetric addition of *n*-BuLi to benzaldehyde at -116 °C.

Entry	chiral amine	Name	conversion (%)	ee (%)	er
1		Li-1a	80	93 *(R)*	28
2		Li-2a	80	97 *(R)*	66
3		Li-1b	71	98 *(S)*	99
4		Li-2b	82	98.5 *(S)*	132
5		Li-3b	96	96 *(S)*	49
6		Li-1c	93	82 *(R)*	10
7		Li-2c	87	68 *(R)*	3

2.4.2. Computational studies on the enantioselectivitie addition

To understand what features are responsible for the enantioselectivity, we undertook a theoretical study of alll plausible TS. The e.r is determined by the difference in the activation barriers in the formation of the *(R)*- and *(S)*-alcohol, i.e. eventually by the difference in free energy between *(R)*- and *(S)*-TS (Figure5, Figure 25).

TS-Li-1x
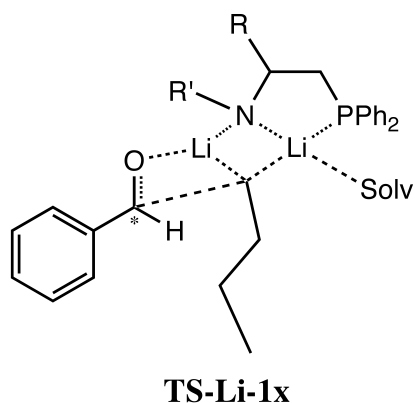
Figure 25. The structure of the TS in the butylation reaction.
R = Ph, Bn, *i*-Pr and R' = Me, *i*-Pr. x=a-e

As for the ligand dimers discussed in Sec. 2.2.2, the high conformational flexibility of the ligands, gives rise to a large manifold of conformations and a systematic conformation search is required to determine accurate energy differences. The procedure used resembles the one used in Sec. 2.2.2 and is shown in Scheme 44 and and is described in more detail in Paper IV.[149]

**TS Template
Optimization
B3LYP/6-31G****

**Mixed complex
MM3*
Conformational Search**

**TS Template
IRC and QRC
B3LYP/6-31G****

Merging

**(R)-TS and (S)-TS
Optimization
B3LYP/6-31G**
with constraints**

**(R)-TS and (S)-TS
Transition State Search
B3LYP/6-31G****

**Low-energy TS
Solvation SM8
B3LYP/6-31+G****

Dispersion
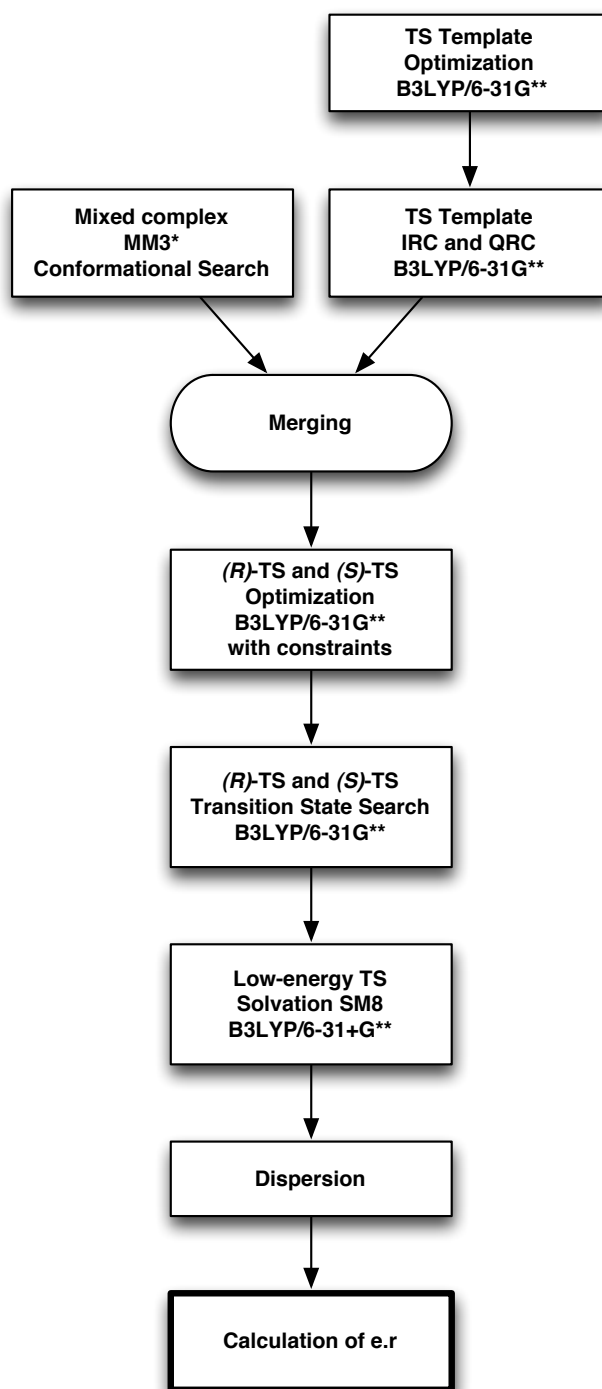
Calculation of e.r

Scheme 44. Prodecure for the calculations of the transition states and ee.

To get a an efficient TS geometry optimization it is important to make a good initial guess and, hence, a template for the initial TS was carefully modelled. An optimized DME-solvated mixed dimer, **Li-1/*n*-BuLi•DME**, from one of the ligands was reconstructed by replacing the butyl group with an ethyl group and both R, R´ were replaced by methyl groups (Figure 26). A benzaldehyde molecule was merged with the resulting scaffold and a TS geometry search was performed. The

geometry optimized *(S)*-T1 was then used as a template for the modelling of all *(R)*-TS-Li-1 and *(S)*-TS-Li-1 (Figure 26).
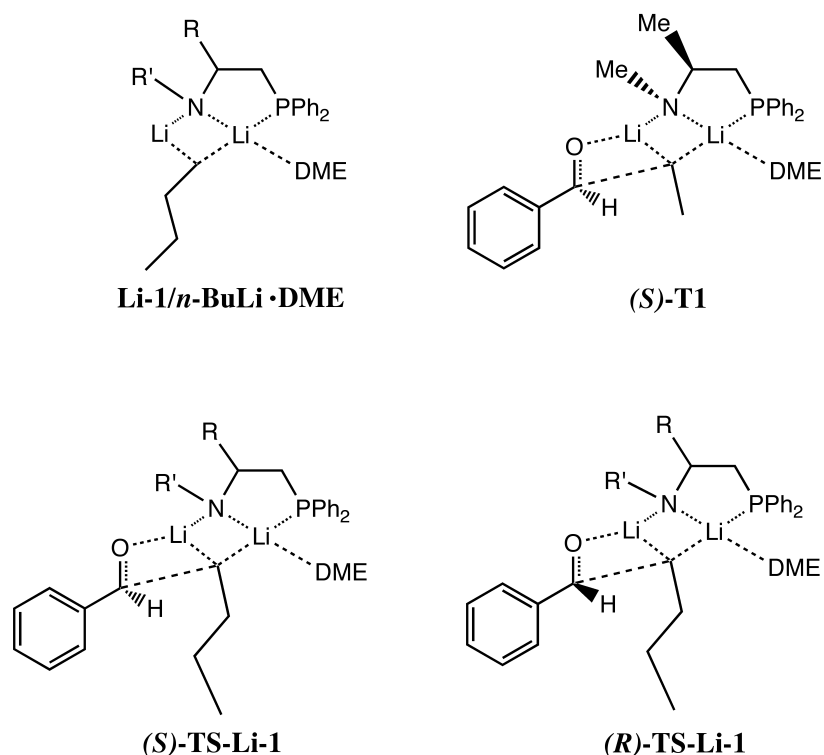
Figure 26. The template *(S)*-T1, **Li-1/n-BuLi•DME** and transition states *(R)*-TS-Li-1, (S)-TS-Li-1. R = Ph, Bn, i-Pr and R' = Me, *i*-Pr.

Both IRC and QRC analysis were performed on *(S)*-T1 to ensure that the correct reactants are connected with the correct products. i.e. that the relevant TS were investigated (Figure 27).[87]
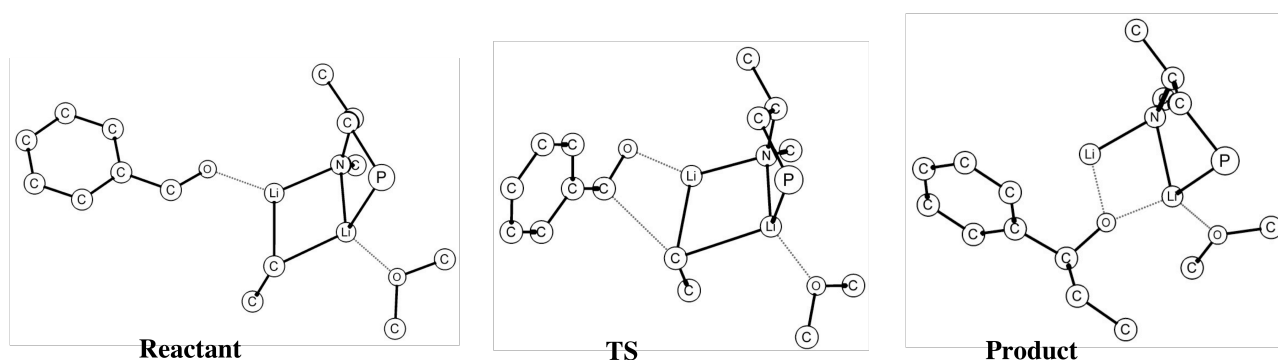
Figure 27. Minima and transition state like structures for benzaldehyde entry in the QRC approach. The butyl group has been truncated to an ethyl group for simplicity.

For the full ligands with *n*-BuLi, MM3* conformational searches were performed. Given the large number of TS searches needed, to save computational time the following optimizations were performed with Macro Model, using a local version of the MM3* force field.[150, 151] To all mixed complexes within 8 kJ mol⁻¹, benzaldehyde was merged using the template described above and the

TSs were optimized with Jaguar in two steps with DFT. In the first step, five bonds of Li-C-C-O were constrained (Figure 27). In the second step a TS search was then performed on the partially optimized TS, with the constraints lifted, and a frequency calculation performed.

The energies for the resulting low-energy TS were recalculated at the B3LYP/6-31+G**level[141] using the SM8 solution model with THF as solvent.[89, 152, 153] The e.r of the resulting alcohol formation from the respective free energies and with dispersion correction added (DFT-D3), was calculated and the results were compared to the experimental values and rationalized from the structures and geometries of the TS.

The calculations of the TSs show that benzaldehyde can coordinate to the ligands in three esentially different ways. We adopted the nomenclature *syn*, *anti* and in plane, defining the three major coordination types, between benzaldehyde and the phosphorus with respect to the 4-membered N-Li-C-Li ring (Figure 28).
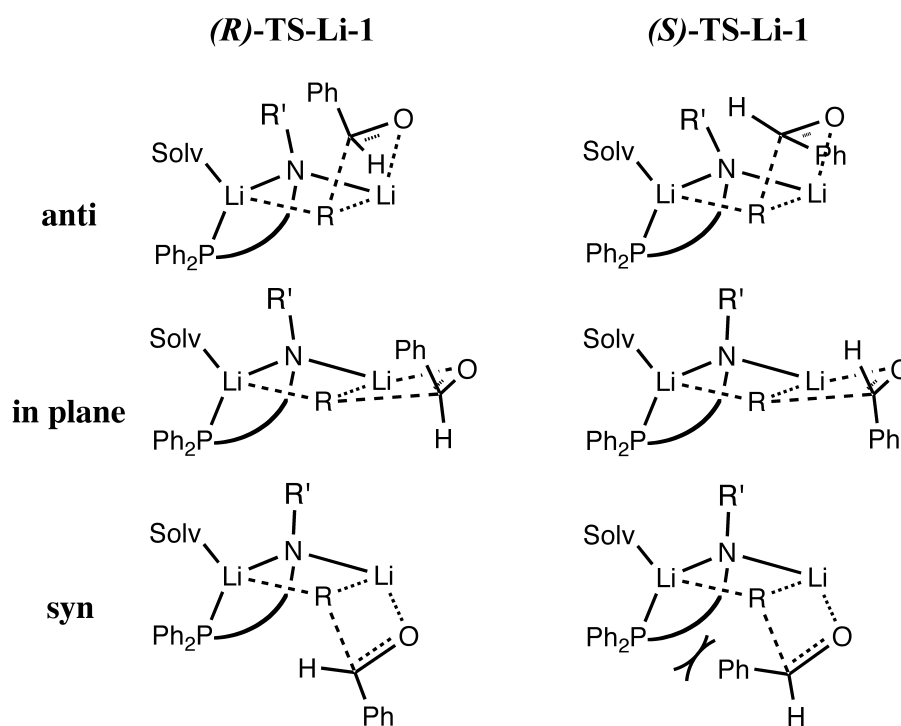
Figure 28. The different coordination modes of benzaldehyde in TS.

In general, the *anti*-conformation is the most frequently observed coordination mode. For some of the ligands in plane conformations exist, but they are always slightly higher in energy than the corresponding *anti*-conformation. Due to steric repulsion of the phenyl ring on benzaldehyde and PPh$_2$ moiety no *syn*-conformation was observed in *(S)*-TS-Li-1. Most importantly, this exception is

also the most stable conformation of all TS in **(R)-TS-Li-1e.** All conformations of **(R)-TS-Li-1c** and most of all **(R)-TS-Li-1b-e** are in *anti*-conformation, although the latter **(R)-TS** have some in plane-conformations. Hence, there are two energetically available paths for **(R)-TS** (*syn, anti*) and only one for **(S)-TS** (*anti*). The various coordination modes for some geometry optimized TS are shown in Figure 29.

anti-*(R)*-TS-Li-1e   **anti-*(S)*-TS-Li-1e**

syn-*(R)*-TS-Li-1e
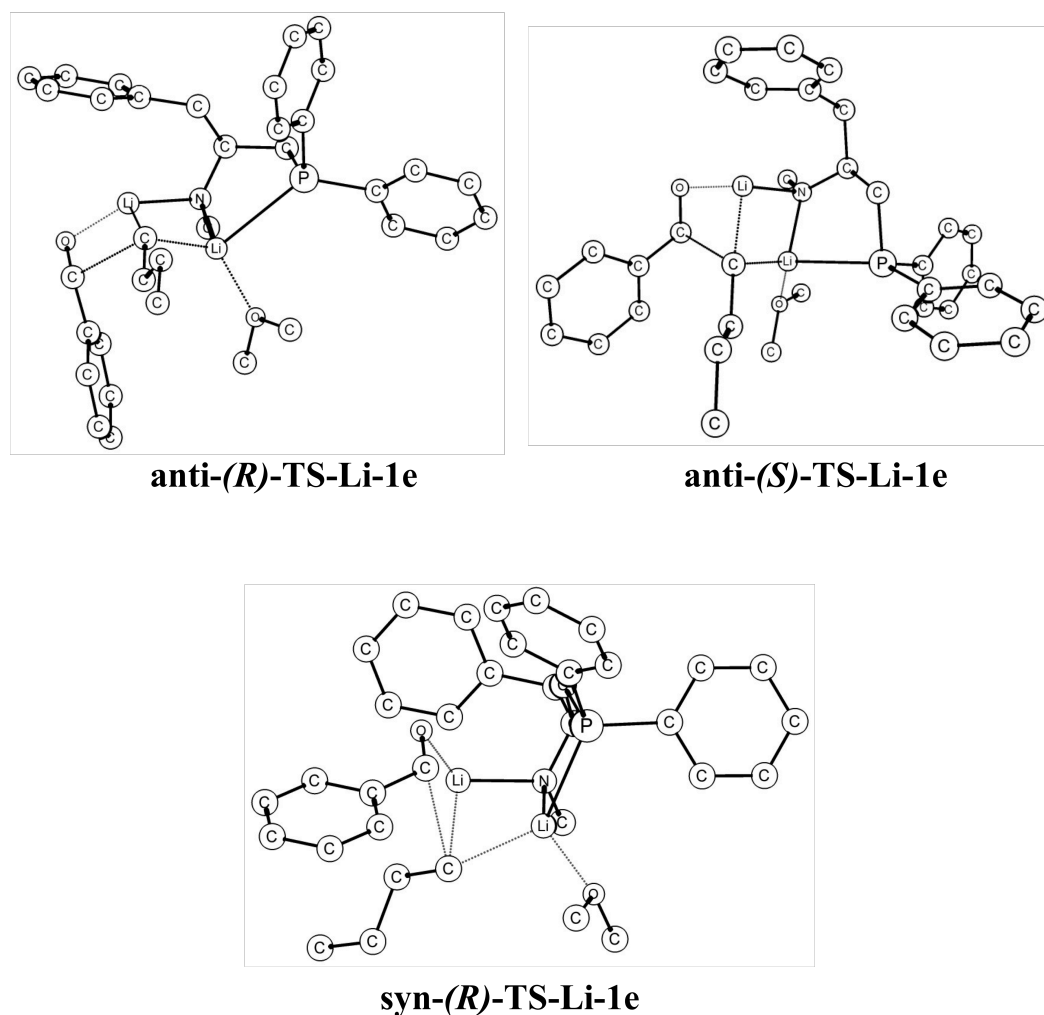
Figure 29. The various coordination modes of **(R)-TS-Li-1e** and **(S)-TS-Li-1e.**

The computational study could confirm the experimentally preferred enantiomer for all TS (Table 4). However, to properly rank ligands **1a-e** with regard to the e.r one has to take dispersion corrections into account. Without dispersion correction the calculations predict that **Li-1c** has the highest e.r of ligands in this study, while it has the lowest in experiment. However, calculated enantioselectivities are often overestimated.[149] Different amounts of Grimme's dispersion correction were tested to reproduce the experimental trend, 100% dispersion correction had to be added, and the highest e.r in the butylation reaction is obtained for **Li-1b**, in accordance with experiments. No experimental e.r are available for **(R)-TS-Li-1d** and **(R)-TS-Li-1e**. From the calculations we predict

that **(R)-TS-Li-1d** will give a lower e.r, whereas **(R)-TS-Li-1e** will give second best e.r of all the TS in this study.

In the study of the dimers we found it necessary to reduce the effect of the dispersion correction to 20% in order to reproduce experimental observation. The scaling of dispersion correction for the dimers is due to the strongly overestimated desolvation equilibria in gas phase (Table 4).[57] This arise from that the magnitude of the entropy of any ligand is expected to be smaller in solvent than in gas phase. The continuum solvation models available to us capture none of the effects that arise from this. The difference of the TS study to the dimers, regarding dispersion correction, is that no desolvation take place and therefore no scaling factor needs to be introduced for the TS, resulting in 100% dispersion.

Table 4 Calculated and experimental enantiomeric ratios.

Ligand (R)-TS-Li-1x	Calc. 0% dispersion	Calc. 20% dispersion	Calc. 100% dispersion	Exp.
x = a	120	120	150	28[a]
b	60	260	71000	99[b]
c	6300	3800	500	10[a]
d	180	160	120	-[c]
e	940	1100	2400	-[c]

(R)-1-phenyl pentanol b) *(S)*-1-phenyl pentanol. In the computational study we rather modelled the *(R)*-alcohol as the preferred in order to have a uniform basis for discussion c) Not determined

There are a number of stablilizing effects in the TS. The phenyl and benzyl rings in **(R)-TS-Li-1b-d** position themselves to Li, creating a Li-π interaction. In **(R)-TS-Li-1b-c** the phenyl ring of benzaldehyde and one of the phenyl rings in PPh$_2$ interact with the α-H in DME. This stabilizes the TS and simultaneously makes it feasible for the aromatic group on α-C in the ligand to coordinate to lithium. These interactions does not occur in their respective enantiomer **(S)-TS-Li-1b-c**, hence, these TS are less stable. We investigated what caused the large dispersion effects in **(R)-TS** in two ways. First, we used non-covalent interaction (NCI) plots to visualize the dispersion interactions. These plots[154] clearly show that the biggest difference between **(R)-TS** and **(S)-TS** is the interaction of α-H in DME to the phenyl ring in benzaldehyde, which is not found in **(S)-TS** (Figure 30). The

dispersion effect from the aromatic group on the α-C in the chiral lithium amide coordinating to lithium is also visualized.
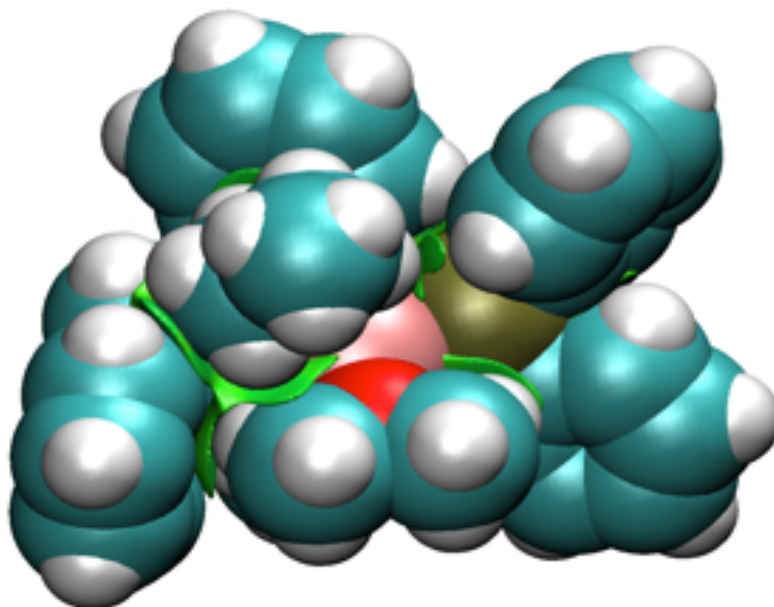
Figure 30. Dispersion effects (green) in *(R)*-**TS-Li-1b** visualized by NCI.

The butyl group interacts with the phenyl ring in benzaldehyde and this dispersion effect is larger in *(S)*-**TS** than in *(R)*-**TS**, thus reducing the enantioselectivity. Interestingly, for this interaction *(R)*-**TS-Li-1b** has the lowest dispersion effect. However, in total it has the largest dispersion effect. The alkyl group on nitrogen also affects the stabilization. Due to steric effects, the bulky *i*-Pr group can interact with both the phenyl ring of benzaldehyde and the α-H in DME. This stablizing effect is only found in *(R)*-**TS** and not *(S)*-**TS**. TS with methyl on nitrogen lack this effect.

To be able to predict the essential features for the selectivity in the butylation reaction, we further investigated which dispersion interactions are important in the TS. Thus, an analysis was performed by decomposing the TS into four units; A) benzaldehyde, B) *n*-BuLi, C) Li-DME and D) ligand (Table 5) and calculated the contributions to the dispersion interaction from the interactions between these fragments as well as inside fragment D. The results were then ranked for the individual contribution, and these partial ranks were summed up to give the total rank. The lower the score, the higher the selectivity for *(R)*-**TS**.

Table 5. Ranking of the different dispersion interaction energies in each *(R)*-TS.

TS *(R)*-TS-Li-1x	A-B	A-C	A-D	B-C	B-D	C-D	D	Total rank
a	4	2	2	3	2	2	3	18
b	2	1	3	4	1	1	1	13
c	3	3	4	2	3	4	4	23
e	1	4	1	1	4	3	2	16

a) Ranks marked in bold italics are strong interactions, larger than 5 kJ mol-1 and favours the **(R)-TS**. **(R)-TS-Li-1d** has been excluded since the differences in dispersion effects between TSs were less than 1 kJ mol-1.

From this analysis it is evident that *(R)*-TS-Li-1b has the lowest rank, that is, the strongest influence in four out of seven criteria used. It also shows strong interactions in three out of five categories. *(R)*-TS-Li-1c has the highest score. Here, it is found that the interaction between the ligand and DME (C-D, Table 5) is the reason for the lower enantioselectivity. These results are consistent with the experimental results and the calculated e.r in Table 4. The interaction between benzaldehyde and *n*-BuLi is strong in *(R)*-TS-Li-1e. This is due to its *syn*-conformation, which favours the *(R)*-TS over *(S)*-TS. In addition, the benzaldehyde-ligand interaction is very strong (>5 kJ mol^{-1}), which also favours the *(R)*-TS.

Furthermore, it was found that the bulk solvent described by the SM8 solvation model in general stabilizes the *(R)*-TS better than the *(S)*-TS and thus enhances the enantioselectivity. The only exception is ligand **3A** where a very high selectivity is reduced by the solvation model, still it yields the highest selectivity among all ligands. The fact that the largest dispersion energy differences involves interactions between the benzaldehyde and the solvent corresponds well with earlier studies that also show the enantioselectivity is strongly solvent dependent.

3. SUMMARY AND OUTLOOK

The aim of this thesis was to obtain better knowledge of chiral organolithium ligands and the relationship between their structure, aggregation pattern and ability to induce enantioselectivity in order to design improved and more selective ligands. Due to the importance of enantiomerically pure intermediates in drug design there is an ongoing search for economic and efficient methods for their production. A new method for the preparation of chiral N,P-amides was developed for the asymmetric addition of *n*-BuLi to benzaldehyde. By experimental NMR studies a better

understanding of the aggregates was obtained. Theoretical calculations resulted in information that made it possible to verify previous studied structures in solution but also gain knowledge to predict and design other structures and transition states.

Because of the versatility and sulfamidate being an excellent intermediate for new substances polymer supported sulfamidates would be ideally suited for preparation of libraries of different chiral compounds. In addition, another interesting use of silica in this project would be by anchoring the chiral aminophosphines on mesoporous silicas in the application to asymmetric synthesis (Scheme 40) By employing the aminophosphines on silica they can easily be used as heterogenous catalysts in, for example, the asymmetric addition to benzaldehyde. This would provide an easy separation of the product and recovery of the catalytically active ligand.
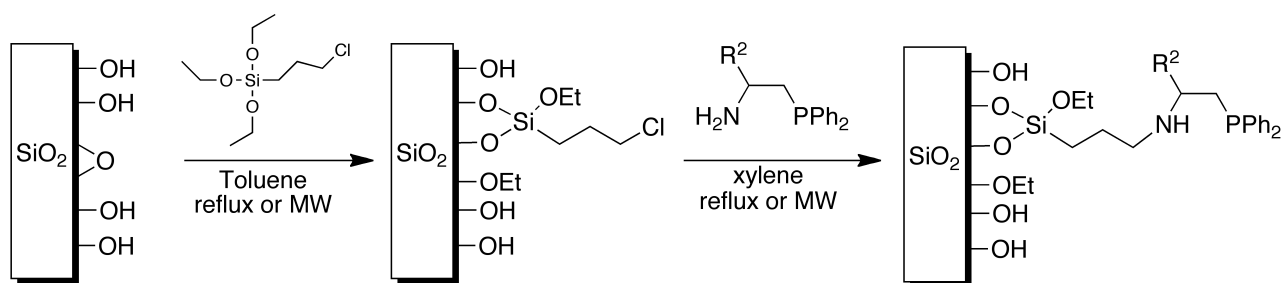
Scheme 40. Synthesis of silica supported aminophosphines.

The computational part of this work shows that the experimental findings can be reproduced well. Both the predicted solvation and aggregation patterns of the ligands and trends in the er for different ligands can be reproduced provided that one takes care to take dispersion interactions and entropic effects into account in a proper way. The calculated structures for the ligand complexes and TSs provided showed which interactions are decisive for the stability of complexes and for the preferred enantiomer in the reaction. Generally, the π systems of the aromatic rings are essential in this connection, e.g. by interaction with Li atoms or α protons of the solvent. Also, experimental NMR properties are reasonably well reproduced by calculations, which means that calculated NMR properties can be used for assigning and analyzing experimental NMR spectra.

There are a number of open questions for future theoretical work:

- One goal of the computational study was to elucidate relationships between structure and chemical behaviour (aggregation patterns, er etc.) By extending the computational study to N,O and N,S ligands, these relationships could be clarified further. For instance, one could

understand the reason for the surprisingly strong Li–P bonds in the N,P ligands as compared to the corresponding Li–O and Li–S bonds in N,O and N,S ligands.

- The calculated NMR properties should be analyzed in more detail. For instance, one could rationalize the dependence of J_{LiP} on r_{LiP} and the aggregation state of Li (see Paper III) using the systematic approach by Podewitz.[155] This would allow using measured Li-P coupling constants as an indicator both for bond lengths and bonding strengths.

- The long-term goal of the investigation is the development of more effective ligands (in terms of yield and er). The findings in this work are a step towards a *de novo* design of new ligands. Existing ligands can be modified in the way that desirable structural features are emphasized and unfavourable ones avoided.

4. EXPERIMENTAL

NMR Measurements

The NMR spectra were recorded using a Varian Unity 400 and 500 MHz spectrometer equipped with three channels using a 5 mm ^{1}H, ^{13}C, ^{6}Li triple-resonance probe head custom-built by Nalorac. Measuring frequencies were 500 MHz (^{1}H) and 74 MHz (^{6}Li). The ^{1}H and ^{13}C spectra were referenced to the solvent signals: THF-d^8 1.73 (^{1}H -CH$_2$) and 25.37 ppm (^{13}C -CH$_2$), Et$_2$O-d^{10} 1.09 (^{1}H -CH$_3$) and 65.5 ppm (^{13}C -CH$_2$). Lithium spectra were referenced to external 0.3 M [^{6}Li]Cl in MeOH-d^4 (δ 0.0 ppm). A typical 90° ^{6}Li pulse was 20 μs.

Preparation of *n*-Bu^{6}Li

^{6}Li (270 mg, 44.85 mmol) was cut into small pieces and washed in dry hexane (3 × 5 ml) in the glovebox. Dry hexane (20 ml) was then added and sonicated for 20 min at 0 °C. BuCl$_3$ (4.72 ml, 44.85 mmol) was added dropwise over a period of 30 min. The reaction started immediately and could be monitored by the change of colourless solution to grey/deep purple. The reaction mixture was sonicated at 0 °C for 2 h and stirred at RT over night. The grey/deep purple suspension was centrifuged and the supernatant was transferred into a glass apparatus equipped with high-vacuum Teflon valves. The solvent was removed under vacuum and the ^{6}Li-*n*-butyllithium (*n*-Bu^{6}Li) was then stored under nitrogen atmosphere in a glass apparatus at -30 °C in the glove box.

General

NMR spectra were recorded on a Varian 400 and 500 MHz spectrometer using CDCl$_3$ as solvent. Optical rotations were measured using Perkin-Elmer 324 LC polarimeter. IR spectra were recorded

on a Perkin-Elmer 1600 Series FTIR spectrometer. Melting points were determined using a Büchi Melting Point B-545 and are uncorrected. GC analyses were carried out using a Varian Star 3400 CX gas chromatograph equipped with a chiral stationary phase column (CP-Chirasil-DEX CB, 25 m, 0.32 mm) from Chrompack. Analysis were done using H_2 (1.5 ml /min) as carrier gas (injector 225°C, detector 250°C). *n*-BuLi and NMR-tubes were prepared and stored in a glovebox (Mecaplex GB 80 equipped with a gas purification system removing oxygen and moisture) containing a nitrogen atmosphere. Dried solvents were distilled from sodium/benzophenone. Column chromatography were performed with SiO_2-60 (40-63 μm) from Fluka at ambient/atmospheric pressure. TLC were SiO_2-60 F254, Merck and visualized by UV light at 254 nm and by staining with a solution of $H_3[P(Mo_3O_{10})_4] \cdot xH_2O$ (10 g) in 95% EtOH (100 ml). MS were recorded on a Micromass LCTP using ESI+ as ionization mode and 5% ACN to 95% ACN in 6 minutes; 40mM ammonia 5 mM carbonate, pH 10 as gradient.

Glassware and syringes were dried at 150 °C in a vacuum oven before transfer into a glovebox (Braun equipped with a gas purification system that removes oxygen and moisture) containing a nitrogen atmosphere. Typical moisture content was less than 1.5 ppm. Ether solvents were distilled under nitrogen from sodium/benzophenone and were kept over 4 Å molecular sieves in septum sealed flasks inside the glove box.

The microwave experiments were performed in a Biotage Initiater Microwave Synthesiser producing controlled radiation at 2450 MHz and using a fixed hold-time.

General procedure for the addition of BuLi to benzaldehyde
n-BuLi (0.30 mmol, 120 μL, 2.5 M in hexane) was added dropwise, over a period of 5 min, to a solution of the chiral aminophosphine (0.20 mmol, 4.0 eq.) in dry Et_2O/THF 1:1 (2.0 ml) at -78 °C under N_2. After 15 minutes, the solution was cooled to –116 °C, using an Et_2O/liquid nitrogen cooling bath, and after a further 15 minutes at this temperature, a solution of benzaldehyde (1.0 M in hexane, containing n-decane as an internal standard, 50 μL, 0.05 mmol, 1.0 eq.) was added dropwise, during ca 5 min. The mixture was allowed to react for another 15 minutes before methanol (1.0 ml) was added to quench the remaining organolithum species. The resulting mixture was allowed to warm up to room temperature and aqueous HCl (1 M, 1.0 ml) and MTBE (2.0 ml) were added, followed by rigorous stirring during 5 min. The stirring was discontinued and an

aliquot of the organic phase was diluted with MTBE and analysed using chiral stationary phase gas chromatography.

In this thesis the trivial nomenclature sulfamidate describes the 2,2-dioxo-1,2,3-oxathiazolidine-4-carboxylate system, and sulfamidite describes the 2-oxo-1,2,3-oxathiazolidine-4-carboxylate system.
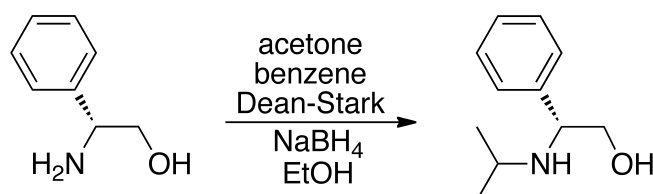
Reactions
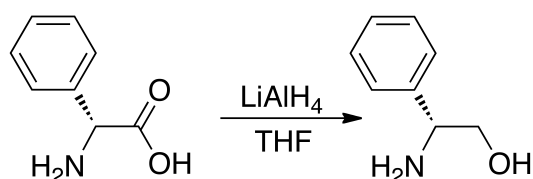
2-amino-2-phenylethanol (1)

LiAlH$_4$ (5.0 g, 138.7 mmol) was added slowly to distilled THF (250 ml) and cooled to 0°C. *(R)*-phenylglycine (10.0 g, 66.82 mmol) was carefully added portionwise. The mixture was stirred at RT for 1 h, then refluxed over night. The yellow reaction mixture was cooled to RT and quenched with NaOH (20 ml, 2 M). The yellow suspension was filtrated and the filtrate washed with THF (4 × 50 ml). The organic phase was concentrated in vacuo and NaOH (80 ml, 2 M) was added and the aqueous phase extracted with DCM (4 × 50 ml). The combined organic phases were washed with brine (2 × 50 ml), dried over MgSO$_4$ and concentrated to yield crude **1** as yellow crystals (9.0 g, 98% crude yield) NMR of the crude product shows the desired product. NMR was according to the litterature.

2-(isopropylamino)-2-phenylethanol (2a)

To a solution of **1** (500 mg, 3.64 mmol) in DCE (10 ml) was acetone (0.27 ml, 3.64 mmol) added at RT, under nitrogen and stirred for 20 min. A clear, yellow solution was formed and NaBH(OAc)$_3$ (1.37 g, 6.47 mmol) was added and an yellow suspension was received. After 2h of stirring at RT the reaction was quenched by adding saturated NaHCO$_3$ (5 ml) and the aqueous phase was

separated and extracted with DCM (3 × 15 ml). The combined organic layers were washed with brine, dried over MgSO₄ and concentrated to yield **2a** (578 mg, 89% crude yield) as a yellow solid as crude product. NMR showed the desired product. ^{1}H NMR (400 MHz, CDCl₃) δ 8.00 (d, J=44.9 Hz, 1 h), 7.51 (d, J=6.9 Hz, 1 h), 7.40 (dt, J=14.5, 7.0 Hz, 1 h), 7.26 (s, 0H), 4.37 – 4.22 (m, 0H), 4.09 – 3.93 (m, 0H), 3.86 (dd, J=12.3, 4.1 Hz, 0H), 3.73 (s, 1 h), 2.98 (dt, J=12.7, 6.4 Hz, 0H), 1.29 (d, J=6.6 Hz, 1 h), 1.21 (d, J=6.4 Hz, 1 h).


2-(isopropylamino)-2-phenylethanol (2b)

1 (1.0 g, 6,6 mmol) in benzene (30 ml) and acetone (1.96 ml, 26.4 mmol) were stirred for 1 h at RT, then refluxed for 1.5 h. The reaction mixture was evaporated and EtOH (20 ml, 99.7%) was added, which gave a cloudy, orange mixture. NaBH₄ (500 mg, 13.2 mmol) was added portionwise and stirred at RT over night (21 h). Water (10 ml) was added to quench the yellow suspension. The organic solvent was evaporated and the aqueous residue was extracted with DCM (4 × 25 ml). The combined organic phases were washed with brine (2 × 30 ml), dried over Na₂SO₄ and concentrated to yield **2b** as a yellow solid (1.16 g, 91% crude yield) as crude product.
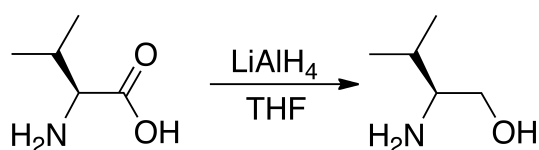
2-amino-3-methylbutan-1-ol (3)

LiAlH₄ (6.9 g, 180.84 mmol) was added slowly to distilled THF (250 ml) and cooled to 0°C. L-valine (10.0 g, 84.51 mmol) was carefully added portionwise. The mixture was stirred at RT for 1 h, then refluxed over night. The grey reaction mixture was cooled to RT and quenched with NaOH (20 ml, 2 M). The yellow suspension was filtrated and the filtrate washed with THF (4 × 50 ml). The organic phase was concentrated in vacuo and NaOH (80 ml, 2 M) was added and the aqueous phase extracted with DCM (4 × 50 ml). The combined organic phases were washed with brine (2 × 50

ml), dried over MgSO$_4$ and concentrated to yield crude **3** as yellow oil (10.51 g, 84% crude yield). NMR of the crude product shows the desired product and a very small amount of impurity.
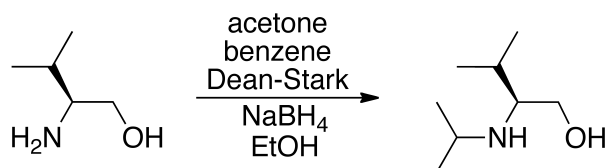
2-(isopropylamino)-3-methylbutan-1-ol (4)

To a solution of **3** (4.23 g, 41.0 mmol) in benzene (275 ml) was acetone (12 ml, 164 mmol) added at RT. The yellow solution was stirred at RT for 1 h and then refluxed with a Dean-Stark over night (14h). The solvent was evaporated to give a yellow oil (6.34 g) and EtOH (225 ml, 99.6%) was added, followed by portionwise addition of NaBH$_4$ (3.13 g, 165.5 mmol). The reaction mixture was stirred at RT over night and then refluxed for 1.5 h. Water (20 ml) was added and the organic solvent evaporated. The aqueous residue was extracted with DCM (3 × 40 ml). The combined organic layers were washed with brine, dried over MgSO$_4$ and concentrated to yield **4** (3.65 g, 61% crude yield) as yellow oil crude. NMR shows desired product.
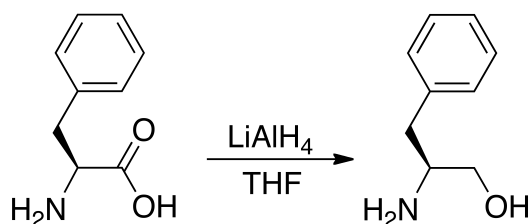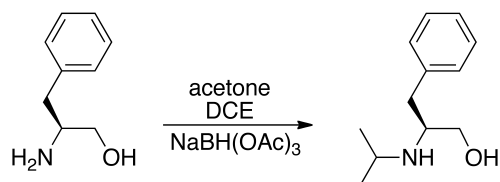

2-amino-3-phenylpropan-1-ol (5)

LiAlH$_4$ (9.2 g, 242.0 mmol) was added slowly to distilled THF (250 ml) and cooled to 0°C. Phenylalanine (10.0 g, 84.51 mmol) was carefully added portionwise. The mixture was stirred at RT for 1 h, then refluxed for 1 h. The reaction mixture was cooled to RT and quenched with NaOH (20 ml, 2 M). The yellow suspension was filtrated and The "LAH-cake" was refluxed for another 30 min. The suspension was filtrated and the combined organic phases was dried over Na$_2$SO$_4$ to yield crude **5** as yellow oil (8.96 g, 98% crude yield). NMR shows desired product with a small amount of impurities. ^{1}H NMR (400 MHz, CDCl$_3$) δ 7.22-7.37 (m, 5H), 3.68 (dd, J=10.7, 3.6 Hz, 1 h), 3.43 (dd, J=10.6, 7.3 Hz, 1 h), 3.16 (s, 1 h), 2.83 (dd, J=13.5, 5.2 Hz, 1 h), 2.58 (dd, J=13.4, 8.6 Hz, 1 h), 2.36 (s, 3H). ^{13}C NMR (400 MHz, CDCl$_3$) δ 138.67, 129.23, 128.59, 126.43, 77.48, 77.16, 76.84, 66.01, 54.25, 40.61, 30.38.

2-(isopropylamino)-3-phenylpropan-1-ol (6a)

To a solution of **5** (1.0 g, 6.6 mmol) in DCE (10 ml) was acetone (0.49 ml, 6.6 mmol) added at RT, under nitrogen and stirred for 10 min. When a clear, orange solution had formed NaBH(OAc)$_3$ (2.49 g, 11.76 mmol) was added and an orange suspension was received. After 3h of stirring at RT the reaction had gone to completion according to TLC (EtOAc/HOAc/H$_2$O, 3:1:1). The reaction was quenched by adding saturated NaHCO$_3$ (7 ml) and the aqueous phase was separated and extracted with DCM (3 × 20 ml). The combined organic layers were washed with brine, dried over MgSO$_4$ and concentrated to yield **6a** as yellow solid (1.25 g, 97% crude yield) as crude product. NMR shows the desired product. ^{1}H NMR (400 MHz, CDCl$_3$) δ 7.29 (m, 5H), 4.57 (s, 2H), 3.78 (m, 2H), 3.34 (q, J=9.2 Hz, 1 h), 3.23 (m, 0H), 3.14 (dd, J=13.7, 5.9 Hz, 1 h), 3.04 (dd, J=13.7, 9.2 Hz, 1 h), 1.40 (dd, J=13.9, 6.5 Hz, 1 h).
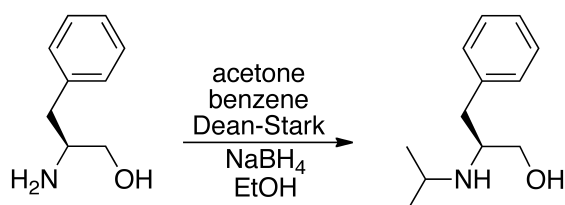
2-(isopropylamino)-3-phenylpropan-1-ol (6b)

To a solution of **5** (3.0 g, 19.84 mmol) in benzene (60 ml) was acetone (6.2 ml, 79.36 mmol) added at RT. The orange solution was stirred at RT for 1.5 h and then refluxed with a Dean-Stark for 2h. The solvent was evaporated and EtOH (70 ml, 99.6%) was added, followed by portionwise addition of NaBH$_4$ (1.5 g, 79.30 mmol). The reaction mixture was stirred at RT over night. Water (20 ml) was added and the organic solvent evaporated. The aqueous residue was extracted with DCM (3 × 40 ml). The combined organic layers were washed with brine, dried over MgSO$_4$ and concentrated to yield a brown oil (3.54 g, 92% crude yield) as crude product of **6b**. NMR shows desired product. ^{1}H NMR (400 MHz, CDCl$_3$) δ 7.24 (ddd, J=32.1, 19.8, 7.2 Hz, 2H), 3.55 (dd, J=10.3, 3.8 Hz, 0H), 3.23 (m, 1 h), 2.96 (m, 0H), 2.86 (m, 1 h), 2.73 (qd, J=13.5, 6.9 Hz, 1 h), 1.02 (d, J=6.2 Hz, 3H), 0.97 (d, J=6.2 Hz, 3H). ^{13}C NMR (400 MHz, CDCl$_3$) δ 138.57, 129.29, 128.60, 126.47, 115.04, 63.11, 57.32, 45.99, 38.64, 23.51.
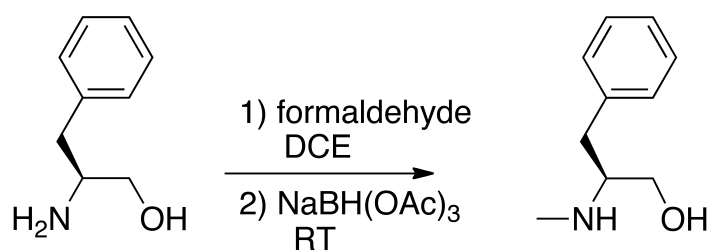
2-(methylamino)-3-phenylpropan-1-ol (7)

To a solution of **5** (760 mg, 5.03 mmol) in DCE (8 ml) was formaldehyde (0.41 ml, 5.5 mmol) added at RT, under nitrogen and stirred for 10 min. When a clear, orange solution had formed NaBH (OAc)$_3$ (4.26 g, 20.1 mmol) was added and an orange suspension was received. After 20h of stirring at RT the reaction was quenched by adding saturated NaHCO$_3$ until no gas evolution was observed. The aqueous phase was separated and extracted with DCM (3 × 20 ml). The combined organic layers were washed with brine, dried over MgSO$_4$ and concentrated to yield **7** as brown oil (728 mg, 89% crude yield) as crude product. NMR shows the desired product and some impurities.
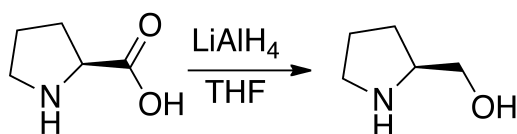
Pyrrolidin-2-ylmethanol (8)

LiAlH$_4$ (6.6 g, 173.3 mmol) was added slowly to distilled THF (300 ml) and cooled to 0°C. L-Proline (10.0 g, 86.9 mmol) was carefully added portionwise. The mixture was stirred at RT for 1 h, then refluxed for 1 h. The reaction mixture was cooled to RT and quenched with NaOH (20 ml, 2 M). The yellow suspension was filtrated and the resulting LiOH was refluxed for another 30 min. The slurry was filtrated and the combined organic phases was dried over Na$_2$SO$_4$ to yield crude **8** as yellow oil (8.91 g, 100% crude yield). ^{1}H NMR (400 MHz, a few drops of MeOD in CDCl$_3$) δ 3.50 (dd, J=11.2, 4.0 Hz, 3H), 3.32 (dd, J=11.1, 7.3 Hz, 1 h), 3.15 (m, 1 h), 2.83 (dd, J=11.7, 6.6 Hz, 2H), 1.72 (m, 3H), 1.35 (qd, J=12.2, 7.8 Hz, 1 h). ^{13}C NMR (400 MHz, a few drops of MeOD in CDCl$_3$) δ 64.53, 59.86, 46.15, 27.38, 25.66. ^{13}C NMR (400 MHz, CDCl$_3$) δ 64.41, 59.95, 46.27, 27.52, 25.82.
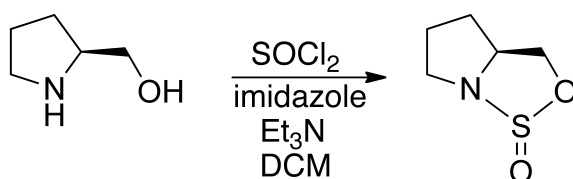
Tetrahydro-3H-pyrrolo[1,2-c][1,2,3]oxathiazole 1-oxide (9)

To a solution of **8** (12.55 g, 124.07 mmol) in distilled DCM (60 ml) was Et₃N (33.9 ml, 248.1 mmol) and imidazole (33.0 g, 496.0 mmol) added to give a brown suspension. This was cooled to 0°C and thionyl chloride (18.0 ml, 248.1 mmol) was added dropwise. After complete addition (2h) the reaction mixture was stirred at RT for 1 h and put on icebath over night. The reaction mixture was filtered and the organic phase washed with brine and water. The aqueous phase was extracted with EtOAc (3 × 40 ml). The combined organic phases were dried over Na₂SO₄ and concentrated to yield crude **9** as yellow oil (16.98 g, 93% crude yield). NMR shows pure desired product as a mixture of two rotamers in a 1:2 ratio. ^{1}H NMR (400 MHz, CDCl₃) δ 4.81 (m, 1 h), 4.41 (m, J=6.2 Hz, 1 h), 4.21 (m, 1 h), 4.15 (m, J=6.6 Hz, 1 h), 4.00 (m, J=17.1, 8.7 Hz, 1 h), 3.39 (m, 2H), 3.23 (m, 1 h), 3.05 (m, J=14.5, 7.1 Hz, 3H), 2.81 (m, J=4.3 Hz, 1 h), 2.02-1.51 (m, 3H), 1.64-1.54 (m, J=1 h). ^{13}C NMR (400 MHz, CDCl3) δ 74.25, 71.38, 65.66, 64.79, 48.17, 44.75, 31.21, 30.43, 28.65, 28.44, 25.26.
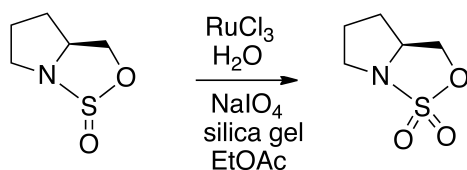
Tetrahydro-3H-pyrrolo[1,2-c][1,2,3]oxathiazole 1,1-dioxide (10)

RuCl₃ (2.0 mg, 0.15 mol%) was added to water (3.4 ml) and a black solution was formed. This solution was stirred at a brisk pace and NaIO₄ (1.55 g, 7.23 mmol) was then added, giving an immediate colour change resulting in a clear, yellow solution of RuO₄. Not all of the NaIO₄ was dissolved, but as much of the NaIO₄ was added to the solution and the rest of NaIO₄ was added directly to the reaction flask as a solid. This RuO₄ solution was added dropwise to silica gel (6.8 g) in a 100 ml round bottom flask with a magnetic stirring bar. After complete addition the rate of stirring was increased and the solid was stirred until a free flowing solid was obtained, to give a white solid. EtOAc (25 ml) was added to the wet silica gel and put on an ice bath. **9** (958 mg, 6.51 mmol) was dissolved in EtOAc (5 ml) and the solution was added dropwise to the slurry of silica gel at 0 °C. After complete addition the ice bath was removed and stirred at a brisk pace throughout the reaction. An orange slurry was formed and TLC (silica, hexane/EtOAc 3:1) indicated complete consumption of the starting material after 20 min. The slurry was filtrated through a short pad of silica gel, dried over Na₂SO4, filtrated and concentrated in vacuo to give crude **10** (756.6 mg, 4.64, mmol 71% crude) as yellow crystals. ^{1}H NMR (400 MHz, CDCl₃) δ 4.54 (m, 1 h), 4.27 (dt, J=12.8,

6.5 Hz, 1 h), 4.03 (dd, *J*=8.5, 6.3 Hz, 1 h), 3.66 (m, 1 h), 3.25 (dt, *J*=11.0, 7.2 Hz, 1 h), 2.17 (dq, *J*=14.7, 7.3 Hz, 1 h), 1.94 (m, 2H), 1.81 (dt, *J*=12.0, 5.3 Hz, 1 h). ^{13}C NMR (400 MHz, CDCl$_3$) δ 71.90, 62.56, 51.14, 31.30, 25.18.
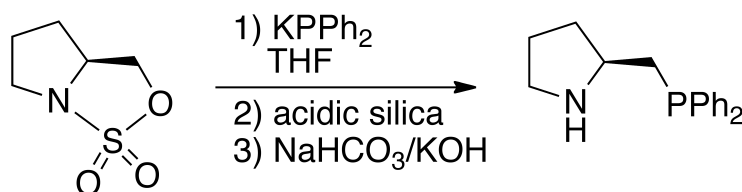
**2-((diphenylphosphino)methyl)pyrrolidine (11)**

To a solution of **10** (4.6 g, 28.19 mmol) in dry THF (55 ml) at -78 °C, a solution of KPPh$_2$ (0.5 M in THF, 62.0ml, 31.0 mmol) was added dropwise to give a red solution. After 10 min of stirring at -78 °C, TLC (hexane/EtOAc/Et$_3$N, 10:1:0.1) indicated complete disappearance of the starting material. Acidic silica (22g silica and 0.8 ml 3.5 M aq. H$_2$SO$_4$, evenly mixed to a white powder) was added portionwise until pH=1. The resulting white slurry was stirred at RT for 1 h, followed by the addition of saturated aqueous NaHCO$_3$ (50 ml) and KOH (2 M, 83 ml). The mixture was stirred for 1 h and filtered off and washed with brine (3 × 50 ml). The combined aqueous layers were extracted with CH$_2$Cl$_2$ (3 × 10 ml) and the combined organic layers were dried over Na$_2$SO$_4$ and evaporated under reduced pressure to give a yellow oil (12.69 g, 167% crude), which was purified by column chromatography (MeOH/DCM/NH$_4$OH, 10:70:1) to yield **11** (6.67 g, 88%) as a beige foam. ^{1}H NMR (400 MHz, CDCl$_3$) δ 7.43 (m, 5H), 7.29 (m, 6H), 3.35 (m, 2H), 3.20 (m, *J*=14.5, 10.7 Hz, 1 h), 2.90 (dd, *J*=13.2, 5.5 Hz, 1 h), 2.49 (dd, *J*=13.2, 9.7 Hz, 1 h), 2.09 (m, 1 h), 2.00 (m, *J*=9.6 Hz, 1 h), 1.83 (m, 1 h), 1.72 (m, 1 h). ^{13}C NMR (400 MHz, CDCl$_3$) δ 137.08, 136.28, 133.31, 133.12, 132.88, 132.69, 129.28, 129.16, 128.90, 128.81, 128.74, 58.56, 58.35, 44.47, 31.63, 31.48, 31.40, 23.71. ^{1}h NMR (400 MHz, THF-d$_8$) δ 7.60 (t, *J*=7.4 Hz, 1 h), 7.32 (ddd, *J*=41.2, 15.3, 7.1 Hz, 6H), 3.32 (dd, *J*=15.7, 6.9 Hz, 1 h), 3.21 (t, *J*=5.2 Hz, 1 h), 3.05 (d, *J*=13.9 Hz, 1 h), 2.03 (t, *J*=12.4 Hz, 1 h), 1.71 (dd, *J*=15.1, 9.9 Hz, 2H). ^{13}C NMR (400 MHz, THF-d$_8$) δ 141.76, 141.62, 139.36, 139.23, 134.06, 133.87, 133.76, 133.57, 129.40, 129.33, 129.31, 129.14, 129.07, 128.96, 59.30, 59.08, 50.72, 37.43, 37.30, 33.31, 33.24. ^{1}h NMR (400 MHz, DMSO-d$_6$) δ 7.53 (t, *J*=7.4 Hz, 1 h), 7.32 (m, 2H), 3.46 (s, 1 h), 2.98 (ddd, *J*=17.8, 15.0, 8.9 Hz, 1 h), 1.92 (t, *J*=12.4 Hz, 1 h), 1.77 (dt, *J*=14.9, 7.6 Hz, 1 h), 1.60 (m, 1 h). ^{13}C NMR (400 MHz, DMSO-d$_6$) δ 140.05, 139.91, 138.08, 137.95, 132.72, 132.53, 132.33, 132.15, 128.49, 128.46, 128.42, 128.35, 128.30, 57.20, 56.98, 49.28, 35.51, 35.39, 31.94, 31.86, 23.92. ^{13}C NMR (400 MHz, CDCl$_3$) δ

137.08, 136.16, 133.31, 133.12, 132.88, 132.69, 129.28, 129.16, 128.90, 128.81, 128.74, 58.56, 58.35, 44.47, 31.63, 31.48, 31.40, 23.71.
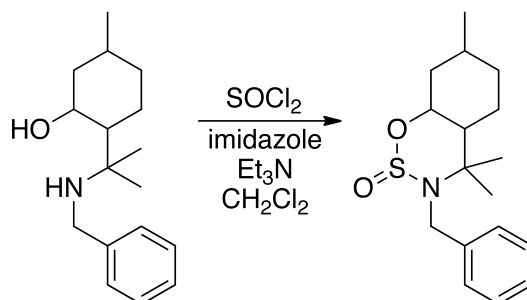
**3-benzyl-4,4,7-trimethyloctahydrobenzo[e][1,2,3]oxathiazine 2-oxide (12)**

To a solution of 3-benzyl-4,4,7-trimethyloctahydrobenzo[e][1,2,3]oxathiazine 2-oxide (100 mg, 0.383 mmol) in distilled DCM (1 ml) was Et₃N (0.11 ml, 0.765 mmol) and imidazole (104 mg, 1.53 mmol) added. This was cooled to 0°C and thionyl chloride (0.04 ml, 0.574 mmol) was added dropwise and a white thick slurry was formed. After complete addition the icebath was removed. TLC in heptan/EtOAc/MeOH/NH₄OH (1:1:10%:1) showed the reaction had gone to completion after 10 min. Water (1 ml) was added to quench the reaction. The organic phase was washed with brine and dried over Na₂SO₄ and evaporated under reduced pressure to yield **12** as white crystals (120 mg, 102% crude yield). NMR shows desired product as a mixture of two rotamers. ^{13}C NMR (400 MHz, CDCl₃) δ 140.93, 139.62, 128.52, 128.35, 127.35, 127.25, 126.70, 76.39, 66.26, 60.90, 59.29, 49.63, 47.63, 45.91, 44.53, 41.80, 41.05, 40.66, 34.56, 34.35, 31.56, 31.39, 27.63, 25.24, 22.15, 22.01, 21.62.
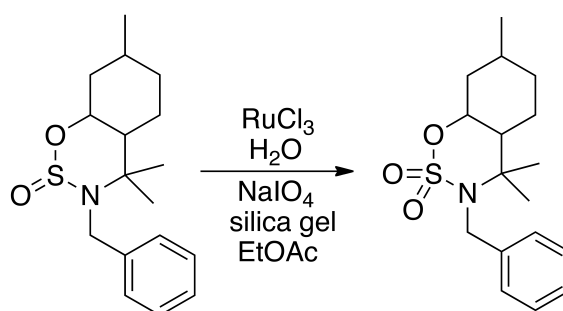
3-benzyl-4,4,7-trimethyloctahydrobenzo[e][1,2,3]oxathiazine 2,2-dioxide (13)

RuCl₃ (0.10 mg, 0.15 mol%) was added to water (0.78 ml) and a brown solution was formed. This solution was stirred at a brisk pace and NaIO₄ (108.5 g, 0.507 mmol) was then added, giving an immediate colour change resulting in a clear, yellow solution of RuO₄. Not all of the NaIO₄ was dissolved, but as much of the NaIO₄ was added to the solution and the rest of NaIO₄ was added directly to the reaction flask as a solid. This RuO₄ solution was added dropwise to silica gel (1.95 g)

in a 100 ml round bottom flask with a magnetic stirring bar. After complete addition the rate of stirring was increased and the solid was stirred until a free flowing solid was obtained, to give a white solid. EtOAc (25 ml) was added to the wet silica gel and put on an ice bath. The **12** (120 mg, 0.390 mmol) was dissolved in EtOAc (5 ml) and the solution was added dropwise to the slurry of silica gel at 0 °C. After complete addition the ice bath was removed and stirred at a brisk pace throughout the reaction. TLC heptan/EtOAc/MeOH/NH$_4$OH (1:1:10%:1) indicated complete consumption of the starting material after 10 min. The slurry was filtrated through a short pad of silica gel, dried over Na$_2$SO$_4$, filtrated and concentrated in vacuo to yield crude **13** (105 mg, 0.324 mmol, 83% crude) as yellow oil. NMR shows desired product. ^{1}H NMR (400 MHz, DMSO-d$_6$) δ 7.40 (m, J=7.5 Hz, 2H), 7.32 (t, J=7.5 Hz, 2H), 7.23 (m, 2H), 4.69 (m, J=10.9, 6.5 Hz, 2H), 4.20 (d, J=17.4 Hz, 1 h), 2.16 (m, J=12.2 Hz, 1 h), 1.78 (m, 3H), 1.56 (s, 3H), 1.36 (s, 3H), 1.09 (s, 3H), 0.99 (d, J=6.5 Hz, 3H). ^{13}C NMR (400 MHz, CDCl$_3$) δ 139.47, 128.49, 127.09, 126.90, 81.92, 64.47, 49.38, 46.76, 40.16, 33.84, 31.36, 27.35, 25.55, 21.86, 18.31.
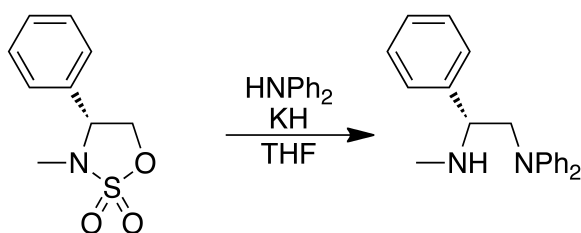
**N^1-isopropyl-N^2,N^2,1-triphenylethane-1,2-diamine (14)**

A solution of HNPh$_2$ (618.0 mg, 3.65 mmol) in dry THF (2.5 ml) was added to a slurry of KH (180.0 mg, 4.49 mmol) and dry THF (2 ml) in the glovebox. Stirred at RT for 2h. **36** (874.0 mg, 3.62 mmol) dissolved in dry THF (3 ml) was added dropwise to the slurry and gave an orange solution. The reaction mixture was refluxed over night. Acidic silica (22g silica and 0.8 ml 3.5 M aq. H$_2$SO$_4$, evenly mixed to a white powder) was added portionwise until pH=1. The resulting slurry was stirred at RT for 2h, followed by the addition of saturated aqueous NaHCO$_3$ (10 ml) and NaOH (5M, 3 ml). The mixture was stirred for 20 min. TLC (hexane/EtOAc, 6:1) shows desired product. The reaction mixture was filtered off and washed with brine (2 × 10 ml). The combined aqueous layers were extracted with CH$_2$Cl$_2$ (3 × 10 ml) and the combined organic layers were dried over Na$_2$SO$_4$ and evaporated under reduced pressure to give an orange oil (1.07 g, 89% crude), which was purified by column chromatography (hexane/EtOAc, 6:1) to yield crude **14** (724 mg, 88%) as an orange oil. ^{1}H NMR (400 MHz, CDCl$_3$) δ 7.34 (m, 4H), 7.25 (m, J=8.9, 6.5 Hz, 5H), 6.96 (m, J=13.9, 7.6 Hz, 6H), 4.08 (dd, J=8.1, 5.6 Hz, 1 h), 3.82 (m, 2H), 2.57 (m, 1 h), 1.50 (s, 01

h), 0.92 (d, J=6.4 Hz, 3H), 0.87 (d, J=6.1 Hz, 3H). ^{13}C NMR (400 MHz, CDCl$_3$) δ 148.36, 143.01, 129.34, 128.49, 127.55, 121.69, 121.49, 77.48, 77.16, 76.84, 60.18, 58.59, 46.47, 24.59, 22.29.
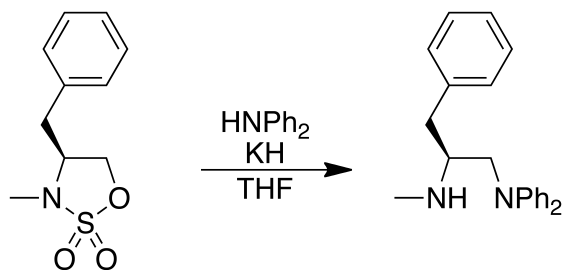
**N^2-methyl-N^1,N^1,3-triphenylpropane-1,2-diamine (15)**

A solution of HNPh$_2$ (446.4 mg, 2.64 mmol) in dry THF (3 ml) was added to a slurry of KH (100 mg, 2.49 mmol) and dry THF (2 ml) in the glovebox. Stirred at RT for 10 min. **17** (400 mg, 1.76 mmol) dissolved in dry TH (2 ml) was added dropwise to the slurry. The reaction mixture was refluxed for 2h. Acidic silica (22g silica and 0.8 ml 3.5 M aq. H$_2$SO$_4$, evenly mixed to a white powder) was added portionwise until pH=1. The resulting slurry was stirred at RT for 1.5 h, followed by the addition of NaOH (2 M) until a pH=10. The mixture was stirred for 20 min. The reaction mixture was filtered off and washed with brine (2 × 10 ml). The combined aqueous layers were extracted with CH$_2$Cl$_2$ (3 × 10 ml) and the combined organic layers were dried over Na$_2$SO$_4$ and evaporated under reduced pressure to give an orange oil (495.6 mg, 89% crude), which was purified by column chromatography (hexane/EtOAc, 6:1) to yield **15** (445.5 mg, 80%) as a brown oil. ^{13}C NMR (400 MHz, CDCl$_3$) δ 148.46, 143.19, 138.66, 129.43, 129.39, 129.34, 129.18, 128.61, 126.53, 121.82, 121.49, 121.06, 117.88, 59.50, 55.91, 38.59, 34.37, 30.46.
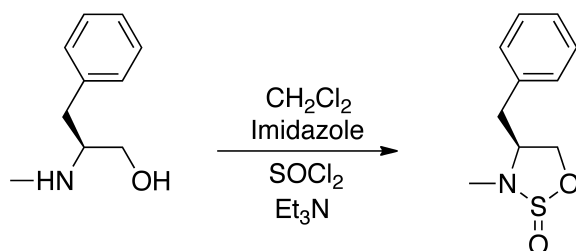
4-benzyl-3-methyl-1,2,3-oxathiazolidine 2-oxide (16)

A solution of 2-(methylamino)-3-phenylpropan-1-ol (1.8 g, 10.89 mmol), imidazole (10.09 g, 148.2 mmol), and Et$_3$N (3.0 ml, 21.78 mmol) in dry CH$_2$Cl$_2$ (10 ml) was cooled to 0 °C on an ice bath. To the stirred yellow solution, SOCl$_2$ (1.18 ml, 16.34 mmol) was added dropwise. TLC (EtOAc/HOAc/ H$_2$O, 3:1:1) showed the reaction was completed after 10 min of stirring. Water was added and the

aqueous phase was extracted with DCM (3 × 20 ml). The organic phase was washed with brine, dried over $MgSO_4$, and concentrated to yield **16** (2.41 g, 104% crude) as a yellow liquid. NMR of the crude product shows the desired sulfamidites as a mixture of two diastereoisomers. ^{1}H NMR (400 MHz, $CDCl_3$) δ 7.33 (m, 10H), 4.70 (t, *J*=7.7 Hz, 2H), 4.45 (t, *J*=7.8 Hz, 0H), 4.19 (t, *J*=8.0 Hz, 1 h), 3.88 (m, 1 h), 3.63 (m, 1 h), 3.29 (dd, *J*=13.5, 5.3 Hz, 1 h), 3.16 (dd, *J*=13.4, 5.2 Hz, 1 h), 2.97 (dd, *J*=13.5, 9.2 Hz, 1 h), 2.91 (s, 3H), 2.76 (s, 3H), 2.72 (dd, *J*=13.7, 8.9 Hz, 1 h). ^{13}C NMR (400 MHz, $CDCl_3$) δ 137.33, 136.58, 134.87, 128.89, 128.80, 128.76, 127.02, 126.91, 121.39, 75.81, 75.11, 66.02, 60.75, 38.29, 37.67, 32.25, 30.51.
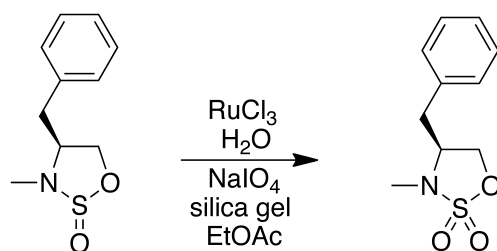
### 4-benzyl-3-methyl-1,2,3-oxathiazolidine 2,2-dioxide (17)

$RuCl_3$ (3.4 mg, 0.15 mol%) was added to water (4 ml) and a brown solution was formed. This solution was stirred at a brisk pace and $NaIO_4$ (3.03 g, 14.16 mmol) was then added, giving an immediate colour change resulting in a clear, yellow solution of RuO_4. Not all of the $NaIO_4$ was dissolved, but as much of the $NaIO_4$ was added to the solution and the rest of $NaIO_4$ was added directly to the reaction flask as a solid. This RuO_4 solution was added dropwise to silica gel (10 g) in a 250 ml round bottom flask with a magnetic stirring bar. After complete addition the rate of stirring was increased and the solid was stirred until a free flowing solid was obtained, to give a white solid. EtOAc (30 ml) was added to the wet silica gel and put on an ice bath. **16** (2.3 g, 10.89 mmol) was dissolved in EtOAc (10 ml) and the solution was added dropwise to the slurry of silica gel at 0 °C. The slurry changed from a yellow to a beige slurry. After complete addition the ice bath was removed and stirred at a brisk pace throughout the reaction. TLC (EtOAc/HOAc/H_2O, 3:1:1) indicated complete consumption of the starting material after 1.5 h. The slurry was filtrated through a short pad of silica gel, dried over Na_2SO_4, filtrated and concentrated in vacuo to yield crude 4-benzyl-3-methyl-1,2,3-oxathiazolidine 2,2-dioxide (2.29 g, 10.3 mmol, 92% crude) as brown oil. NMR shows desired product. The crude product was purified by column chromatography (hexane/ EtOAc, 6:1, 3:1) to yield **17** as a brown oil (971 mg, 39%). ^{1}H NMR (400 MHz, $CDCl_3$) δ 7.28 (ddd, *J*=45.4, 24.3, 7.1 Hz, 5H), 4.35 (t, *J*=7.6 Hz, 1 h), 4.20 (t, *J*=8.1 Hz, 1 h), 3.71 (m, 1 h), 3.16

(dd, *J*=13.3, 5.5 Hz, 1 h), 2.81 (m, 4H). ^{13}C NMR (400 MHz, CDCl$_3$) δ 134.67, 129.21, 129.14, 127.67, 70.98, 61.80, 38.06, 32.81.
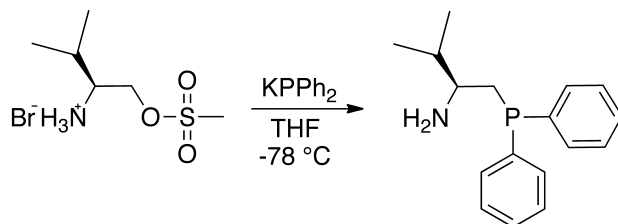

1-(diphenylphosphino)-3-methylbutan-2-amine (18)

To a solution of 2-((methylsulfonyl)oxy)-1-isoporpylethanaminium bromide (2.0 g, 7.63 mmol) in distilled THF (40 ml) at -78°C was KPPh$_2$ (0.5M in THF, 32.0 ml, 16.02 mmol) added dropwise over a period of 25 min. A clear, orange solution was formed and stirred on the dry ice bath over night.(14h) The day after an orange slurry had formed and was filtered through Celite. The organic phase was dried over Na$_2$SO$_4$, filtrated and concentrated in vacuo to give **18** (3.93 g, 14.48 mmol, 190% crude) as yellow oil as crude product, which was purified by column chromatography (hexane/EtOAc/Et$_3$N, 4:1:0.02, 1:2:0.02) to yield **18** (1.73 g, 84%) as a colourless oil.
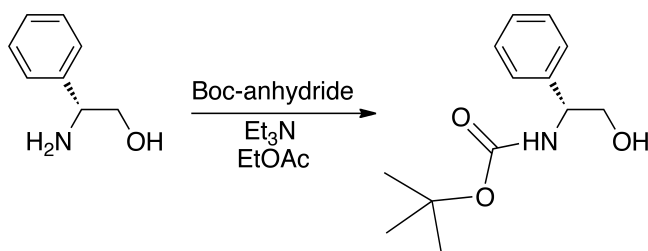
***Tert*-butyl (2-hydroxy-1-phenylethyl)carbamate (19)**

To a solution of **1** (8.0 g, 58.32 mmol) in EtOAc (120 ml) was Et$_3$N (8.9 ml, 64.15 mmol) added. A clear yellow solution was formed and di-*tert*-butyl dicarbonate (13.12 g, 60.12 mmol) was added in portions. A yellow precipitate was formed and after 3h of stirring at RT TLC (hexane/EtOAc, 1:1) showed the reaction had gone to completion. KHSO$_4$ (1 M, 100 ml) was added and the aqueous phase separated and extracted with Et$_2$O (4 × 50 ml). The combined organic phases were washed with brine (2 × 50 ml), dried over Na$_2$SO$_4$ and filtrated, concentrated in vacuo to yield crude **19** as yellow crystals (14.37 g, 98%) as crude product. NMR shows desired product. The NMR was found to be identical with those reported in the literature.
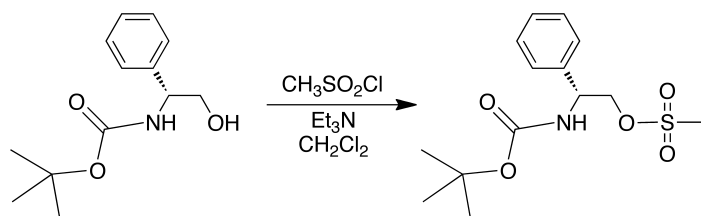
2-((tert-butoxycarbonyl)amino)-2-phenylethyl methanesulfonate (20)

A yellow solution of 19 (16.03 g, 63.78 mmol) and Et₃N (10.5 ml, 76.54 mmol) in DCM (250 ml) was cooled to -78°C and methanesulfonyl chloride (5.48 ml, 70.51 mmol) was added dropwise. After complete addition the reaction mixture was stirred at RT over night (19h). Water was added and the aqueous phase was extracted with DCM (3 × 80 ml). The combined organic layers were washed with NaOH (1 M, 70 ml), HCl (1 M, 80 ml), brine (2 × 50 ml) and dried over Na_2SO_4, filtrated and concentrated in vacuo to give **20** as a yellow solid (20.98 g, 104%) as crude product. Recrystallization of the crude product resulted in the desired product as white crystals (12.66 g, 64% yield). NMR shows desired product and a small amount of impurity. The NMR was found to be identical with those reported in the literature.
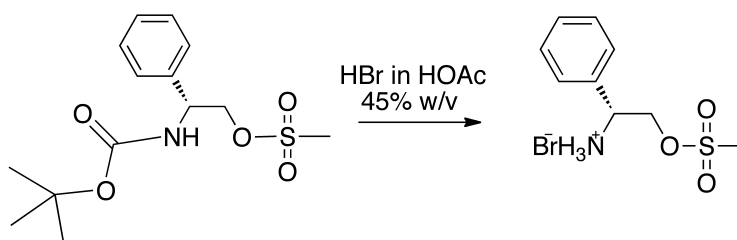
2-((methylsulfonyl)oxy)-1-phenylethanaminium bromide (21)

To a solution of HBr in HOAc (45 %, 1.37 ml, 7.96 mmol) at RT was **20** (1.51 g, 4.80 mmol) added slowly and portionwise, which gave a dark yellow solution. After 5 min of stirring a white precipitate was formed. Et₂O was added after 1.5 h of stirring, then stirred for another 10 min. The reaction mixture was filtrated and concentrated in vacuo to give **21** (1.12 g, 79% crude) as white crystals. NMR shows desired product.
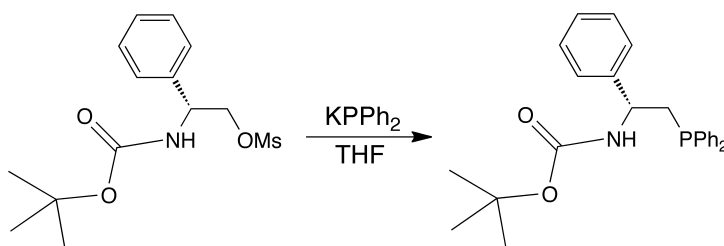
Tert-butyl (2-(diphenylphosphino)-1-phenylethyl)carbamate (22)

20 (3.45 g, 10.94 mmol) was added dropwise to a solution of KPPh$_2$ (21.9 ml, 10.94 mmol) in dry THF (30 ml). A clear red solution was formed. The reaction mixture was stirred at RT over night and a beige suspension was formed. The suspension was stirred at RT over night (22h). The received slurry was refluxed and TLC (hexane/EtOAc, 6:1) showed desired product after 1.5 h. After 3.5 h of refluxing Et$_2$O was added to dilute the slurry and the mixture was washed with water (2 × 25 ml). The combined organic phases were dried over MgSO$_4$, filtered and concentrated in vacuo to give tert-butyl (2-(diphenylphosphino)-1-phenylethyl)carbamate (5.84 g, 132%) as a yellow solid as crude product. The crude product was purified by column chromatography (hexane/ EtOAc, 6:1, 1:1) to yield crude **22** as white crystals. Recrystallisation in hexane/EtOAc gave **22**(4.0 g, 90%) as white crystals. NMR showed pure desired product.
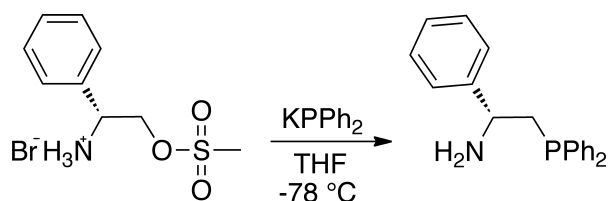
2-(diphenylphosphino)-1-phenylethanamine (23a)

To a solution of **21** (1.5 mg, 5.06 mmol) in distilled THF (150 ml) at -78 °C was KPPh$_2$ (0.5M in THF, 21.3 ml, 10.64 mmol) added dropwise. A yellow solution was formed and stirred at -78 °C for 1 h, then at RT over night. The day after a yellow suspension had formed and was filtered through Celite. The organic phase was dried over Na$_2$SO$_4$, filtrated and concentrated in vacuo to yield crude 2-(diphenylphosphino)-1-phenylethanamine (2.9 g, 187% crude) as crude product, which was purified by column chromatography (hexane/EtOAc/Et$_3$N, 4:1:0.3, 4:4:0.3) to yield **23a** (1.21 g, 78%) as a colourless oil. NMR shows pure desired product.
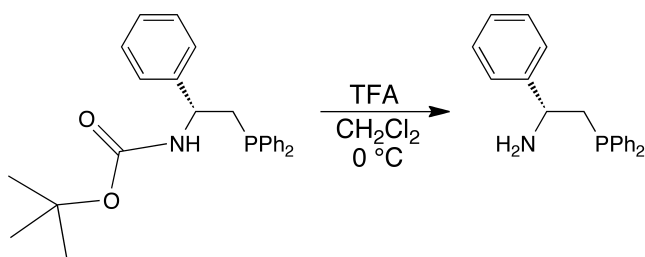
2-(diphenylphosphino)-1-phenylethanamine (23b)

To a solution of **22** (160 mg, 0.40 mmol) in DCM at 0 °C was trifluoroacetic acid (1.40 ml, 18.95 mmol) added dropwise and stirred at 0°C for 1 h, then at RT over night. TLC (hexane/EtOAc, 6:1)

showed the reaction had gone to completion and was quenched by adding water. The organic phase was neutralized with NaOH (5M) and the aqueous phase was extracted with DCM (3 × 50 ml). The combined organic phases were washed with saturated NaHCO₃, brine and dried over MgSO₄ and concentrated in vacuo to yield crude 2-(diphenylphosphino)-1-phenylethanamine (240 mg, 200%) as a light yellow oil as crude product, which was purified by column chromatography (aluminium oxide, hexane/EtOAc, 1:4) to yield **23b** (60 mg, 60 %) as a colourless oil.
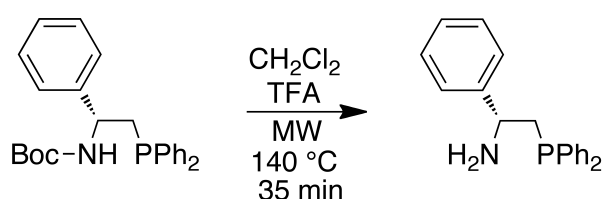
2-(diphenylphosphino)-1-phenylethanamine (24c)

To a solution of **22** (160 mg, 0.40 mmol) in DCM (5 ml) was trifluoroacetic acid (2.1 ml, 12.0 mmol) added and put under microwave irradiation and using fixed hold-time for 35 min in a sealed vial. NMR shows dersired product **24c** and some aziridine as by-product (25%).
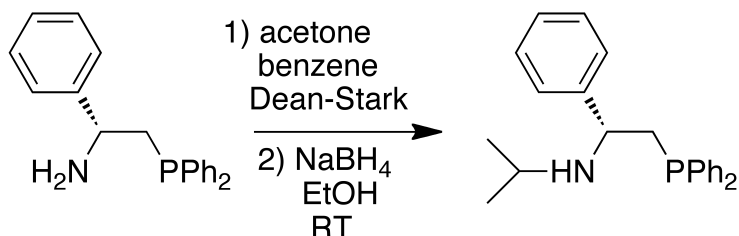
N-(2-(diphenylphosphino)-1-phenylethyl)propan-2-amine (25)

To a solution of **24c** (360 mg, 1.18 mmol) in benzene (10 ml) was acetone (0.35 ml, 4.72 mmol) added and stirred for 30 min at RT, then refluxed with Dean-Stark over night. The reaction mixture was concentrated in vacuo and dissolved in EtOH (96%, 15 ml). NaBH₄ (137 mg, 3.62 mmol) was added slowly and stirred at RT over night. Water (5 ml) was added to the reaction mixture and concentrated in vacuo. The residue was extracted with DCM (3 × 40 ml) and the combined organic phases were washed with brine (2 × 20 ml), dried over Na₂SO₄, filtrated and concentrated in vacuo to give N-(2-(diphenylphosphino)-1-phenylethyl)propan-2-amine (400 mg, 98%) as a yellow oil, which was purified by column chromatography (3% Et₃N in hexane) to give **25** (370 mg, 90%) as a colourless oil. NMR shows desired product.

_N_-(2-hydroxy-1-phenylethyl)-N-isopropylformamide (26)

A solution of **2a** (778.6 mg, 4.34 mmol) in ethylformiate (0.45 ml, 5.65 mmol) was subjected to microwave irradiation at 150 °C and using fixed hold-time for 10 min in a sealed vial. The orange oil was concentrated in vacuo and gave _N_-(2-hydroxy-1-phenylethyl)-N-isopropylformamide (959 mg, 107% crude) as an orange oil as crude product, which was purified by column chromatography (hexane/EtOAc, 1:4) to yield **26** (230 mg, 26%) as a beige solid. NMR shows desired p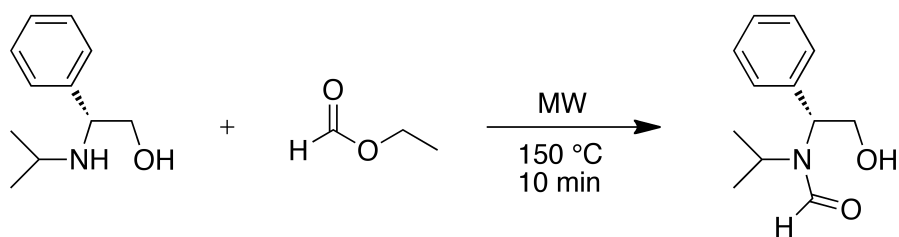roduct as diastereoisomers in 1:2.4 ratio. ^{1}H NMR (400 MHz, CDCl$_3$) δ 8.41 (s, 1 h), 8.40 (s, 1 h), 7.2-7.4 (m, 5H), 4.85 (m, 1 h), 4.56 (t, 1 h), 4.23 (m, 2H), 4.05 (m, 2H), 3.65 (m, 2H), 2 (t, 1 h), 1.32 (m, 6H), 1.07 (d, 3H), 1.01 (d, 3H).
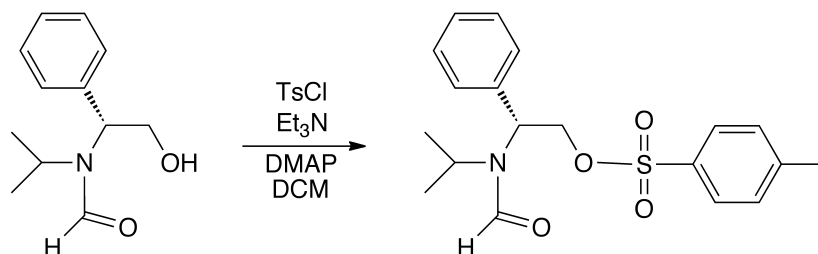
2-(N-isopropylformamido)-2-phenylethyl benzenesulfonate (27)

Tosyl chloride (212 mg, 1.11 mmol, purified in Soxlet) was added in portions to a solution of **26** (230 mg, 1.11 mmol), Et$_3$N (0.17 ml, 1.22 ml) and DMAP (5.5 mg, 0.045 mmol) at RT. The light yellow solution that was stirred at RT for 23h. Saturated NH$_4$Cl (20 ml) was added and the aqueous phase was extracted with DCM (2 × 15 ml). The combined organic phases were dried over NaSO$_4$ and concentrated in vacuo to give 2-(N-isopropylformamido)-2-phenylethyl benzenesulfonate (383 mg, 96%) as a yellow oil as crude product, which was purified by column chromatography (hexane/ EtOAc, 2:1) to yield **27** (60.5 mg, 15 %) as a yellow oil. NMR shows pure desired product as two rotamers (1:2 ratio).
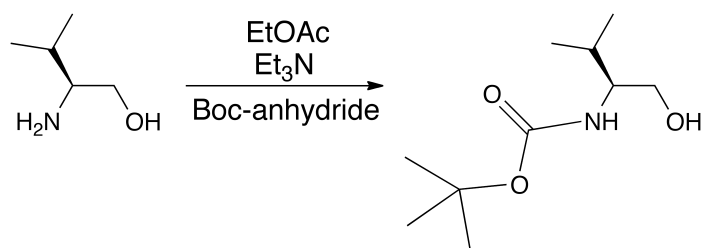
Tert-butyl (1-hydroxy-3-methylbutan-2-yl)carbamate (28)

To a solution of **3** (5.32 g, 51.57 mmol) in EtOAc (100 ml) was Et$_3$N (7.91 ml, 56.7 mmol) added. A clear yellow solution was formed and di-tert-butyl dicarbonate (13.12 g, 60.12 mmol) was added in portions and stirred at RT over night. KHSO$_4$ (1 M, 2 × 50 ml) was added and the aqueous phase separated and extracted with Et$_2$O (3 × 50 ml). The combined organic phases were washed with brine (2 × 50 ml), dried over MgSO$_4$ and filtrated, concentrated in vacuo to give **28** (11.06 g, 106%) as a yellow oil as crude product. NMR shows desired product.
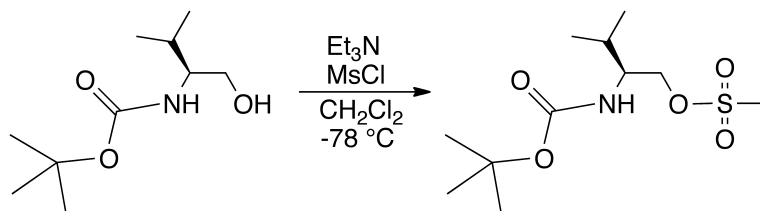
2-((tert-butoxycarbonyl)amino)-3-methylbutyl methanesulfonate (29)

A solution of **28** (10.48 g, 51.57 mmol) and Et$_3$N (8.6 ml, 61.88 mmol) in DCM (250 ml) was cooled to -78°C and methanesulfonyl chloride (4.42 ml, 57.01 mmol) was added dropwise. After complete addition a yellow suspension had formed and was stirred at RT over night. Water (80 ml) was added and the aqueous phase was extracted with DCM (4 × 50 ml). The combined organic layers were washed with NaOH (1 M, 70 ml), HCl (1 M, 80 ml), brine (2 × 70 ml) and dried over Na$_2$SO$_4$, filtrated and concentrated in vacuo to give yellow solid (13.11 g, 104%) as crude product. Recrystallization (hexane/EtOAc) of the crude product resulted in **29** as the desired product as beige crystals (7.83 g, 54% yield). NMR shows desired product. ^{1}H NMR (400 MHz, CDCl$_3$) δ 6.17 (s, 1 h), 4.43 (t, *J*=8.6 Hz, 1 h), 4.09 (dd, 1 h), 3.60 (dd, *J*=14.7, 7.3 Hz, 1 h), 1.73 (m, *J*=13.5, 6.8 Hz, 1 h), 1.44 (m, 1 h), 1.26 (s, 9H), 1.09 (m, 2H), 0.95 (d, *J*=6.7 Hz, 3H), 0.89 (d, *J*=6.7 Hz, 3H).
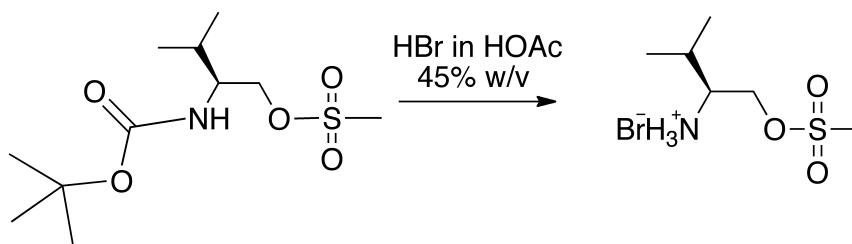
2-((methylsulfonyl)oxy)-1-isoporpylethanaminium bromide (30)

To a solution of HBr in HOAc (45%, 6.4 ml, 102.7 mmol) at RT was **29** (7.83 g, 27.83 mmol) added slowly and portionwise, which gave a dark yellow solution. Et$_2$O (120 ml) was added after 2h of stirring and a precipitate was formed. The yellow suspension was filtrated and concentrated in vacuo to give **30** (3.97 g, 54% crude) as white crystals. NMR shows pure desired product.
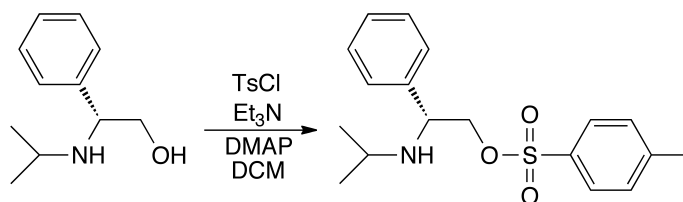
2-(isopropylamino)-2-phenylethyl 4-methylbenzenesulfonate (31a)

Tosyl chloride (351 mg, 1.84 mmol, purified in Soxlet) dissolved in dry DCM (2 ml) and Et$_3$N (0.26 ml, 1.84 ml) and DMAP (3 mg, 0.25 mmol) was added to a solution of (*R*)-*N*-isopropyl-phenylglycinol (300 mg, 1.67 mmol) in dry DCM (5 ml) at 0 °C. After 1.5 h of stirring the reaction had gone to completion. The reaction mixture was stirred over night. Water (4 ml) was added and the aqueous phase was extracted with DCM (4 × 10 ml). The combined organic phases were washed with HCl (5%, 2 × 10 ml), brine (2 × 15 ml) and then dried over NaSO$_4$ and concentrated in vacuo to give **31a** (209 mg, 37%) as a yellow oil as crude product. This was purified by column chromatography (hexane/EtOAc, 3:1) to yield **31a** (41.5 mg, 7%) as a yellow oil.
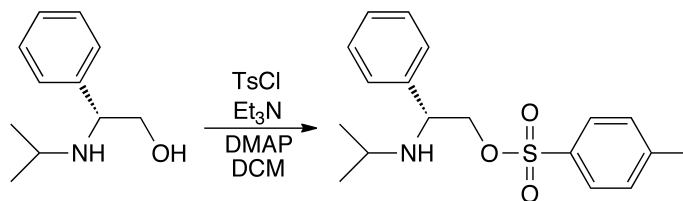
2-(isopropylamino)-2-phenylethyl 4-methylbenzenesulfonate (31b)

Tosyl chloride (351 mg, 1.84 mmol, purified in Soxlet) dissolved in dry DCM (2 ml) and Et$_3$N (0.26 ml, 1.84 ml) and DMAP (3 mg, 0.25 mmol) was added to a solution of **2a** (300 mg, 1.67 mmol) in

dry DCM (5 ml) at 0 °C. After 1.5 h of stirring the reaction had gone to completion. The reaction mixture was stirred over night and the day after a dark red mixture had formed. EtOAc (20 ml) was added and washed with HCl (1 M, 2 × 20 ml), water (20 ml) and then dried over Na_2SO_4 and concentrated in vacuo to give 2-(isopropylamino)-2-phenylethyl 4-methylbenzenesulfonate (69.4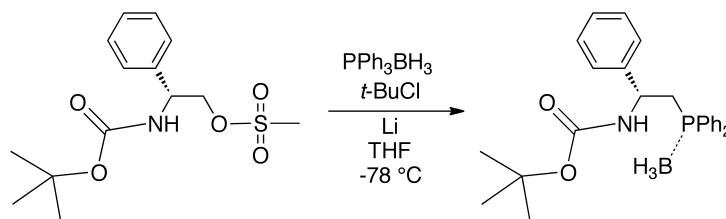 mg, 12%) as a red oil as crude product. NMR shows some of desired product. The aqueous phase was extracted with DCM (3 × 20 ml) and the combined organic phases were washed with water (20 ml), dried over Na_2SO_4 and concentrated in vacuo to give a red oil (58.8 mg) as a crude product.

Tert-butyl (2-(diphenylphosphino)-1-phenylethyl)carbamate borane (32)

To a white suspension of **20** (2.03 g, 7.13 mmol) in distilled THF (5 ml) was finely cut strips of Li metal (excess), that beforehand had been washed in MeOH and THF, added. The reaction mixture was turned dark red and was stirred at RT over night. The excess of Li was removed and tBuCl (0.79 ml, 7.16 mmol) was added dropwise. This was cooled to -78°C and stirred for 30 min and added to a solution of 2-((tert-butoxycarbonyl)amino)-2-phenylethyl methanesulfonate (1.5 g, 4.77 mmol) in distilled THF. A light yellow solution was formed and after 1.5 h of stirring it had turned orange and was slowly warmed to RT. While warming to RT a yellow suspension was formed. After 25.5 h of stirring TLC (hexane/EtOAc, 6:1) shows no 2-((tert-butoxycarbonyl)amino)-2-phenylethyl methanesulfonate. The reaction mixture was poured onto water and concentrated in vacuo. The aqueous phase was extracted with Et_2O (3 × 50 ml) and the combined organic phases were washed with brine, dried over $MgSO_4$ and concentrated in vacuo to give **32** (2.88 g, 144%) as a yellow oil as crude product, which was purified by column chromatography (hexane/EtOAc, 10:1, 6:1), then DCVC to yield **32** (1.2 g, 60 %) as a colourless oil. NMR shows desired product and impurities.
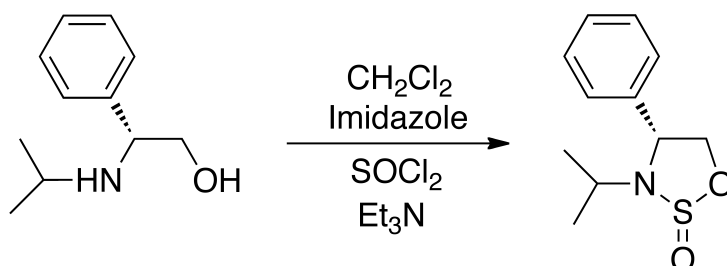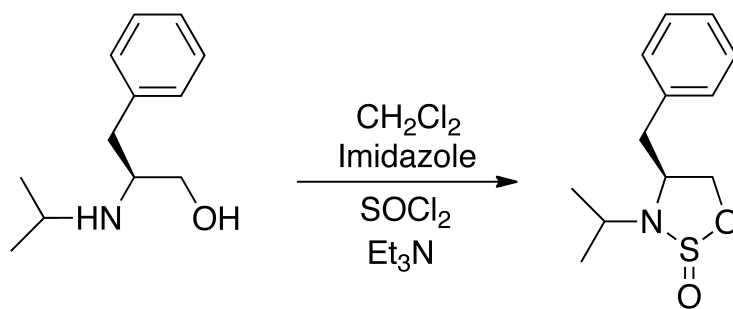
(4*R*)-3-isopropyl-4-phenyl-1,2,3-oxothiazolidine *S*-oxide (33)

A solution of **2a** (47.0 g, 0.26 mol), imidazole (72 g, 1.1 mmol), and Et₃N (73 ml, 0.52 mol) in dry CH₂Cl₂ (800 ml) was cooled on an icebath. To the stirred yellow solution, SOCl₂ (28 ml, 0.39 mol) was added dropwise over ca 20 min, keeping the internal temperature below +10 °C. After complete addition the ice bath was removed and the resulting mixture allowed to warm to RT overnight, and then filtrated through a short pad of silica gel, washed with brine, dried over MgSO₄, and concentrated to give 4c (58.0 g, 98% crude) as a yellowish oil, which solidified upon standing. The crude product, which was used in the next step without further purification, was judged >95% pure by [1 h] NMR and GC. If needed, the mixture of sulfamidites can be purified, but not easily separated into the individual diastereomers, using silica gel chromatography (silica, hexane / EtOAc 9:1 to 3:1). Filtration and concentration in vacuo gave the crude product as a brown solid. NMR of the crude product shows the desired sulfamidites **33** as a mixture of two diastereoisomers. ¹H NMR (CDCl₃): 1.16 (d, *J*=6.6 Hz, 6H), 1.34 (d, *J*=6.8 Hz, 3 H),), 1.39 (d, *J*=6.8 Hz, 3 H), 3.3-3.4 (m, 1 h), 4.2 (dd, *J*=3.8 Hz, 1 h), 4.5-4.6 (m, 2H), 4.74 (dd, *J*=3.8 Hz, 1 h), 4.86 (dd, *J*=6.8 Hz, 1 h), 5.07 (dd, *J*=7.8 Hz, 1 h), 7.3-7.6 (m, 5H). ¹³C NMR (CDCl₃): 21.0, 21.9, 22.1, 23.0, 46.7, 48.2, 60.0, 65.9, 76.0, 127.9, 128.1, 128.5, 129.1, 137.1, 138.0.
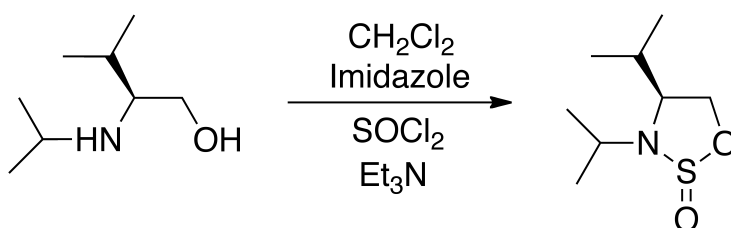
(4*S*)-3-isopropyl-4-isopropyl-1,2,3-oxothiazolidine *S*-oxide (34)

Using the procedure described for **33**; **4** (28 g, 0.20 mol) gave crude **34** as a 1:1 mixture of inseparable diastereoisomers (36.5 g, 97%), as a yellowish oil, which solidified upon standing. The crude product thus obtained was directly used in the next step without further purification. ¹H NMR (CDCl₃): δ 0.82 (d, *J*=6.9 Hz, 3H), 0.92 (d, *J*=7.0 Hz, 3H), 0.98 (d, *J*=6.8 Hz, 3H), 1.20 (d, *J*=6.9 Hz, 3H), 1.21 (d, *J*=6.6 Hz, 3H), 1.3 (d, *J*=6.6 Hz, 3H), 1.36 (d, *J*=6.9 Hz, 3H), 1.47 (d, *J*=6.9 Hz, 3H), 3.25 (q, *J*=7.57 Hz, 1 h), 3.38 (q, *J*=6.70 Hz, 1 h), 3.52 (q, *J*=6.70 Hz, 1 h), 3.68-3.74 (m, 1 h), 4.24 (dd, *J*=8.80 Hz, 1 h), 4.49 (dd, *J*=7.37 Hz, 1 h), 4.57 (dd, *J*=8.42 Hz, 1 h), 4.70 (dd, *J*=7.74 Hz, 1 h). ¹³C NMR (CDCl₃): δ 15.02, 18.37, 19.62, 20.40, 21.07, 21.43, 22.26, 23.11, 28.64, 31.95, 46.86, 50.85, 60.41, 67.26, 69.60, 72.34.
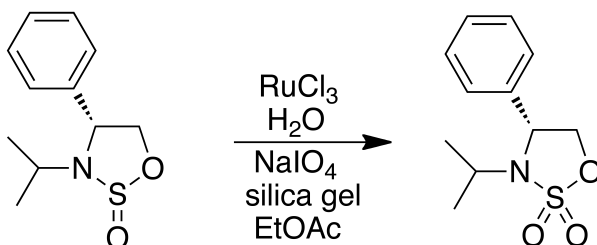
(4*S*)-3-isopropyl-4-benzyl-1,2,3-oxothiazolidine *S*-oxide (35)

Using the procedure described for **34**; **6a** (6.5 g, 34 mmol) gave **35** a 1:1 mixture of inseparable diastereoisomers (7.5 g, 87%), as a brown oil, which solidified upon standing. The crude product thus obtained was directly used in the next step without further purification. A mixture of 1:1 epimers at sulfur of **35** was received: ^{1}H NMR (CDCl$_3$): δ 1.21 (d, *J*=6.7 Hz, 3 H), 1.35 (d, *J*=6.7 Hz, 6 H), 1.35 (d, *J*=6.7 Hz, 3 H), 2.56 (dd, *J*=9.8, 13.5 Hz, 1 H), 2.91-3.04 (m, 2H), 3.23 (dd, *J*=5.8, 13.5 Hz, 1 H), 3.46 (sept, *J*=6.7 Hz, 1 H), 3.61 (sept, *J*=6.7 Hz, 1 H), 3.69-3.79 (m, 1 H), 3.93-4.02 (m, 1 H), 4.16 (t, *J*=4.0, 8.6 Hz, 1 H), 4.29-4.37 (m, 1 h), 4.54-4.66 (m, 2H). ^{13}C NMR (CDCl$_3$): δ 21.5, 22.0, 22.20, 22.7, 39.5, 40.7, 47.0, 48.5, 57.4, 61.5, 72.9, 75.6, 126.9, 127.1, 128.9, 129.2, 137.2, 138.0.

(4*R*)-3-isopropyl-4-phenyl-1,2,3-oxothiazolidine *S,S*-dioxide (36)

RuCl$_3$ (0.7 mg, 0.15 mol%) was added to water (1.25 ml) yielding a black solution. This solution was stirred at a brisk pace and small portions of NaIO$_4$ (1.19 g, 5.55 mmol) were then added, the black solution immediately turned yellow (RuO$_4$). Note that only the amount of NaIO4 that dissolved was added. The RuO$_4$ solution and the remaining NaIO$_4$ was added directly to silica gel (2.5 g) in a 100 ml round bottom flask with a magnetic stirring bar. The rate of stirring was increased and the solid was stirred until a free flowing white solid was obtained. EtOAc (9 ml) was added to the wet silica gel and put on an ice bath. The sulfamidite **33** (500 mg, 2.22 mmol) was dissolved in EtOAc (9 ml), a few drops of CH$_2$Cl$_2$ was added to dissolve all of the sulfamidite. The solution of the substrate was added dropwise to the slurry of silica gel at 0 °C. After complete

90

addition the ice bath was removed and stirred at a brisk pace throughout the reaction. A white slurry is formed and stirred until TLC (silica/hexane/EtOAc 3:1) indicated complete consumption of the starting material, Typically this requires 10 min-2 h depending on sulfamidite. The slurry was filtrated through a short pad of silica gel, dried over Na_2SO_4, filtrated and concentrated in vacuo to give **36** (503.3 mg, 2.086, mmol 95% crude) as a colourless oil as crude product, which solidifies upon standing. In most cases, the crude product was essentially pure (>95% by NMR and GC) and used in the next step without further purification. Occasionally, however, the crude product contains traces of the Ru catalyst (brown to black). This may be removed by re-dissolving in hexane/EtOAc (4:1) and filtering again through a silica plug (ca 5 cm), followed by evaporation. ^{1}H NMR (CDCl$_3$): δ 1.13 (d, *J*=6.73 Hz 3H), 1.37 (d, *J*=6.89 Hz 3H), 3.7-3.6 (m, 1 h), 4.24-4.30 (dd, *J*=8.17, 8.17 Hz 1 h), 4.64-4.70 (dd, *J*=15.52, 15.52 Hz, 1 h), 4.80-4.86 (dd, *J*=7.33, 7.33 Hz, 1 h), 7.39-7.47 (m, 5H). ^{13}C NMR (CDCl$_3$): δ 19.82, 20.12, 49.09, 60.73, 72.49, 127.40, 129.44, 129.51, 136.90.

v_{max} (neat): 2981, 2359, 1604, 1456, 1338, 1194 cm^{-1}. α_D^{19} = -87.3° (c=1.00, CDCl$_3$).

HRMS (FAB): MH$^+$, found 242.0856, $C_{11 h16}NO_3S$ requires 242.0853.
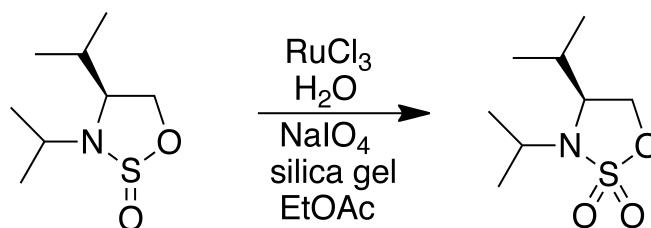
(4*S*)-3-isopropyl-4-isopropyl-1,2,3-oxothiazolidine *S,S*-dioxide (37)

Following the procedure described for **36**; sulfamidite **34** (2.00 g, 10.5 mmol) was oxidized to give sulfamidate **37** (2.02 g, 93%) as a colourless oil. ^{1}H NMR (CDCl$_3$): δ 0.97 (dd, *J*=7.38 Hz, 6H), 1.29 (d, *J*=6.83 Hz, 3H), 1.36 (d, *J*=6.83 Hz, 3H), 2.03 (sext, 1 h), 3.50 (sext, 1 h), 3.70 (q, 1 h), 4.25 (dd, *J*=8.82 Hz, 1 h), 4.40 (m, 1 h). ^{13}C NMR (CDCl$_3$): δ 16.49, 18.89, 19.64, 20.57, 30.87, 50.63, 61.44, 67.93. v_{max} (neat): 2969, 2359, 1718, 1469, 1338, 1196 cm^{-1}. α_D^{19} = -12.11 (c=1.14, CDCl$_3$). HRMS (FAB): MH$^+$, found 208.1011, $C_8H_{18}NO_3S$ requires 208.1009.
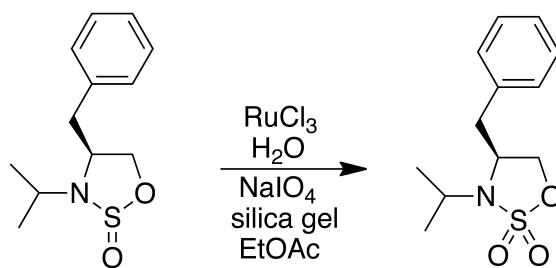
(4*S*)-3-isopropyl-4-benzyl-1,2,3-oxothiazolidine *S,S*-dioxide (38)

Following the procedure described for **36**, sulfamidite **35** (5.49 g, 28.76 mmol) was oxidized to give sulfamidate **38** (6.39 g, 93%) as a colourless oil. ^{1}H NMR (CDCl$_3$): δ 1.11 (d, *J*=6.79 Hz 3H), 1.32 (d, *J*=6.82 Hz 3H), 2.85-2.95 (m, 1 h), 3.10-3.20 (m, 1 h), 3.68 (sext, *J*=6.8 Hz, 1 h), 3.90-4.00 (m, 1 h), 4.20-4.30 (m, 1 h), 4.20-4.35 (m, 1 h), 7.20-7.45 (m, 5H). ^{13}C NMR (CDCl$_3$): 19.28, 20.66, 39.75, 50.13, 57.36, 70.68, 127.20, 128.78, 129.38, 135.90. ν$_{max}$ (neat): 2979, 2257, 1604, 1455, 1338, 1189 cm^{-1}.
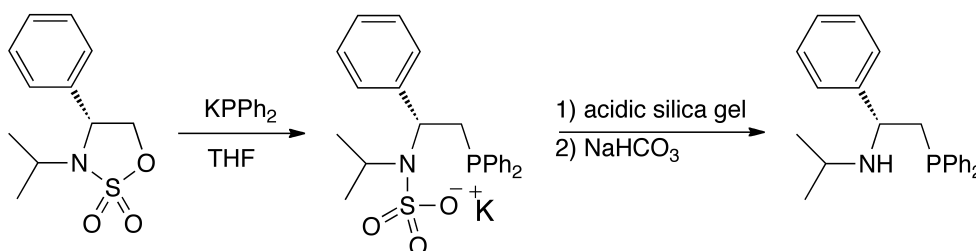
(*R*)-2-isopropylamino-2-phenyl-1-(diphenylphosphino)ethane (39)

To a solution of **36** (1.0 g, 4.14 mmol) in dry THF (5 ml) at -78 °C, a solution of KPPh$_2$ (0.5 M in THF, 8.7 ml, 4.35 mmol) was added dropwise, over 15 min, to give a red solution. After complete additon the ice bath was removed and stirred for another 5 min, when TLC (hexane/EtOAc/Et$_3$N, 10:1:0.1) indicated complete disappearance of the starting material (5-45 min depending on the sulfamidate and concentration in the reaction mixture). Acidic silica (2 g silica and 0.8 ml 3.5 M aq. H$_2$SO$_4$, evenly mixed to a white powder) was added portionwise until pH=1. The resulting white slurry was stirred at RT during 40 min, followed by the addition of saturated aqueous NaHCO$_3$ (35 ml). The mixture was filtered off and washed with brine (2 × 10 ml). The combined aqueous layers were extracted with CH$_2$Cl$_2$ (3 × 10 ml) and the combined organic layers were dried over Na$_2$SO$_4$ and evaporated under reduced pressure to give a white solid (1.75 g, 122% crude), which was purified by column chromatography (hexane/EtOAc/Et$_3$N, 10:1:0.1) to yield **39** (1.17 g, 81%) as a colourless oil, which solidified upon standing. ^{1}H NMR (CDCl$_3$): δ 0.94 (t, *J*=5.52 Hz, 6H), 1.6 (bs, 1 h), 2.44 (d, 2H, *J*=6.93 Hz), 2.50-2.60 (m, 1 h), 3.75-3.80 (q, *J*=7.13 Hz, 1 h), 7.20-7.50 (m, 15H). ^{13}C NMR (CDCl$_3$): δ 22.0, 24.26, 38.99, 39.13, 45.87, 57.44, 57.59, 126.80,

126.98, 128.31, 128.38, 128.75, 132.47, 132.66, 133.06, 133.25, 138.05, 138.18, 138.77, 138.89, 145.15, 145.21. ^{31}P NMR (CDCl$_3$): δ -22.30. ν_{max} (neat): 3314, 3055, 2960, 1952, 1883, 1811, 1585, 1477, 1433, 1378, 1169 cm^{-1}. α_D^{19}= -60.12° (c=1.60, THF).

HRMS (FAB): MH$^+$, found 348.1883, C$_{23}$H$_{27}$NP requires 348.1912.
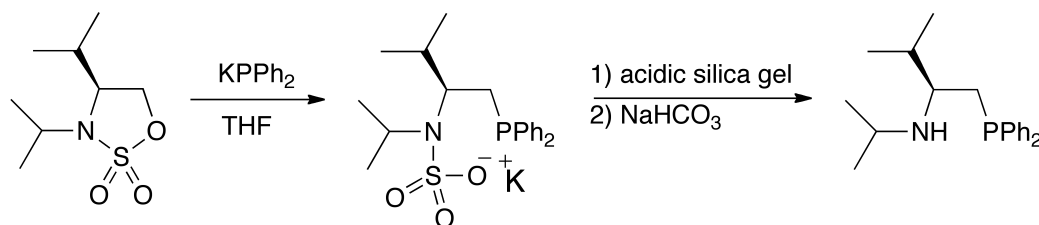
***(S)*-2-isopropylamino-3-metyl-1-(diphenylphosphino)butane (40)**

Using the procedure described for the synthesis of **39,** starting from **37** (0.79 g, 3.83 mmol) was phosphinated to yield **40** (0.55 g, 46% yield) as a colourless syrup. ^1H NMR (CDCl$_3$): δ 0.83 (d, *J*=6.86 Hz, 3H, 0.89 (d, *J*=6.86 Hz, 3H), 0.93 (t, *J* =6.86 Hz, 6H), 1.94–2.05 (m, 2H), 2.23 (m, 1 h), 2.48 (m, 1 h), *J*=4.26 Hz), 2.77 (m, 1 h), 7.35-7.50 (m, 10H). ^{13}C NMR (CDCl$_3$): δ 17.20, 18.13, 23.11, 23.73, 30.52, 30.60, 30.86, 30.99, 45.96, 56.85, 56.97, 128.22, 128.29, 128.35, 128.63, 132.43, 132.61, 133.06, 133.25, 138.45, 138.48, 139.50, 139.63. ^{31}P NMR (CDCl$_3$): δ -21.68. ν_{max} (neat): 3314, 3053, 2957, 1952, 1883, 1810, 1585, 1477, 1434, 1377, 1169 cm^{-1}. α_D^{19}= +37.04° (c =1.73, THF). HRMS (FAB): MH$^+$, found 314.2015, C$_{20}$H$_{29}$NP requires 314.2039.
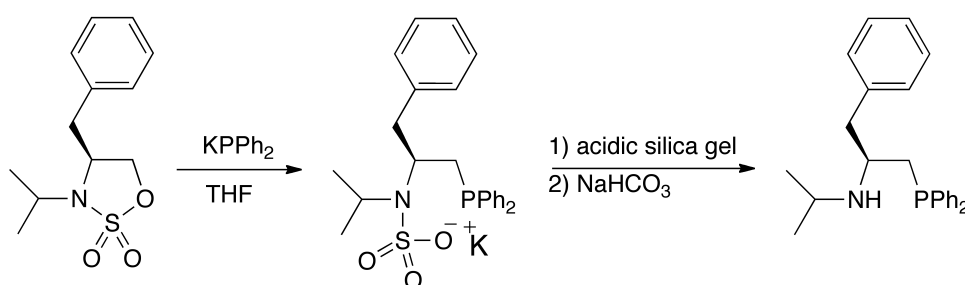
(S)-2-isopropylamino-3-phenyl-1-(diphenylphosphino)propane (41)

Using the procedure described for the phosphination of **39,** sulfamidate **38** (0.79 g, 3.83 mmol) was converted into **41** (1.10 g, 4.3 mmol, 80% yield) as a viscous, colourless oil. ^1H NMR (CDCl$_3$): δ 0.86 (d, *J*=6.27 Hz, 3H), 0.91 (d, *J*=6.27 Hz, 3H), 1.1-1.2 (bs, 1 h), 2.11 (t, *J*=6.6 Hz, 1 h), 2.23 (m, 1 h), 2.76-2.92 (m, 4H). ^{13}C NMR (CDCl$_3$): δ 22.76, 23.97, 33.58, 34.29, 42.30, 42.40, 45.94, 52.19, 52.22, 126.54, 128.80, 129.78, 130.65, 130.75, 130.95, 131.04, 131.78, 132.50, 133.47, 133.70, 134.68, 138.79. ^{31}P NMR (CDCl$_3$): δ -22.97. ν_{max} (neat): 3314, 3056, 2960, 1951, 1882,

1810, 1585, 1478, 1434, 1377, 1171 cm^{-1}. α_D^{19} = +25.74° (c=2.02, THF). HRMS (FAB): MH$^+$, found 362.2043, C$_{24}$H$_{29}$NP requires 362.2039.

ACKNOWLEDGEMENTS

REFERENCES

1. Tansjö, L., Från Lavoisier till Strindberg. **2008,** *8*, 293.

2. Theophilus Scheffer, H., Framledne directeuren herr H.T. Scheffers chemiske föreläsningar rörande, salter, jord-arter, metaller, vatten, fetmor och färgning; med anmärkningar utgifne; jemte anledning til föreläsningar öfver chemiens beskaffenhet och nytta, samt naturlige kroppars allmännaste skiljaktigheter. **1779.**

3. Wöhler, F., Ueber künstliche Bildung des Harnstoffs. *Annalen der Physik und Chemie* **1828,** *88,* 253-256.

4. Reed, A., Natural population analysis. *J. Chem. Phys.* **1985,** *83*, 735.

5. Würthwein, E. U.; Sen, K. D.; Pople, J. A.; Schleyer, P. v. R., Lithiated ammonia, amide anions, and ammonium ions. An ab initio study of structures, bonding, and energetic relationships. *Inorganic Chemistry* **1983,** *22*, 496-503.

6. Armstrong, D. R.; Perkins, P. G.; Walker, G. T., The electronic structure of the monomers, dimers, a trimer, the oxides and the borane complexes of the lithiated ammonias. *Journal of Molecular Structure: THEOCHEM* **1985,** *122*, 189-204.

7. Clayden, J., Organolithiums: selectivity for synthesis. *Tetrahedron Organic Chemistry Series Vol 23* **2002**.

8. Braunstein, P.; Naud, F., Hemilability of Hybrid Ligands and the Coordination Chemistry of Oxazoline-Based Systems. *Angewandte Chemie International Edition* **2001,** *40*, 680-699.

9. LoPachin, R.; Gavin, T.; DeCaprio, A.; Barber, D. S., APPLICATION OF THE HARD AND SOFT, ACIDS AND BASES (HSAB) THEORY TO TOXICANT-TARGET INTERACTIONS. *Chemical Research in Toxicology* **2011**.

10. Ho, T.-L.; Ho, H. C.; Hamilton, L. D., Biochemical significance of the hard and soft acids and bases principle. *Chemico-Biological Interactions* **1978,** *23*, 65-84.

11. Ralph G, P., Hard and soft acids and bases—the evolution of a chemical concept. *Coordination Chemistry Reviews* **1990,** *100,* 403-425.

12. Pearson, R. G.; Songstad, J., Application of the Principle of Hard and Soft Acids and Bases to Organic Chemistry. *Journal of the American Chemical Society* **1967,** *89*, 1827-1836.

13. Granander, J.; Sott, R.; Hilmersson, G., Chiral lithium amido sulfide ligands for asymmetric addition reactions of alkyllithium reagents to aldehydes. *Tetrahedron: Asymmetry* **2003,** *14*, 439-447.

14. Granander, J.; Sott, R.; Hilmersson, G., Asymmetric addition of n-butyllithium to aldehydes: new insights into the reactivity and enantioselectivity of the chiral amino ether accelerated reaction. *Tetrahedron* **2002,** *58*, 4717-4725.

15. Gavrilov, K. N.; Bondarev, O. G.; Korostylev, A. V.; Polosukhin, A. I.; Tsarev, V. N.; Kadilnikov, N. E.; Lyubimov, S. E.; Shiryaev, A. A.; Zheglov, S. V.; Gais, H.-J.; Davankov, V. A., Novel P,N-bidentate phosphite ligands in asymmetric catalysis. *Chirality* **2003,** *15*, S97-S103.

16. Sott, R.; Granander, J.; Dinér, P.; Hilmersson, G., Solution structures of chiral lithium amides with internal sulfide coordination: sulfide versus ether coordination in chiral lithium amides. *Tetrahedron: Asymmetry* **2004,** *15*, 267-274.

17. Rönnholm, P.; Södergren, M.; Hilmersson, G., Improved and Efficient Synthesis of Chiral N,P-Ligands via Cyclic Sulfamidates for Asymmetric Addition of Butyllithium to Benzaldehyde. *Organic Letters* **2007,** *9*, 3781-3783.

18. Lait, S. M.; Rankic, D. A.; Keay, B. A., 1,3-Aminoalcohols and Their Derivatives in Asymmetric Organic Synthesis. *Chemical Reviews* **2007,** *107*, 767-796.

19. Hedberg, C.; Källström, K.; Brandt, P.; Hansen, L. K.; Andersson, P. G., Asymmetric Hydrogenation of Trisubstituted Olefins with Iridium-Phosphine Thiazole Complexes: A Further Investigation of the Ligand Structure. *Journal of the American Chemical Society* **2006,** *128*, 2995-3001.

20. Shirai, R.; Aoki, K.; Sato, D.; Kim, H.-D.; Murakata, M.; Yasukata, T.; Koga, K., Stereoselective Reactions. XXII. Design and Synthesis of Chiral Chelated Lithium Amides for Enantioselective Reactions. *Chemical & pharmaceutical bulletin* **1994,** *42*, 690-693.

21. Curthbertson, E.; O'Brien, P.; Towers, T. D., Practical One-Step Synthesis of Koga's Chiral Bases. *Synthesis* **2001,** *2001*, 0693-0695.

22. de Sousa, S. E.; O'Brien, P.; Poumellec, P., Two expedient methods for the preparation of chiral diamines. *Journal of the Chemical Society, Perkin Transactions 1* **1998**, 1483-1492.

23. Bhuniya, D.; DattaGupta, A.; Singh, V. K., Design, Synthesis, and Application of Chiral Nonracemic Lithium Amide Bases in Enantioselective Deprotonation of Epoxides. *The Journal of Organic Chemistry* **1996,** *61*, 6108-6113.

24. de Sousa, S. E.; O'Brien, P.; Poumellec, P., Two useful methods for the preparation of (R)- and (S)-N-methyl-1-phenyl-2-(1-pyrrolidinyl)ethanamine. *Tetrahedron: Asymmetry* **1997,** *8*, 2613-2618.

25. Miao, G.; Rossiter, B. E., Influence of the Aromatic Substituent on the Reactivity of (R)-N-Methyl-1-phenyl-2-(1-piperidinyl)ethanamine Cuprates in Enantioselective Conjugate Addition. *The Journal of Organic Chemistry* **1995,** *60*, 8424-8427.

26. Dieter, R. K.; Deo, N.; Lagu, B.; Dieter, J. W., Stereo- and regioselective synthesis of chiral diamines and triamines from pseudoephedrine and ephedrine. *The Journal of Organic Chemistry* **1992,** *57*, 1663-1671.

27. Anderson, J. C.; Cubbon, R.; Harding, M.; James, D. S., Concepts for ligand design in asymmetric catalysis: a study of chiral amino thiol ligands. *Tetrahedron: Asymmetry* **1998,** *9*, 3461-3490.

28. Kang, J.; Bum Kim, J.; Whan Kim, J.; Lee, D., The effects of sulfur substitution in chiral amino thiols on the enantioselective addition of organozinc reagents to aldehydes: a novel method for estimation of free energies of dimerization in monomer-dimer equilibria. *Journal of the Chemical Society, Perkins Transactions* **1997**, 189-194.

29. Krause, N., Copper-Catalyzed Enantioselective Michael Additions: Recent Progress with New Phosphorus Ligands. *Angewandte Chemie International Edition* **1998,** *37*, 283-285.

30. Dahlenburg, L.; Götz, R., Funktionelle Phosphane: Part XI. Optisch reine β-Aminophosphane und β-Aminophosphinite für die komplexkatalysierte Reduktion organischer Carbonylverbindungen. Molekülstrukturen von [(1R,2R)-Ph$_2$PCH(Ph)CH(Me)NH$_2$Me]Cl, (1R,2S)-Ph$_2$PCH(Ph)CH(Me)NHSO$_2$Me und [{(1R,2R)-Ph$_2$PCH(Ph)CH(Me)NHMe-κN,κP}Rh(η4-1,5-C$_8$H$_{12}$)]BF$_4$. *Journal of Organometallic Chemistry* **2001,** *619*, 88-98.

31. Rossiter, B. E.; Eguchi, M.; Miao, G.; Swingle, N. M.; Hernández, A. E.; Vickers, D.; Fluckiger, E.; Greg Patterson, R.; Vásavi Reddy, K., Enantioselective conjugate addition to cyclic enones with scalemic lithium organo(amido)cuprates, Part IV. Relationship between ligand structure and enantioselectivity. *Tetrahedron* **1993,** *49*, 965-986.

32. Saitoh, A.; Morimoto, T.; Achiwa, K., A phosphorus-containing chiral amidine ligand for asymmetric reactions: enantioselective Pd-catalyzed allylic alkylation. *Tetrahedron: Asymmetry* **1997,** *8*, 3567-3570.

33. Quirmbach, M.; Holz, J.; Tararov, V. I.; Börner, A., Synthesis of Heterofunctionalized Multidentate Diphosphines. *Tetrahedron* **2000,** *56*, 775-780.

34. Anderson, J. C.; Cubbon, R. J.; Harling, J. D., Investigation of the importance of nitrogen substituents in a N-P chiral ligand for enantioselective allylic alkylation. *Tetrahedron: Asymmetry* **2001,** *12*, 923-935.

35. Kanai, M.; Nakagawa, Y.; Tomioka, K., Catalytic enantioselective conjugate addition of Grignard reagents to cyclic α,β-unsaturated carbonyl compounds. *Tetrahedron* **1999,** *55*, 3843-3854.

36. Jalil, M. A.; Hui, E. B., A general and efficient method for the preparation of unsymmetrical bidentate P,N and P,S ligands. *Tetrahedron Letters* **2006,** *47*, 1473-1475.

37. Mukaiyama, T.; Soai, K.; Sato, T.; Shimizu, H.; Suzuki, K., Enantioface-differentiating (asymmetric) addition of alkyllithium and dialkylmagnesium to aldehydes by using (2S,2'S)-2-hydroxymethyl-1-[(1-alkylpyrrolidin-2-yl)methyl]pyrrolidines as chiral ligands. *Journal of the American Chemical Society* **1979,** *101*, 1455-1460.

38. Ye, M.; Logaraj, S.; Jackman, L. M.; Hillegass, K.; Hirsh, K. A.; Bollinger, A. M.; Grosz, A. L.; Mani, V., Enantioselective addition of alkyllithium reagents to aldehydes induced by chiral lithium alkoxides. *Tetrahedron* **1994,** *50*, 6109-6116.

39. Schön, M.; Naef, R., New 1-amino-1,2-diphenylethanols as ligands for the enantioselective addition of alkyllithiums to benzaldehyde. *Tetrahedron: Asymmetry* **1999,** *10*, 169-176.

40. Eleveld, M. B.; Hogeveen, H., Enantioselective addition of n-butyllithium to benzaldehyde in the presence of chiral lithium amides. *Tetrahedron Letters* **1984,** *25*, 5187-5190.

41. Corruble, A.; Valnot, J.-Y.; Maddaluno, J.; Duhamel, P., Structure-Selectivity Relationship in Alkyllithium–Aldehyde Condensations Using 3-Aminopyrrolidine Lithium Amides as Chiral Auxiliaries. *The Journal of Organic Chemistry* **1998,** *63*, 8266-8275.

42. Arvidsson, P. I.; Davidsson, Ö.; Hilmersson, G., Enantioselective butylation of aliphatic aldehydes by mixed chiral lithium amide/n-BuLi dimers. *Tetrahedron: Asymmetry* **1999,** *10*, 527-534.

43. Corruble, A.; Valnot, J.-Y.; Maddaluno, J.; Duhamel, P., Structure-Selectivity Relationship in Alkyllithium,àíAldehyde Condensations Using 3-Aminopyrrolidine Lithium Amides as Chiral Auxiliaries. *The Journal of Organic Chemistry* **1998,** *63*, 8266-8275.

44. Mazaleyrat, J. P.; Cram, D. J., Chiral catalysis of additions of alkyllithiums to aldehydes. *Journal of the American Chemical Society* **1981,** *103*, 4585-4586.

45. Uhlenbeck, G. E.; Goudsmit, S., *Naturwissenschaften* **1925,** *47*.

46. *www.nobelprize.org*.

47. Aue, W. P.; Bartholdi, E.; Ernst, R. R., Two-dimensional spectroscopy. Application to nuclear magnetic resonance. *The Journal of Chemical Physics* **1976,** *64*, 2229-2246.

48. Brown, T. L., Nuclear magnetic resonance studies of organometallic exchange processes. *Accounts of Chemical Research* **1968,** *1*, 23-32.

49. Darensbourg, M. Y.; Kimura, B. Y.; Hartwell, G. E.; Brown, T. L., Organometallic exchange reactions. X. Cross-association of tert butyllithium. Kinetics of tert butyllithium dissociation. *Journal of the American Chemical Society* **1970,** *92*, 1236-1242.

50. Lewis, H. L.; Brown, T. L., Association of alkyllithium compounds in hydrocarbon media. Alkyllithium-base interactions. *Journal of the American Chemical Society* **1970,** *92*, 4664-4670.

51. Fraenkel, G.; Henrichs, M.; Hewitt, J. M.; Su, B. M.; Geckle, M. J., Dynamic behavior and aggregation of propyllithium from carbon-13 and lithium-6 NMR at high field. *Journal of the American Chemical Society* **1980,** *102*, 3345-3350.

52. Fraenkel, G.; Fraenkel, A. M.; Geckle, M. J.; Schloss, F., Structure and dynamic behavior of propyllithium from carbon-13, lithium-7, and lithium-6 NMR. *Journal of the American Chemical Society* **1979,** *101*, 4745-4747.

53. Roland, W. K., An Investigation of Charge Effects on NMR. Coupling Constants. The Charge Induced Variation of s-Densities at the Nucleus. *Helvetica Chimica Acta* **1980,** *63*, 2054-2070.

54. Dieter, S.; Robert, H.; Josef, G., ^{13}C-NMR.-Spektroskopie von Organolithiumverbindungen bei tiefen Temperaturen. Strukturinformation aus der ^{13}C, ^{6}Li-Kopplung. *Helvetica Chimica Acta* **1983,** *66*, 308-337.

55. Hilmersson, G.; Davidsson, O., A Multinuclear NMR Study of a Chiral Lithium Amide with an Intramolecular Chelating Methoxy Group in Coordinating Solvents at the Slow Ligand Exchange Limit. *The Journal of Organic Chemistry* **1995,** *60*, 7660-7669.

56. Sato, D.; Kawasaki, H.; Shimada, I.; Arata, Y.; Okamura, K.; Date, T.; Koga, K., Crystallographic and lithium-6 and nitrogen-15 NMR studies of a chiral bidentate lithium amide. An effect of aggregation states on an enantioselective deprotonation reaction. *Journal of the American Chemical Society* **1992,** *114*, 761-763.

57. Rönnholm, P.; Nilsson Lill, S. O.; Gräfenstein, J.; Norrby, P.-O.; Pettersson, M.; Hilmersson, G., Aggregation and Solvation of Chiral N,P-amide Ligands in Coordinating Solvents - A Computational and NMR Study. *submitted to the European Journal of Organic Chemistry* **2011**.

58. Nichols, M. A.; Williard, P. G., Solid-state structures of n-butyllithium-TMEDA, -THF, and -DME complexes. *Journal of the American Chemical Society* **1993,** *115*, 1568-1572.

59. Holm, T., Association of Butyllithium in Diethyl Ether and in Tetrahydrofuran. *Acta Chemica Scandinavica, Series B* **1978,** *32*, 162-166.

60. McGarrity, J. F.; Ogle, C. A., High-field proton NMR study of the aggregation and complexation of n-butyllithium in tetrahydrofuran. *Journal of the American Chemical Society* **1985,** *107*, 1805-1810.

61. Hilmersson, G., An NMR and Computational Study of a Lithium Amide and Ethereal Ligand Exchange. *Chemistry – A European Journal* **2000,** *6*, 3069-3075.

62. Arvidsson, P. I.; Hilmersson, G.; Davidsson, Ö., Rational Design of Chiral Lithium Amides for Asymmetric Alkylation Reactions - NMR Spectroscopic Studies of Mixed Lithium Amide/ Alkyllithium Complexes. *Chemistry - A European Journal* **1999,** *5*, 2348-2355.

63. Born, M.; Oppenheimer, R., Zur Quantentheorie der Molekeln. *Annalen der Physik (Leipzig)* **1927,** *84*, 457–484.

64. Hohenberg, P.; Kohn, W., Inhomogeneous Electron Gas. *Physical Review B* **1964,** *136*, B864-B871.

65. Kohn, W.; Sham, L. J., Self-Consistent Equations Including Exchange and Correlation Effects. *Physical Review* **1965,** *140*, A1133-A1138.

66. Vosko, S. H.; Wilk, L.; Nusair, M., Accurate Spin-Dependent Electron Liquid Correlation Energies for Local Spin-Denity Calculations - A Critical Analysis. *Canadian Journal of Physics* **1980,** *58*, 1200-1211.

67. Perdew, J. P., Density-Functional Approximation for the Correlation Energy of the Inhomogeneous Electron Gas. *Physical Review B* **1986,** *33*, 8822-8824.

68. Becke, A. D., Density-Functional Exchange-Energy Approximation With Correct Asymptotic-Behavior. *Physical Review A* **1988,** *38*, 3098-3100.

69. Lee, C. T.; Yang, W. T.; Parr, R. G., Development of the Colle-Salvetti Correlation-Energy Functional into a Functional of the Electron Density. *Physical Review B* **1988,** *37*, 785-789.

70. Perdew, J. P.; Yue, W., Accurate and Simple Density Functional for the Electronic Exchange Energy - Generalized Gradient Approximation. *Physical Review B* **1986,** *33*, 8800-8802.

71. Becke, A. D., A New Mixing of Hartree-Fock and Local Density-Functional Theories. *Journal of Chemical Physics* **1993,** *98*, 1372-1377.

72. Stephens, P. J.; Devlin, F. J.; Chabalowski, C. F.; Frisch, M. J., Ab Initio Calculation of Vibrational Absorption and Circular Dichroism Spectra Using Density Functional Force Fields. *The Journal of Physical Chemistry* **1994,** *98*, 11623-11627.

73. Sousa, S. F.; Fernandes, P. A.; Ramos, M. J., General performance of density functionals. *Journal of Physical Chemistry A* **2007,** *111*, 10439-10452.

74. Zhao, Y.; Schultz, N. E.; Truhlar, D. G., Design of density functionals by combining the method of constraint satisfaction with parametrization for thermochemistry, thermochemical kinetics, and noncovalent interactions. *Journal of Chemical Theory and Computation* **2006,** *2*, 364-382.

75. Kümmel, S.; Kronik, L., Orbital-dependent density functionals: Theory and applications. *Reviews of Modern Physics* **2008,** *80*, 3-60.

76. Janesko, B. G.; Henderson, T. M.; Scuseria, G. E., Long-range-corrected hybrids including random phase approximation correlation. *The Journal of Chemical Physics* **2009,** *130*, 081105-4.

77. Grimme, S., Semiempirical GGA-type density functional constructed with a long-range dispersion correction. *Journal of Computational Chemistry* **2006,** *27*, 1787-1799.

78. Andrews, D. H., The Relation Between the Raman Spectra and the Structure of Organic Molecules. *Physical Review* **1930,** *36*, 544–554.

79. Burkert, U.; Allinger, N. L., *Molecular Mechanics*. Americal Chemical Society: 1982.

80. Allinger, N. L., Conformational analysis. 130. MM2. A hydrocarbon force field utilizing V1 and V2 torsional terms. *Journal of the American Chemical Society* **1977,** *99*, 8127-8134.

81. Norrby, P.-O.; Liljefors, T., Automated molecular mechanics parameterization with simultaneous utilization of experimental and quantum mechanical data. *Journal of Computational Chemistry* **1998,** *19*, 1146-1166.

82. Jensen, F., Introduction to Computational Chemistry. *John Wiley & Sons* **1999**.

83. Henkelman, G.; Uberuaga, B. P.; Jonsson, H., A climbing image nudged elastic band method for finding saddle points and minimum energy paths. *The Journal of Chemical Physics* **2000,** *113*, 9901-9904.

84. Peng, C.; Ayala, P. Y.; Schlegel, H. B.; Frisch, M. J., Using redundant internal coordinates to optimize equilibrium geometries and transition states. *Journal of Computational Chemistry* **1996,** *17*, 49-56.

85. Deng, L.; Ziegler, T., The determination of intrinsic reaction coordinates by density functional theory. *International Journal of Quantum Chemistry* **1994,** *52*, 731-765.

86. Deng, L., A combined density functional and intrinsic reaction coordinate study on the ground state energy surface of H2CO. *J. Chem. Phys.* **1993,** *99*, 3823.

87. Goodman, J. M.; Silva, M. A., QRC: a rapid method for connecting transition structures to reactants in the computational analysis of organic reactivity. *Tetrahedron Letters* **2003,** *44*, 8233-8236.

88. Lee, M. S.; Salsbury, F. R.; Olson, M. A., An efficient hybrid explicit/implicit solvent method for biomolecular simulations. *Journal of Computational Chemistry* **2004,** *25*, 1967-1978.

89. Marenich, A. V.; Cramer, C. J.; Truhlar, D. G., Performance of SM6, SM8, and SMD on the SAMPL1 Test Set for the Prediction of Small-Molecule Solvation Free Energies. *The Journal of Physical Chemistry B* **2009,** *113*, 4538-4543.

90. Olson, R. M.; Marenich, A. V.; Cramer, C. J.; Truhlar, D. G., Charge Model 4 and Intramolecular Charge Polarization. *Journal of Chemical Theory and Computation* **2007,** *3*, 2046-2054.

91. Marenich, A. V.; Olson, R. M.; Kelly, C. P.; Cramer, C. J.; Truhlar, D. G., Self-Consistent Reaction Field Model for Aqueous and Nonaqueous Solutions Based on Accurate Polarized Partial Charges. *Journal of Chemical Theory and Computation* **2007,** *3*, 2011-2033.

92. Pérez-Jordá, J., Density-functional study of van der Waals forces on rare-gas diatomics: Hartree-Fock exchange. *J. Chem. Phys.* **1999,** *110,* 1916.

93. Pérez-Jordá, J.; Becke, A. D., A density-functional study of van der Waals forces: rare gas diatomics. *Chemical Physics Letters* **1995,** *233*, 134-137.

94. Kurita, N.; Sekino, H., Ab initio and DFT studies for accurate description of van der Waals interaction between He atoms. *Chemical Physics Letters* **2001,** *348*, 139-146.

95. Couronne, O.; Ellinger, Y., An ab initio and DFT study of (N2)2 dimers. *Chemical Physics Letters* **1999,** *306*, 71-77.

96. Romesberg, F. E.; Bernstein, M. P.; Gilchrist, J. H.; Harrison, A. T.; Fuller, D. J.; Collum, D. B., Structure of lithium hexamethyldisilazide in the presence of hexamethylphosphoramide. Spectroscopic and computational studies of monomers, dimers, and triple ions. *Journal of the American Chemical Society* **1993,** *115*, 3475-3483.

97. Popenova, S.; Mawhinney, R. C.; Schreckenbach, G., Density Functional Study of Lithium Hexamethyldisilazide (LiHMDS) Complexes: Effects of Solvation and Aggregation. *Inorganic Chemistry* **2007,** *46*, 3856-3864.

98. Grimme, S., Density functional theory with London dispersion corrections. *Wiley Interdisciplinary Reviews: Computational Molecular Science* **2011,** *1*, 211-228.

99. Andersson, Y.; Langreth, D. C.; Lundqvist, B. I., van der Waals interactions in density-functional theory. *Physical Review Letters* **1996,** *76*, 102-105.

100. Dion, M.; Rydberg, H.; Schroder, E.; Langreth, D. C.; Lundqvist, B. I., Van der Waals density functional for general geometries. *Physical Review Letters* **2004,** *92*.

101. Grafenstein, J.; Cremer, D., An efficient algorithm for the density-functional theory treatment of dispersion interactions. *Journal of Chemical Physics* **2009,** *130*.

102. Zhao, Y.; Truhlar, D. G., A new local density functional for main-group thermochemistry, transition metal bonding, thermochemical kinetics, and noncovalent interactions. *Journal of Chemical Physics* **2006,** *125*.

103. von Lilienfeld, O. A.; Tavernelli, I.; Rothlisberger, U.; Sebastiani, D., Optimization of effective atom centered potentials for London dispersion forces in density functional theory. *Physical Review Letters* **2004,** *93*.

104. Nilsson Lill, S. O., Application of Dispersion-Corrected Density Functional Theory. *The Journal of Physical Chemistry A* **2009,** *113*, 10321-10326.

105. Gino A, D., Accurate treatment of van der Waals interactions using standard density functional theory methods with effective core-type potentials: Application to carbon-containing dimers. *Chemical Physics Letters* **2008,** *455*, 348-353.

106. Hehre, W. J.; Ditchfield, R.; Pople, J. A., Self-Consistent Molecular Orbital Methods. XII. Further Extensions of Gaussian-Type Basis Sets for Use in Molecular Orbital Studies of Organic Molecules. *The Journal of Chemical Physics* **1972,** *56*, 2257-2261.

107. Goerigk, L.; Grimme, S., Accurate Dispersion-Corrected Density Functionals for General Chemistry Applications. In *Modeling of Molecular Properties*, Wiley-VCH Verlag GmbH & Co. KGaA: 2011; pp 1-16.

108. Grimme, S.; Antony, J.; Ehrlich, S.; Krieg, H., A consistent and accurate ab initio parametrization of density functional dispersion correction (DFT-D) for the 94 elements H-Pu. *The Journal of Chemical Physics* **2010,** *132*, 154104-19.

109. Goerigk, L.; Grimme, S., A thorough benchmark of density functional methods for general main group thermochemistry, kinetics, and noncovalent interactions. *Physical Chemistry Chemical Physics* **2011,** *13*, 6670-6688.

110. Theilacker, K.; Arbuznikov, A. V.; Bahmann, H.; Kaupp, M., Evaluation of a Combination of Local Hybrid Functionals with DFT-D3 Corrections for the Calculation of Thermochemical and Kinetic Data. *The Journal of Physical Chemistry A* **2011,** *115*, 8990-8996.

111. Christoffers, J., An Unusual Acyliminium Cyclization and Other Drawbacks during an Attempted Synthesis of a Chiral Primary alpha-Phosphinoalkanamine. *Helvetica Chimica Acta* **1998,** *81*, 845-852.

112. Wallén, E. A. A.; Christiaans, J. A. M.; Saario, S. M.; Forsberg, M. M.; Venäläinen, J. I.; Paso, H. M.; Männistö, P. T.; Gynther, J., 4-Phenylbutanoyl-2(S)-acylpyrrolidines and 4-phenylbutanoyl--prolyl-2(S)-acylpyrrolidines as prolyl oligopeptidase inhibitors. *Bioorganic & Medicinal Chemistry* **2002,** *10*, 2199-2206.

113. Ghosh, A.; Sieser, J. E.; Caron, S.; Watson, T. J. N., Synthesis of the kappa-agonist CJ-15,161 via a palladium-catalyzed cross-coupling reaction. *Chemical Communications* **2002**, 1644-1645.

114. El Moncef, A.; El Hadrami, E. M.; González, M. A.; Zaballos, E.; Zaragozá, R. J., Experimental and DFT study of the conversion of ephedrine derivatives into oxazolidinones. Double SN2 mechanism against SN1 mechanism. *Tetrahedron* **2010,** *66*, 5173-5184.

115. Heathcock, C.; Hassner, A., Bildung von 2-Oxazolidonen aus beta-Jodurethanen Stereospezifische Synthese von cis-beta-Aminoalkoholen. *Angewandte Chemie* **1963,** *75*, 344.

116. Malkov, A. V.; Hand, J. B.; Kocovsky, P., A long-range chiral relay via tertiary amide group in asymmetric catalysis: new amino acid-derived N,P-ligands for copper-catalysed conjugate addition. *Chemical Communications* **2003**, 1948-1949.

117. Abdel-Magid, A. F.; Carson, K. G.; Harris, B. D.; Maryanoff, C. A.; Shah, R. D., Reductive Amination of Aldehydes and Ketones with Sodium Triacetoxyborohydride. Studies on Direct and Indirect Reductive Amination Procedures1. *The Journal of Organic Chemistry* **1996,** *61*, 3849-3862.

118. Ali, M. H., Stricklin, S., Catalytic oxidation of sulfides to sulfones with silica gel supported $RuCl_3$/$NaIO_4$ in non-aqueous media. *Synthetic Communications* **2006,** *36*.

119. MelÈndez, R. E.; Lubell, W. D., Synthesis and reactivity of cyclic sulfamidites and sulfamidates. *Tetrahedron* **2003,** *59*, 2581-2616.

120. Huibers, M.; Manuzi, Å.; Rutjes, F. P. J. T.; van Delft, F. L., A Sulfitylation‚àíOxidation Protocol for the Preparation of Sulfates. *The Journal of Organic Chemistry* **2006,** *71*, 7473-7476.

121. Al-Horani, R. A.; Desai, U. R., Chemical sulfation of small molecules--advances and challenges. *Tetrahedron* **2010,** *66*, 2907-2918.

122. Berridge, M. S.; Franceschini, M. P.; Rosenfeld, E.; Tewson, T. J., Cyclic sulfates: useful substrates for selective nucleophilic substitution. *The Journal of Organic Chemistry* **1990,** *55*, 1211-1217.

123. Kuyl-Yeheskiely, E.; Lodder, M.; van der Marel, G. A.; van Boom, J. H., One-step synthesis of optically active benzyl N-trityl-L-aziridine-2-carboxylic esters. *Tetrahedron Letters* **1992,** *33*, 3013-3016.

124. Tao, B.; Schlingloff, G.; Sharpless, K. B., Reversal of regioselection in the asymmetric aminohydroxylation of cinnamates. *Tetrahedron Letters* **1998,** *39*, 2507-2510.

125. Lowe, G.; Reed, M. A., Synthesis and configurational assignment of some novel bicyclic sulphamidites and sulphamidates. *Tetrahedron: Asymmetry* **1990,** *1*, 881-884.

126. Cooper, G. F.; McCarthy, K. E.; Martin, M. G., Alkylation of the cyclic sulfamate of prolinol. Preparation of optically active 2-alkyl-substituted pyrrolidines. *Tetrahedron Letters* **1992,** *33*, 5895-5896.

127. Masui, Y.; Watanabe, H.; Masui, T., One-pot synthesis of N-acyl-substituted sulfamides from chlorosulfonyl isocyanate via the Burgess-type intermediates. *Tetrahedron Letters* **2004,** *45*, 1853-1856.

128. Fuhrman, A.; Degering, E. F., Heterocyclic Derivatives of Sulfamide1. *Journal of the American Chemical Society* **1945,** *67*, 1245-1246.

129. Baldwin, J. E.; Spivey, A. C.; Schofield, C. J., Cyclic sulphamidates: New synthetic precursors for [beta]-functionalised [alpha]-amino acids. *Tetrahedron: Asymmetry* **1990,** *1*, 877-880.

130. Williard, P. G.; Sun, C., Mixed Aggregates Containing n-Butyl-, sec-Butyl-, or tert-Butyllithium and a Chiral Lithium Amide Derived from N-Isopropyl-O-methyl Valinol. *Journal of the American Chemical Society* **1997,** *119*, 11693-11694.

131. Keresztes, I.; Williard, P. G., Diffusion-Ordered NMR Spectroscopy (DOSY) of THF Solvated n-Butyllithium Aggregates. *Journal of the American Chemical Society* **2000,** *122*, 10228-10229.

132. Hilmersson, G.; Malmros, B., Mixed Dimer and Mixed Trimer Complexes of nBuLi and a Chiral Lithium Amide. *Chemistry – A European Journal* **2001,** *7*, 337-341.

133. Hilmersson, G.; Malmros, B., Mixed Dimer and Mixed Trimer Complexes of *n*-BuLi and a Chiral Lithium Amide. *Chemistry – A European Journal* **2001,** *7*, 337-341.

134. Rönnholm, P.; Hilmersson, G., NMR studies of chiral lithium amides with phosphine chelating groups reveal strong Li-P-interactions in ethereal solvents. *ARKIVOC* **2011**, 200 - 210.

135. De Vries, T. S.; Goswami, A.; Liou, L. R.; Gruver, J. M.; Jayne, E.; Collum, D. B., Lithium Phenolates Solvated by Tetrahydrofuran and 1,2-Dimethoxyethane: Structure Determination Using the Method of Continuous Variation. *Journal of the American Chemical Society* **2009,** *131*, 13142-13154.

136. Pratt, L. M., Modeling lithium dialkylamides in ethereal solvents: A test of the microsolvation model. *Journal of Molecular Structure: THEOCHEM* **2007,** *811*, 191-196.

137. Francl, M. M.; Pietro, W. J.; Hehre, W. J.; Binkley, J. S.; Gordon, M. S.; DeFrees, D. J.; Pople, J. A., Self-consistent molecular orbital methods. XXIII. A polarization-type basis set for second-row elements. *The Journal of Chemical Physics* **1982,** *77*, 3654-3665.

138. Ditchfield, R.; Hehre, W. J.; Pople, J. A., Self-Consistent Molecular-Orbital Methods. IX. An Extended Gaussian-Type Basis for Molecular-Orbital Studies of Organic Molecules. *The Journal of Chemical Physics* **1971,** *54*, 724-728.

139. Hariharan, P. C.; Pople, J. A., The influence of polarization functions on molecular orbital hydrogenation energies. *Theoretical Chemistry Accounts: Theory, Computation, and Modeling (Theoretica Chimica Acta)* **1973,** *28*, 213-222.

140.   Frisch, M. J.; Pople, J. A.; Binkley, J. S., Self-consistent molecular orbital methods 25. Supplementary functions for Gaussian basis sets. *The Journal of Chemical Physics* **1984,** *80*, 3265-3269.

141.   Clark, T.; Chandrasekhar, J.; Spitznagel, G. W.; Schleyer, P. V. R., Efficient diffuse function-augmented basis sets for anion calculations. III. The 3-21+G basis set for first-row elements, Li–F. *Journal of Computational Chemistry* **1983,** *4*, 294-301.

142.   Capriati, V.; Florio, S.; Perna, F. M.; Salomone, A.; Abbotto, A.; Amedjkouh, M.; Nilsson Lill, S. O., On the Dichotomic Reactivity of Lithiated Styrene Oxide: A Computational and Multinuclear Magnetic Resonance Investigation. *Chemistry – A European Journal* **2009,** *15*, 7958-7979.

143.   Yoshida, T.; Sakakibara, K.; Asami, M.; Chen, K.-H.; Lii, J.-H.; Allinger, N. L., Molecular mechanics (MM3) calculations on lithium amide compounds. *Journal of Computational Chemistry* **2003,** *24*, 319-327.

144.   Allinger, N. L.; Yuh, Y. H.; Lii, J. H., Molecular mechanics. The MM3 force field for hydrocarbons. 1. *Journal of the American Chemical Society* **1989,** *111*, 8551-8566.

145.   Lii, J. H.; Allinger, N. L., Molecular mechanics. The MM3 force field for hydrocarbons. 2. Vibrational frequencies and thermodynamics. *Journal of the American Chemical Society* **1989,** *111*, 8566-8575.

146.   Lii, J. H.; Allinger, N. L., Molecular mechanics. The MM3 force field for hydrocarbons. 3. The van der Waals' potentials and crystal data for aliphatic and aromatic hydrocarbons. *Journal of the American Chemical Society* **1989,** *111*, 8576-8582.

147.   Timofeeva, T. V.; Lii, J.-H.; Allinger, N. L., Molecular Mechanics Explanation of the Metallocene Bent Sandwich Structure. *Journal of the American Chemical Society* **1995,** *117*, 7452-7459.

148.   Granander, J.; Eriksson, J.; Hilmersson, G., Highly enantioselective 1,2-additions of various organolithium reagents to aldehydes. *Tetrahedron: Asymmetry* **2006,** *17*, 2021-2027.

149.   Rönnholm, P.; Nilsson Lill, S. O.; Gräfenstein, J.; Norrby, P.-O.; Hilmersson, G., A Computational Study of the Enantioselective Addition of *n*-BuLi to Benzaldehyde in the Presence of a Chiral Lithium N,P-Amide. *to be submitted to the Organic & Biomolecular Chemistry* **2011**.

150.   Nilsson Lill, S. O.; Forbes, A.; Donoghue, P.; Verdolino, V.; Wiest, O.; Rydberg, P.; Norrby, P.-O., Application of Q2MM to Stereoselective Reactions. *Current Organic Chemistry* **2010,** *14*, 1629-1645.

151.   Rönnholm, P.; Nilsson Lill, S. O., Tailored force field for lithium organic amides. *Unpublished* **2011**.

152.   Cramer, C. J.; Truhlar, D. G., A Universal Approach to Solvation Modeling. *Accounts of Chemical Research* **2008,** *41*, 760-768.

153.   Chamberlin, A. C.; Levitt, D. G.; Cramer, C. J.; Truhlar, D. G., Modeling Free Energies of Solvation in Olive Oil. *Molecular Pharmaceutics* **2008,** *5*, 1064-1079.

154.   Contreras-García, J.; Johnson, E. R.; Keinan, S.; Chaudret, R.; Piquemal, J.-P.; Beratan, D. N.; Yang, W., NCIPLOT: A Program for Plotting Noncovalent Interaction Regions. *Journal of Chemical Theory and Computation* **2011,** *7*, 625-632.

155.   Podewitz, M., The Effect of Solvation on the NMR Properties of Lithium Amides - A DFT Study. *Master of Science Project Report in Theoretical Chemistry* **2006**.

156.   Jones, A. C.; Sanders, A. W.; Bevan, M. J.; Reich, H. J., Reactivity of Individual Organolithium Aggregates: A RINMR Study of n-Butyllithium and 2-Methoxy-6-(methoxymethyl)phenyllithium. *Journal of the American Chemical Society* **2007,** *129*, 3492-3493.